UNIVERSITY OF CALIFORNIA
RIVERSIDE

An Effector of the Citrus Huanglongbing-Associated Pathogen Provides Mechanistic Insight to Pathogenesis and Potential Strategies to Enhance Disease Management

A Dissertation submitted in partial satisfaction
of the requirements for the degree of

Doctor of Philosophy

in

Microbiology

by

Kelley Jean Clark

December 2019

Dissertation Committee:
Dr. Wenbo Ma, Chairperson
Dr. Georgios Vidalakis
Dr. Mikeal Roose

The Dissertation of Kelley Jean Clark is approved:

_____

_____

_____

Committee Chairperson

University of California, Riverside

ACKNOWLEDGEMETS

My upmost respect goes to those who have embarked on this journey prior to myself, your guidance and advice were never wasted. My deepest gratitude does to my advisor Prof. Wenbo Ma for her mentorship on a multitude of levels. Throughout my PhD she has been like a parent, both nurturing and disciplined, encouraging me to succeed as a scientist. Many thanks also go to my committee members Prof. Mikeal Roose and Prof. Georgios Vidalakis for their recommendations to my research and guidance in my personal career. I want to acknowledge all of the Ma Lab members who have contributed to my development as a young scientist, including present members; Dr. Yingnan Hou, Drs. Agustina De Francesco, Yi Zhai, Morgan Halane, Hui Li, and Eva Hawara, Sara Dorhmi, Alexander McClelland, Jessica Trinh, and Yufei Li, and past members; Drs. Deborah Pagliaccia, Simon Schwizer, Liping Zeng, Jinxia Shi, Ka-Wai Ma, Ariel Tung Kuan, Du Seok Choi, Robert Lui and Yao Zhao.

I would also like to acknowledge our many collaborators whose intellect contributed this research; Prof. Gitta Coaker and Ms. Jessica Franco at the University of California, Davis, Prof. Nian Wang and Dr. Zhiqian Pang at the University of Florida, Lake Alfred, Dr. Veronica Ancona-Contreras and Mr. Fatta Gurung at Texas A&M University, Kingsville, Prof. Ashok Mulchandani and Dr. Thien-Toan Tran at University of California Riverside, Dept. of Chemical and Environmental Engineering, and Prof. Yinsheng Wang and Dr. Pengcheng Wang University of California Riverside, Dept. of Chemistry. Within each chapter special acknowledgements are given for specific contributions. I also thank the Dynamic Genome faculty, staff, and students for their contributions my research including; Prof. Sue Wessler, Dr. Jim Burnette, Dr. Matthew Collin, Mr. Alex Cortez, and Dr. Venki Chetty. Thank you to my undergraduate mentees

for your assistance and enthusiasm in the lab, Thomas Forest, Shellen Lee, Caitlin Tong and Abhi Gowder. And lastly, to my friends and family who have always lent their support, without them this dissertation would not have been possible.

Note: the contents of Chapter 2 of this thesis are adapted from Clark and Franco *et. al.* (2018) *Nature Communications*. 9:1718.

DEDICATION

To my family whom has never wavered in their support or adoration of my accomplishments. Thank you, Mom, Dad, and Jen, for the encouragement and blessings. And to my other half Dr. Michael Matson, who has been with me every step of my PhD journey. And to Kepler, who has sat patiently with me for hours as I wrote the contents of this thesis. I dedicate this thesis to all of you, know that I always love you.

ABSTRACT OF THE DISSERTATION

An Effector of the Citrus Huanglongbing-Associated Pathogen Provides Mechanistic Insight to Pathogenesis and Potential Strategies to Enhance Disease Management

by

Kelley Jean Clark

Doctor of Philosophy, Graduate Program in Microbiology
University of California, Riverside, December 2019
Dr. Wenbo Ma, Chairperson

Huanglongbing (HLB) is currently the most devastating disease of citrus and has created unperceived challenges to global citrus production. In order to properly manage HLB, robust detection methods must be implemented to prevent pathogen expansion and genetic resources must be explored to develop HLB-tolerance in citrus. To achieve this, much is to be elucidated on the pathogen virulence mechanisms and host defense responses involved during HLB disease progression.

The most prevalent HLB-associated disease agent is *Candidatus* Liberibacter asiaticus (*C*Las); a fastidious, gram-negative bacterium. Gram-negative bacterial pathogens possess secretion systems which deliver virulence proteins, known as effectors, into the host. Effectors can modify host physiology and suppress immunity to promote pathogen colonization and subsequent disease. Previous research found that *C*Las encodes Sec-delivered effectors (SDEs), many of which are highly expressed in *C*Las-infected citrus tissues, conserved across *C*Las isolates, and have uncharacterized functions. As such, SDEs can be utilized as molecular probes to better understand pathogen biology.

In this thesis, I employed SDEs of *C*Las to aid in development of detection technologies and to further knowledge of the *C*Las-citrus arms race. In **Chapter I**, I used *C*Las SDE1 and SDE2 as biomarkers in the development of antibodies for serological-based detection technologies. I evaluated and purified antibodies raised against the two biomarker proteins enhancing antibody efficiency and functionality for subsequent detection platforms. These results demonstrated their potential use for *C*Las detection.

In **Chapter II**, I utilized *C*Las SDE1 as a molecular probe to unveil host targets and characterize effector function. I found SDE1 interacts with and inhibits the activity of citrus papain-like cysteine proteases (PLCPs). PLCPs are known to be involved in defense in many other pathosystems and exhibit increased abundance during *C*Las infection. Collectively, these results indicated that SDE1 works as a virulence protein of *C*Las and can promote bacterial infection, likely by inhibiting citrus PLCP activity to suppress host defenses.

In **Chapter III**, I further explored SDE1 function in HLB disease progression. My results demonstrated that SDE1 protein expression in *Arabidopsis thaliana* caused yellowing, reminiscent of HLB symptoms. This SDE1-induced yellowing was associated with the induction of leaf senescence signatures, such as reactive oxygen species and senescence-associated genes. Senescence gene induction was also slightly altered in *SDE1*-transgenic citrus but, only in plants with the additional stress of *C*Las-infection. Thus, manipulation of senescence could be a possible virulence strategy of *C*Las in an SDE1-related manner.

TABLE OF CONTENTS

LIST OF FIGURES

General Introduction

Chapter I

Chapter II

Chapter III

LIST OF TABLES

Chapter I

Chapter II

Chapter III

Appendix

GENERAL INTRODUCTION

Epidemiology and economic significance of citrus Huanglongbing (HLB)

Huanglongbing (HLB), also known as citrus greening disease, is currently considered the most destructive disease of citrus worldwide [1–4]. Origins of the disease were first noted in Asia, between the 18th and 19th century [5,6]; however, today HLB has spread to most of the world's citrus producing regions [3]. HLB is associated with three fastidious bacteria, which are named according to their presumed origins: *Candidatus* Liberibacter asiaticus (*C*Las), *Candiatus* Liberibacter americanus (*C*Lam), and *Candidatus* Liberibacter africanus (*C*Laf) [1]. Although HLB is a century-old disease, it was confirmed in the Americas only over a decade ago [7–11]. *C*Las is the most prevalent species and also the species associated with HLB outbreak in the United States. *C*Lam is present in South America, however the presence and aggressive nature of *C*Las has suppressed *C*Lam populations in this region [12]. *C*Laf is primarily present in Africa and consists of several subspecies [13,14]. *C*Laf and *C*Lam are also reported to be more heat sensitive compared to *C*Las contributing to their less widespread distribution [14,15].

Spread of HLB to the Americas has led to costly and intense control programs. In Sao Paulo, Brazil, 18 million citrus plants have been eradicated between 2005 and 2012, increasing production costs through inspection and replanting [16]. In the United States, HLB has affected the three major citrus producing states, Florida, California, and Texas [7–9]. From 2007-08 to 2017-18 there has been a 72% reduction in juice production and 20% reduction in fresh fruit, from HLB disease infestation in Florida [17]. HLB disease factors, among other issues such as drought and hurricanes, have raised the estimated cost of a box of oranges from $2.89 to $9.67, during the window of time HLB has been present in Florida [18,19]. In Florida, where HLB infestation has spread to at least 90% of

citrus acreage and estimated losses of one-billion-dollars annually threaten economic return [20] and [21]. In Texas and California, current disease incidence is lower. Yet, markets in these states are based on whole-fruit production, so rapid spread of HLB could instantly devastate citrus industries due to unmarketable fruits [17]. Disease incidence in California is increasing rapidly, from 11 trees in 2012-15 after the initial discovery of *C*Las-infected trees, to over 1,600 trees confirmed as of October 2019 (information from California Department of Food and Agriculture, citrusinsider.org) (**Figure Ia**).

HLB disease cycle and symptomology

The HLB disease cycle includes the associated bacterium, psyllid vector, and citrus hosts [1] (**Figure Ib**). Interactions among these organisms, in addition to environmental conditions contribute to the complexity of the disease [22,23]

Candidatus Liberibacters (*C*L) are gram-negative bacteria belonging to the Rhizobiaceae family of the alpha-proteobacteria [24]. These bacteria are phloem-limited and have yet to be cultured outside the host; therefore, Koch's postulates have not been completed. The association of the *C*L with HLB disease is based on metagenomic sequencing data and 16SrRNA analysis [25,26]. *Liberibacter crescens* is the only Liberibacter that can be obtained in pure culture [27].

In the natural environment, *C*Ls are introduced to host plants via insect vectors. The most well-known vector is the Asian citrus psyllid (ACP), *Diaphorina citri* Kuwayama, which can transmit both *C*Las and *C*Lam strains [28,29]. Another vector, known to transmit *C*Laf, is the African citrus psyllid, *Trioza erytreae* Del Guerico. Psyllids feed on young citrus flush where the acquisition of *C*Ls can occur at all psyllid stages, with nymphs having higher acquisition levels than adults [30]. *C*Las transmission has been

reported in a persistent manner and bacteria has been detected in various ACP organs [31]. Acquisition of *C*Las by the ACP can be from 15min to 24hrs, followed by a latency period ranging from 1-25 days in which bacteria enter the psyllid salivary gland, possibly multiply, and then inoculate a new plant [32]. ACP are capable of moving 100m within three days and have been reported to travel up to two km in 12 days further disseminating the disease [33,34]. Such distances are also greatly affected by wind conditions and human transport via shipment trucks [29,35]. Additionally, grafting with contaminated scion or budwood can spread *C*Ls [36] and in principle other *C*Ls and pholem-limited pathogens [37].

Upon *C*L transmission to the host, symptom development is highly variable and can take anywhere from several months to years to occur [1,38,39]. Symptom progression and severity has been observed more rapidly in young trees than mature ones [39]. All citrus cultivars and many citrus relatives can be infected and very few tolerant citrus varieties have been reported [23,40,41]. Disease symptoms include yellowing of leaf veins and shoots, leaf blotchy mottle, reduced fruit production, discolored or deformed fruits, premature fruit drop, stunting and dieback (**Figure Ic**) [1,2,4]. The fruits produced are not viable for commercial purposes due to their altered appearance and off-tasting flavor from lower total sugar and higher citric acid [17,42].

Current management strategies

Currently, no curative method is available to control HLB [43,44]. Management has traditionally focused on a three-pronged approach to 1) area-wide control the psyllid vector, 2) detect and remove infected trees, and 3) plant clean nursey stock [45–47]. However, current strategies are more dependent on local disease infestation.

In Florida, where disease prevalence in high and tree removal is no longer cost effective, management is based on treatments to reduce effects of the disease on crop production [29]. Such treatments include antibiotics, plant hormones, increased nutrient application, and thermotherapy [43,44,48,49]. Since many of these treatments include chemical application, delivery of such compounds to the phloem has been problematic [50]. It is argued that these treatments may not have any value in extending tree productivity [51]; yet, it has also been reported that these strategies are more effective when combined [43].

In California, where disease incidence is still relatively low, prevention strategies support a multi-pronged approach based on inspections and high-risk models. 1) Vector management is based on insecticide application and biocontrol release [32,52]. Insecticide application can protect trees from ACP feeding for 1.5-6 weeks, thus repeated applications are needed for sufficient protection and ACP resistance to insecticides is possible [32,43]. Biological control has been implemented by release of the parasitic wasps (*Tamarixia radiata* and *Diaphorencyrtus aligarhensis*) [52,53]. Yet, the mode of action provided by biological control methods is slower than that of chemical application and can only reduce vector populations to low levels, rather than eradicating them completely. 2) Efficient detection technologies are pertinent for identification and removal of infected trees in lower infestation areas. The current gold-standard for detection is quantitative-polymerase chain reaction (qPCR) which detects for the presence of *C*Las DNA [54,55]. Yet the uneven distribution of *C*Las bacterium in infected citrus tissues poses a challenge to this detection method, spurring the innovation of several alternative "early" detection technologies [56,57] (further discussed in Chapter 1). 3) Quarantine and

regulatory zones implemented by California Department of Food and Agriculture manage or forbid the transportation of nursey stock to non-quarantine zones, reducing spread of the disease. 4) By California law, the use of clean citrus propagative material is mandatory (3060.2. Standard of Cleanliness, California code of regulations) and must be obtained through the Citrus Clonal Protection Program or Citrus Nursery Stock Pest Cleanliness Program.

The most efficient long-term sustainable strategy would be to develop HLB-resistant or tolerant cultivars, yet this will require identification of useful resistance genes. In addition, commercial applications of such trees are years away [17,43]. The only current example of tolerance in citrus is the constitutive expression of NPR1, which exhibits enhanced resistance to HLB and citrus canker [58]. However, overexpression of defense genes almost always leads to growth/yield costs [59]. Efforts to silence homologs of the susceptibility gene downy mildew resistance 6 (*DRM6*) in citrus have also been reported [60]. Conventional breeding for disease tolerance is difficult due to long juvenile stages in citrus plants [61]. Tolerant citrus relatives have been reported and hybrids are in progress [41]. Yet, the fruit quality and similarity to popular cultivars of these hybrids is unknown. In addition, tolerance has been reported in Sugar Belle™ mandarin 'LB8-9' and *Poncirus trifoliata* (L.) Raf. [40,62]. Engineered citrus tristeza virus (CTV) to attack *C*Las has also been presented as possible biocontrol strategy and field trials are underway in Florida, with plans to expand to California, however trials are still in the early stages [63].

Overview of plant-pathogen interactions

To cause disease, plant pathogens must overcome a multitude of hurdles presented by their hosts including physical barriers and immune perception [64]. Upon

infection, conserved pathogen molecules or pathogen-associated molecular patterns (PAMPs) or damage associated molecular patterns (DAMPs) can be perceived by the host's surveillance system, consisting of extracellular pattern recognition receptors (PRRs) [65,66]. Pathogen recognition by these receptor-like proteins triggers the host's first line of immunity, pattern triggered immunity (PTI) (**Figure IIa**). During the PTI response the host turns on defense signaling via mitogen-activated protein kinases (MAPKs), WRKY transcription factors, reactive oxygen species (ROS), and callose deposition to restrict pathogen growth [67]. Coevolution between plants and pathogens has resulted in a vast array of such recognition receptors within plant genomes [67,68]. For pathogens to evade this immune response they must deploy effectors to facilitate infection [69].

Bacterial, fungal, oomycete pathogens and insect pests utilize different secretion mechanisms to deliver effectors into the host [70]. Effectors manipulate the host by suppressing or disrupting the PTI signaling network, resulting in effector-triggered susceptibility (ETS) [69,71] (**Figure IIa**). To counteract this, intracellular immune receptors, host resistance (R) proteins or NB-LRRs (nucleotide-binding leucine-rich repeat proteins) can specifically recognize effectors and/or effector activity, triggering the next layer of innate immunity known as, effector triggered immunity (ETI). ETI is a stronger version of PTI, eliciting similar defense responses but also including pathogenesis-gene expression, hypersensitive response, and systemic acquired resistance [69,72]. The arm's race between plants and their pathogen counterparts persists, as pathogens evolve by editing their effector arsenals to yet again evade the host immune response [67].

However, as PTI and ETI share overlapping effects and pathogen recognition has been noted both inside and outside of plant cells maintaining a strict ETI/PTI model is not always possible. A proposed alternative paradigm of plant defense and

counterdefense includes three layers 1) recognition, 2) signal integration, and 3) defense-action [73] (**Figure IIb**). In this model the pathogen signatures (including PAMPs and effectors) can be perceived in the apoplast or cytoplasm, followed by a signal transduction triggered by recognition (i.e. phosphorylation and ubiquitination cascades, hormone signaling, and transcription factors). These signals initiate a defense-action layer consisting of diverse mechanisms to target specific and/or multiple pathogens (i.e. programmed cell death, phytotoxins, antimicrobial proteins, etc.). Similar rejections of the traditional zigzag model have been made previously suggesting that such models are overgeneralizations of complex biological systems [74,75].

Molecular plant pathology of HLB

Currently, there is a knowledge gap in the plant-microbe interactions undergone during HLB pathogenesis. Both the difficulty in obtaining pure cell cultures of *C*Ls and the time and space requirements for working with citrus greatly contribute to this lack in knowledge of *C*L biology. The *C*Las genome encodes many potential elicitors which include the well-known PAMPs such as, flagellin and lipopolysaccharides (LPS) [76,77]. However, *C*Las flagellin has not been visualized, in addition to being absent from *C*Lam, and the roles of *C*Las LPS are unclear. Although treatment of two different citrus cultivars with *C*Las flagellin did elicit an immune response, it was weaker than compared to treatment with *Xanthomonas citri* flagellin [78]. PTI response to *C*Las remains questionable as PAMP perception normally occurs outside the cell surface and *C*Ls are directly transmitted into phloem cells by their psyllid vectors [2,79]. Transcriptional analysis revealed the upregulation of defense-related receptor kinases (RLK) [80], but these transmembrane-bound proteins work at the cell membrane, so how they recognize *C*Las

PAMPs is unknown. It is possible they use an intermediate molecule to relay signaling or that they have lost function over evolution [2]. Potential PTI responses observed in *C*Las-infected citrus include, callose deposition, phloem cell wall thickening, massive starch accumulation and necrotic phloem [76,81–83].

To subvert host immune responses, it is believed that *C*Las uses encoded proteins such as: serralysin, a metalloprotease reported to degrade antimicrobial proteins; hemolysin, which is thought to be involved in cell lysis; and a salicylate hydroxylase that can convert salicylic acid (SA) in to catechol [4]. *C*Las also has two prophage-encoded secreted peroxidases which can help the bacteria defend itself against oxidative stress and evade early host detection [84]. These microbial virulence factors may play an important role in colonization and survival of *C*Las in the citrus host.

The variability in latency prior to symptom development, and range in tolerance across citrus species suggest an attempted immune response [2]. Comparisons of transcriptomes, proteomes, and metabolomes in *C*Las-infected vs. non-infected citrus reveal drastic differences, further indicating host response [80,81,85,86]. Gene expression analysis in citrus found that many genes with altered expression are defense and stress related including several NBS-LRR genes [80,81]. In addition, *C*Las flagellin peptide, flg22, can trigger salicylic acid (SA) signaling genes in citrus, indicating an attempted defense [78]. It is intriguing to speculate that citrus has not evolved sufficient immunity to *C*Las since there has been little to no observed natural resistance in citrus species and disease occurrence is recent (100 years) in comparison to citrus cultivation (1000s of years) [2,3].

*C*Las encodes Sec-delivered effectors (SDEs)

Many gram-negative bacteria encode secretion systems, which contribute to bacterial pathogenesis by releasing virulence proteins, or effectors [87]. For example, *Pseudomonas syringae* encodes the type III secretion system (T3SS), which is a syringe-like appendage that facilitates injection of effectors directly into host cells [88]. *P. syringae* type III-secreted effectors are well known to suppress host immunity and recognition by targeting host defense-associated processes, thus are required for full virulence [89,90].

*C*Las has a significantly reduced genome size, and does not encode the T3SS; however, *C*Las does possess all the components of the general Sec secretion machinery [77,91]. In addition, genes encoding components of the Sec-secretion system (SecYEG translocase) are expressed 30-folds higher in citrus than in psyllids [92]. The Sec secretion system secretes proteins carrying an N-terminal signal peptide to the periplasmic space (**Figure III**) [91,93,94]. It is predicted these Sec-delivered effectors (SDEs) are further secreted to into their environment via beta barrel proteins on the outer membrane, hijacking of the *flp* pilus (which is evolutionarily related to the type II secretion system), or outer membrane vesicles [91]. Such a delivery mechanism for effectors of intracellular pathogens like *C*Ls can be expected since they are injected into host cells by their insect vector and would therefore release SDEs directly into the phloem.

SDEs of other insect-transmitted, phloem-colonizing bacteria play essential roles in disease development [95]. For instance, Phytoplasma SDEs are small in size allowing them to travel systemically throughout host tissues (**Figure IVa**) and target host proteins. Aster yellows phytoplasma strain witches' broom is predicted to secrete 56 SDEs [95].

Expression of individual phytoplasma SDEs *in planta* has revealed SDEs can contribute to enhanced insect fecundity [96], and disease symptoms such as dwarfing [97] and altered leaf morphology [98] (**Figure IVb**). *C*Ls are similar to Phytoplasmas since they are both insect-transmitted, phloem-colonizing, bacterial pathogens. Therefore, it is likely that the SDEs produced by *C*Las or other *C*Ls can also contribute to HLB symptoms and disease cycle. Thus, effectors are excellent cellular probes to facilitate insight of biological processes behind pathogenesis and vulnerability in host defense [64]

Genome analysis revealed 86 potential SDEs encoded by *C*Las [99]. Among them, CLIBASIA_05315 and CLIBASIA_03230 (SDE1 and SDE2) are highly conserved across *C*Las isolates [100] (Thapa 2019 *in prep*), suggesting they are important virulence factors of *C*Las specifically, and can confer detection for all isolates. SDE1 is expressed ~10-folds higher [100] and SDE2 ~3.5-folds higher [92] in *C*Las-infected citrus compared to *C*Las-infected psyllids, indicating plausible roles in the *C*Las establishment in the plant host, and high abundance for detection in infected tissues (**Figure V**). SDE1 and SDE2 are also both small in size (less than ~17kDa), which could encourage their movement with the phloem flow, allowing potential targeting of host proteins in the pholem and neighboring tissues [101], and potentially higher distrubution throughout citrus tissues compared to *C*Las cells themselves, enhancing detection.

In this thesis, I employed SDE1 and SDE2 to generate, evaluate, and improve antibodies applied to serological methods for *C*Las detection, and utilized SDE1 to identity effector host targets in citrus and characterize effector function, broadening our knowledge on *C*Las virulence mechanisms and HLB pathogenesis.

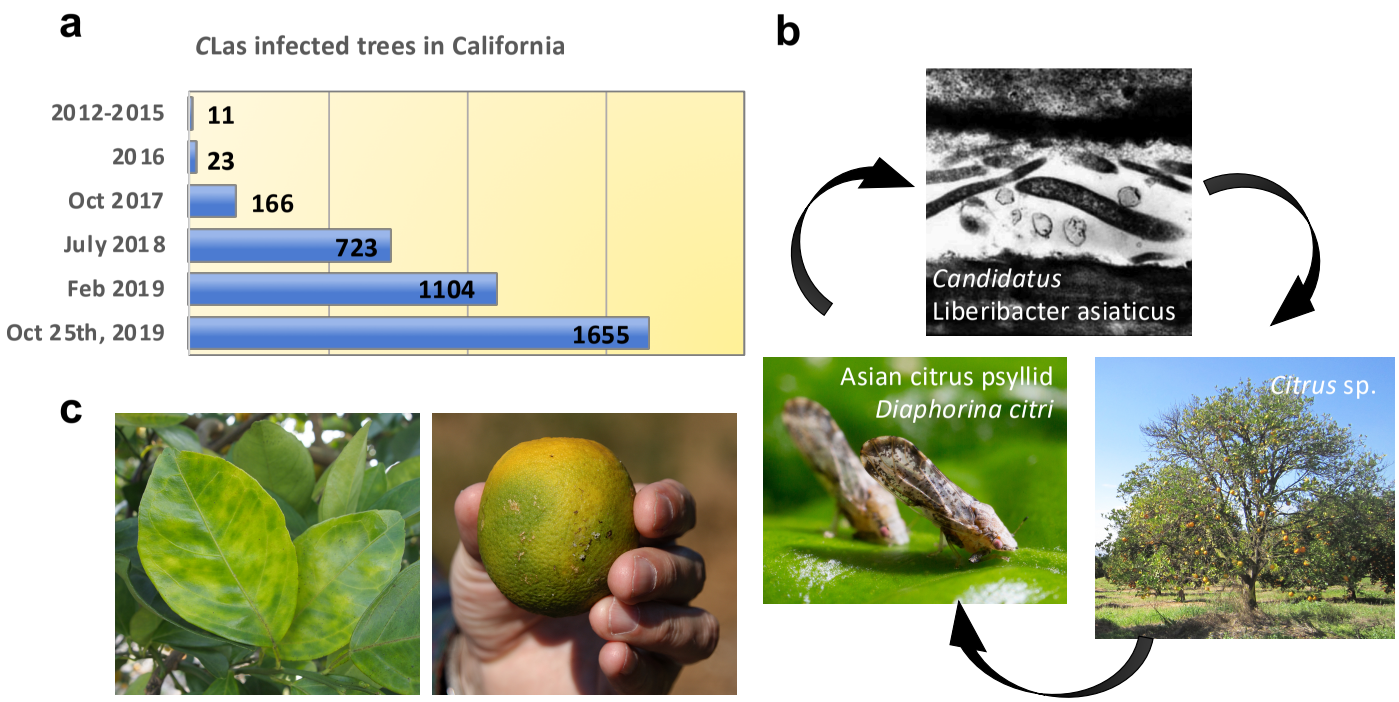
a
CLas infected trees in California
2012-2015
11
2016
23
Oct 2017
166
July 2018
723
Feb 2019
1104
Oct 25th, 2019
1655
b
Candidatus
Liberibacter asiaticus
Asian citrus psyllid
Diaphorina citri
Citrus sp.
c

Figure I – Huanglongbing (HLB) prevalence in California, disease cycle, and symptoms. a) Number of trees in California detected positive for *Candidatus* Liberibacter asiaticus (*C*Las) infection from 2012 to present (October 2019). Information from CDFA (citrusinsider.org). **b)** Disease cycle for *C*Las, which occurs in a feedback loop from transmission by the Asian citrus psyllid (ACP), *Diaphorina citri* Kuwayama, to *C*Las colonization of host tissues consisting of all *Citrus* spp. and many citrus relatives. Images from Bove *et. al.* (2006) *J. of Plant Pathology*, Mike Lewis and Georgios Vidalakis, UC Riverside. **c)** Typical HLB disease symptoms, left, blotchy mottle on leaves, and right, greening of citrus fruit from the stylar end. Images from Citrus Pest and Disease Prevention Program.

a

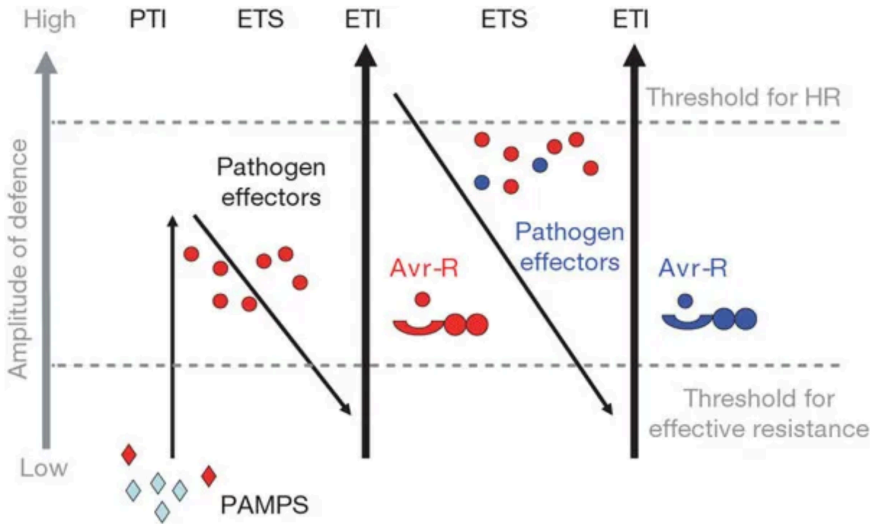
High
PTI
ETS
ETI
ETS
ETI
Amplitude of defence
Threshold for HR
Pathogen effectors
Avr-R
Pathogen effectors
Avr-R
Threshold for effective resistance
Low
PAMPS

b

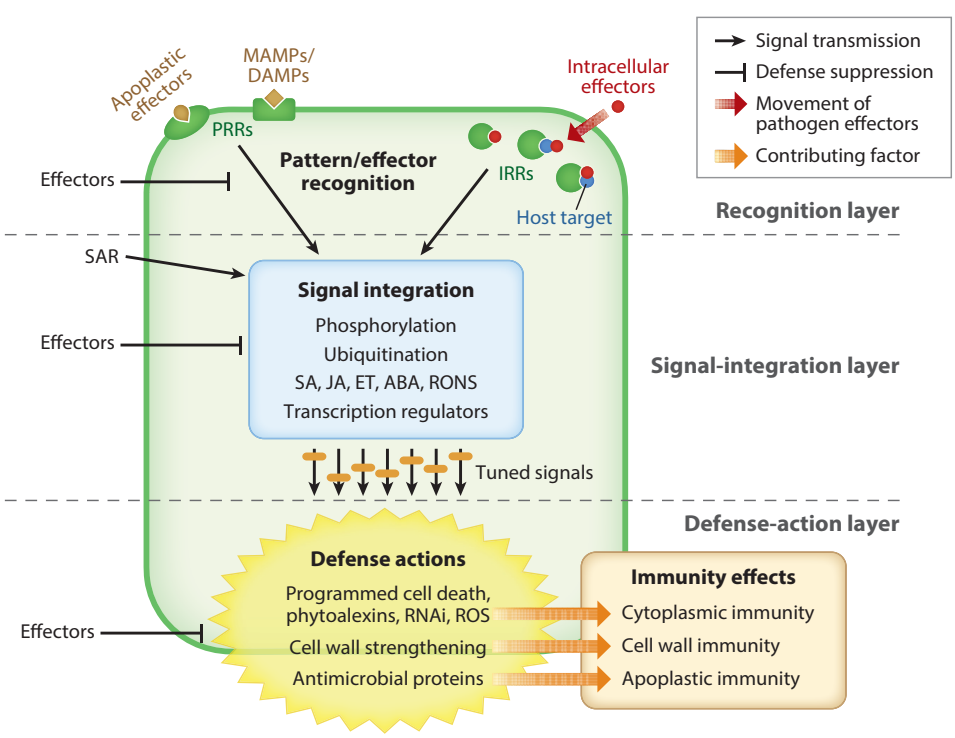
Signal transmission
Defense suppression
Movement of pathogen effectors
Contributing factor
Apoplastic effectors
MAMPs/ DAMPs
Intracellular effectors
PRRs
Pattern/effector recognition
IRRs
Host target
Effectors
Recognition layer
SAR
Signal integration
Phosphorylation
Ubiquitination
SA, JA, ET, ABA, RONS
Transcription regulators
Effectors
Signal-integration layer
Tuned signals
Defense-action layer
Defense actions
Programmed cell death, phytoalexins, RNAi, ROS
Cell wall strengthening
Antimicrobial proteins
Effectors
Immunity effects
Cytoplasmic immunity
Cell wall immunity
Apoplastic immunity

Figure II – Diagrams of the classical and recently proposed models for plant defense and pathogen counterdefense strategies. a) Zigzag model of the plant immune system, pathogen-associated molecular patterns (PAMPs) are recognized by host pattern recognition receptors (PRRs) allowing PAMP-triggered immunity (PTI). Successful pathogens release effectors (Avr) to dampen PTI, resulting in effector-triggered susceptibility (ETS). However, if effectors are recognized by host resistance proteins (R), effector-trigged immunity (ETI), a more robust form of PTI is initiated, which can include the hypersensitive response (HR). Model from Jones and Dangl 2006 *Nature*. **b)** Layered immunity model, pathogen components including PAMPs and effectors are recognized by the host extra- or intercellularly. Recognition initiates a signaling cascade consisting of post-translational modifications, hormones, and gene regulation, effectors can also work to subdue these responses. Defense actions downstream of signal integration may include, programmed cell death, reactive oxygen species (ROS), cell structural modifications, small interfering RNAs or antimicrobial proteins. Model from Wang, Tyler and Wang 2019 *Annual Review Microbiology*.

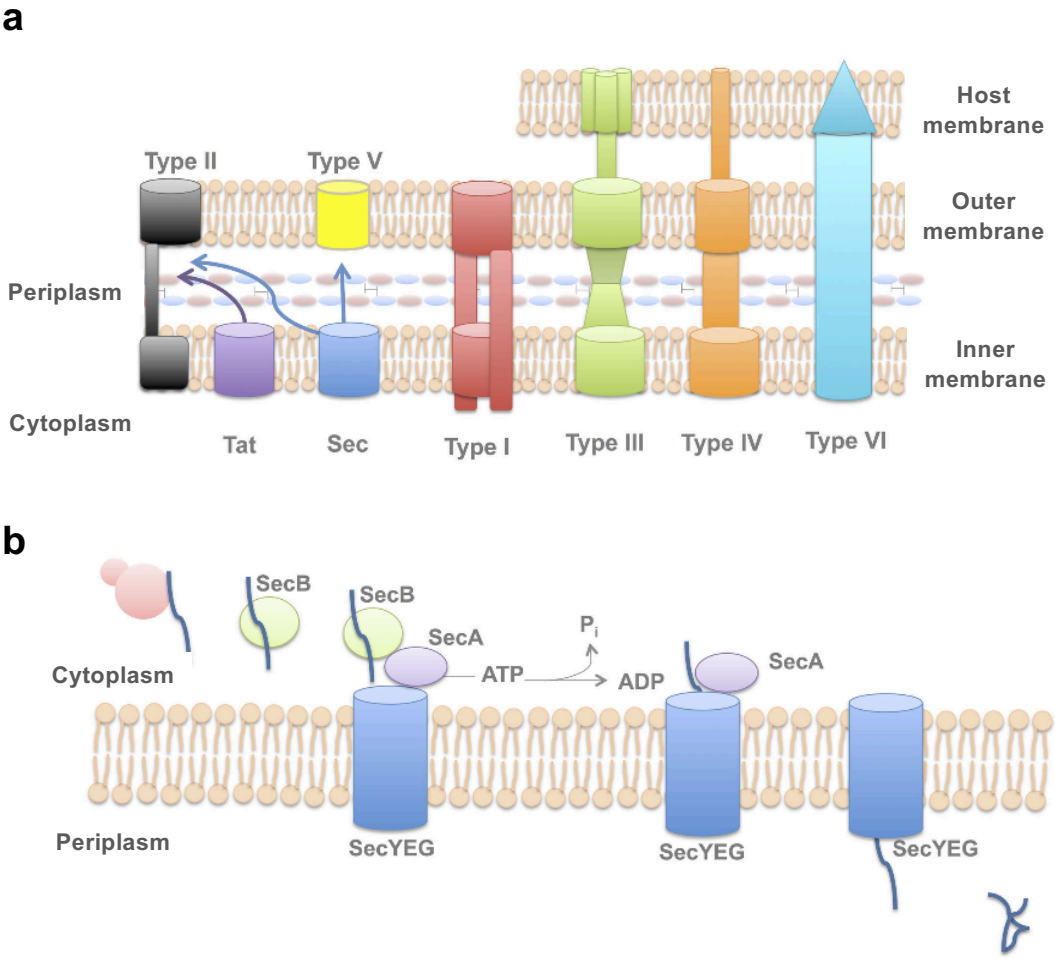

Figure III – Gram-negative bacterial secretion systems and the Sec secretion pathway. a) Multiple secretion pathways are utilized by gram-negative bacteria to transport proteins across the inner cell membrane, outer cell membrane, or through host cell membranes (and cell ways for plant hosts). Sec- and Tat-dependent secretion systems require two steps for protein to exit the outer membrane, for example type II and type V can be utilized as the second step. **b)** The Sec pathway destines unfolded proteins to the periplasm and/or for extracellular release. N-terminal, Sec signal sequences are recognized by SecB, which guides proteins to SecA (an ATPase) aiding in transport through the SecYEG channel. From there Sec secretion signals are cleaved, proteins are folded in the periplasmic space, and potentially secreted outside of the cell through an outer membrane channel or outer membrane vesicles. Figures modified from Green and Mecsas *et al.* 2016 *Microbiol Spectr.*

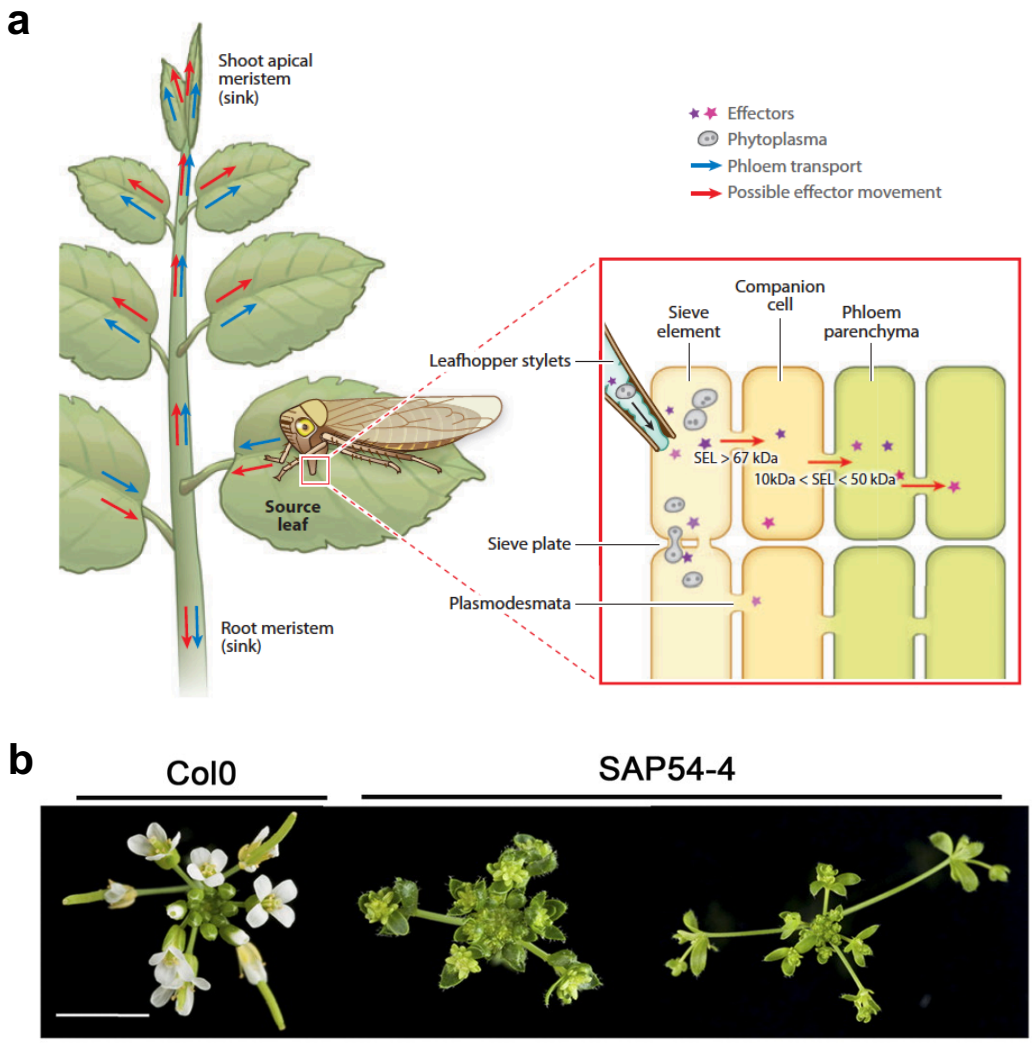

Figure IV – Phytoplasma Sec-delivered effectors (SDEs) as a model. a) SDE secretion from phytoplasma cells and systemic movement via phloem sieve plates and plasmodesmata proposes a potential model for effectors of other phloem-limited, bacterial pathogens such as *Candidatus* Liberibacters spp. Figure from Sugio *et. al.* 2011 *Annual Reviews of Phytopathology*. **b)** The phytoplasma SDE, SAP54 from Aster Yellows phytoplasma strain Witches' Broom (AY-WB; *Candidatuis* Phytoplasma asteris) induces leaf-like development of floral organs, a characteristic symptom of AY-WB infection, when expressed in *Arabidopsis thaliana* ecotype Columbia (Col0). Image modified from MacLean et. al. 2011 *Plant Physiology*.

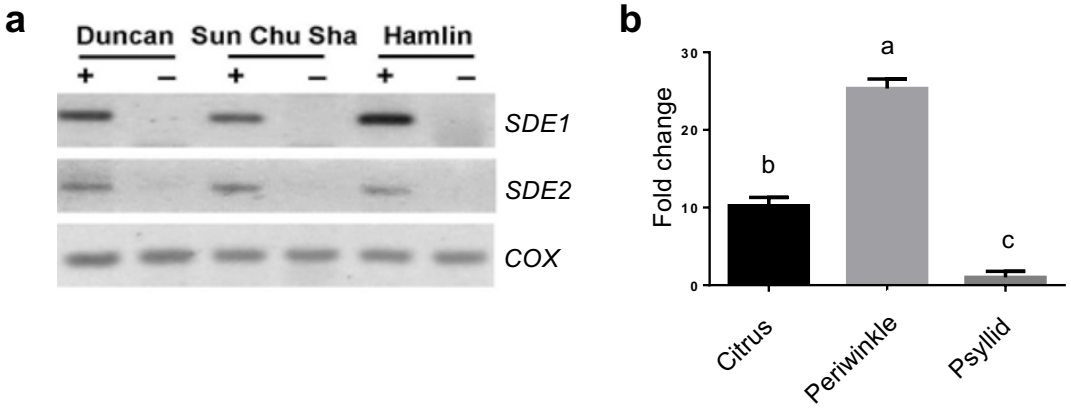

Figure V - SDE1 and SDE2 are expressed in *Candidatus* Liberibacter asiaticus (*C*Las)-infected citrus. a) Semi-quantitative, reverse transcription-PCR (RT-PCR) of *C*Las-positive (+) and non-infected tissues (-) of different citrus varieties including *Citrus paradisi* (L.) Mac. (Duncan grapfruit), *C. reticulata* Blanco (Sun Chu Sha mandarin), and *C. sinensis* (L.) Osb. (Hamlin sweet orange) using primers specific to SDE1 or SDE2. **b)** Quantitative RT-PCR (qRT-PCR) of *C*Las-infected citrus, periwinkle, and psyllids for SDE1. SDE2 expression in citrus relative to psyllids can be found in Yan *et. al.* 2013 *Mol. Plant Pathology*.

REFERENCES

1. Bové, J. M. Huanglongbing: A Destructive, Newly-Emerging, Century-Old Disease of Citrus. *Journal of Plant Pathology* **88**, 7–37 (2006).

2. da Graça, J. V. *et al.* Huanglongbing: An overview of a complex pathosystem ravaging the world's citrus: Citrus Huanglongbing. *J. Integr. Plant Biol.* **58**, 373–387 (2016).

3. Gottwald, T. R. Current Epidemiological Understanding of Citrus Huanglongbing. *Annual Review of Phytopathology* **48**, 119–139 (2010).

4. Wang, N. & Trivedi, P. Citrus huanglongbing: a newly relevant disease presents unprecedented challenges. *Phytopathology* **103**, 652–665 (2013).

5. Lin, K. Observations on yellow shoot on citrus. Etiological studies of yellow shoot of citrus. *Acta Phytopathol.* **2**, 237–242 (1956).

6. Husain, M. & Nath, D. The citrus psylla (Diaphorina citriKuw.) [Psyllidae:Homoptera]. *Mem. Dept. Agric. India, Entomol.* **10**, 1–27 (1927).

7. da Graça, J. V. *et al.* Huanglongbing in Texas: Report on the first detections in commercial citrus. *Journal of Citrus Pathology* **2**, (2015).

8. Halbert, S. E., Manjunath, K., Ramadugu, C. & Lee, R. F. Incidence of Huanglongbing-Associated 'Candidatus Liberibacter Asiaticus' in Diaphorina citri (Hemiptera: Psyllidae) Collected from Plants for Sale in Florida. *Florida Ento.* **95**, 617–624 (2012).

9. Kumagai, L. B. *et al.* First Report of Candidatus Liberibacter asiaticus Associated with Citrus Huanglongbing in California. *Plant Disease* **97**, 283–283 (2012).

10. Teixeira, D. do C. *et al.* 'Candidatus Liberibacter americanus', associated with citrus huanglongbing (greening disease) in São Paulo State, Brazil. *Int. J. Syst. Evol. Microbiol.* **55**, 1857–1862 (2005).

11. Coletta-Filho, H. D. *et al.* First Report of the Causal Agent of Huanglongbing ("Candidatus Liberibacter asiaticus") in Brazil. *Plant Disease* **88**, 1382–1382 (2004).

12. Gasparoto, M. C. G. *et al.* Influence of temperature on infection and establishment of 'Candidatus Liberibacter americanus' and 'Candidatus Liberibacter asiaticus' in citrus plants. *Plant Pathology* **61**, 658–664 (2012).

13. Roberts, R. *et al.* Resolution of the Identity of 'Candidatus Liberibacter' Species From Huanglongbing-Affected Citrus in East Africa. *Plant Disease* **101**, 1481–1488 (2017).

14. Pietersen, G. *et al.* A Survey for 'Candidatus Liberibacter' Species in South Africa Confirms the Presence of Only 'Ca. L. africanus' in Commercial Citrus. *Plant Disease* **94**, 244–249 (2010).

15. Lopes, S. A. *et al.* Liberibacters Associated with Citrus Huanglongbing in Brazil: 'Candidatus Liberibacter asiaticus' Is Heat Tolerant, 'Ca. L. americanus' Is Heat Sensitive. *Plant Disease* **93**, 257–262 (2009).

16. Adami, A. C. O., Miranda, S. H. G. & Bassanezi, R. B. Benefit-cost analysis of Huanglongbing management in Sao Paulo, Brazil. *Journal of Citrus Pathology* **1**, (2014).

17. Dala-Paula, B. M. *et al.* Effect of Huanglongbing or Greening Disease on Orange Juice Quality, a Review. *Front. Plant Sci.* **9**, 1976 (2019).

18. Singerman, A., Lence, S. H. & Useche, P. Is Area-Wide Pest Management Useful? The Case of Citrus Greening. *Applied Economic Perspectives and Policy* **39**, 609–634 (2017).

19. U.S. Department of Agriculture. National Agricultural Statistics Service, Florida Citrus Statistics 2014–2015. (2016).

20. Hodges, A. W. & Spreen, T. H. Economic Impacts of Citrus Greening (HLB) in Florida,. *Food and Resource Economics Department, University of Florida* (2012).

21. Singerman, A. & Useche, P. Impact of Citrus Greening on Citrus Operations in Florida. University of Florida, Institute of Food and Agricultural Sciences (IFAS). *Electronic Data Information Source (EDIS)* **FE983**, (2016).

22. Wang, N. *et al.* The Candidatus Liberibacter–Host Interface: Insights into Pathogenesis Mechanisms and Disease Control. *Annual Review of Phytopathology* **55**, 451–482 (2017).

23. Folimonova, S. Y., Robertson, C. J., Garnsey, S. M., Gowda, S. & Dawson, W. O. Examination of the Responses of Different Genotypes of Citrus to Huanglongbing (Citrus Greening) Under Different Conditions. *Phytopathology* **99**, 1346–1354 (2009).

24. JAGOUEIX, S., BOVE, J.-M. & GARNIER, M. The Phloem-Limited Bacterium of Greening Disease of Citrus Is a Member of the α Subdivision of the Proteobacteria. *International Journal of Systematic and Evolutionary Microbiology,* **44**, 379–386 (1994).

25. Sagaram, U. S. *et al.* Bacterial Diversity Analysis of Huanglongbing Pathogen-Infected Citrus, Using PhyloChip Arrays and 16S rRNA Gene Clone Library Sequencing. *Applied and Environmental Microbiology* **75**, 1566–1574 (2009).

26. Tyler, H. L., Roesch, L. F. W., Gowda, S., Dawson, W. O. & Triplett, E. W. Confirmation of the Sequence of ' *Candidatus* Liberibacter asiaticus' and

Assessment of Microbial Diversity in Huanglongbing-Infected Citrus Phloem Using a Metagenomic Approach. *MPMI* **22**, 1624–1634 (2009).

27. Fagen, J. R. *et al.* Liberibacter crescens gen. nov., sp. nov., the first cultured member of the genus Liberibacter. *International Journal of Systematic and Evolutionary Microbiology,* **64**, 2461–2466 (2014).

28. Halbert, S. E. & Manjunath, K. L. Asian citrus psyllids (Sternorrhyncha: Psyllidae) and greening disease of citrus: a literature review and assessment of risk in Florida. *Florida Entomologist* **87**, 330–353 (2004).

29. Hall, D. G., Richardson, M. L., Ammar, E.-D. & Halbert, S. E. Asian citrus psyllid, Diaphorina citri, vector of citrus huanglongbing disease. *Entomologia Experimentalis et Applicata* **146**, 207–223 (2013).

30. Inoue, H. *et al.* Enhanced proliferation and efficient transmission of Candidatus Liberibacter asiaticus by adult Diaphorina citri after acquisition feeding in the nymphal stage. *Annals of Applied Biology* **155**, 29–36 (2009).

31. Ammar, E.-D., Shatters, R. G. & Hall, D. G. Localization of Candidatus Liberibacter asiaticus, Associated with Citrus Huanglongbing Disease, in its Psyllid Vector using Fluorescence in situ Hybridization. *Journal of Phytopathology* **159**, 726–734 (2011).

32. Grafton-Cardwell, E. E., Stelinski, L. L. & Stansly, P. A. Biology and Management of Asian Citrus Psyllid, Vector of the Huanglongbing Pathogens. *Annu. Rev. Entomol.* **58**, 413–432 (2013).

33. Boina, D. R., Meyer, W. L., Onagbola, E. O. & Stelinski, L. L. Quantifying dispersal of Diaphorina citri (Hemiptera: Psyllidae) by immunomarking and potential impact of unmanaged groves on commercial citrus management. *Environ. Entomol.* **38**, 1250–1258 (2009).

34. Lewis-Rosenblum, H., Martini, X., Tiwari, S. & Stelinski, L. L. Seasonal Movement Patterns and Long-Range Dispersal of Asian Citrus Psyllid in Florida Citrus. *J. Econ. Entomol.* **108**, 3–10 (2015).

35. Halbert, S. E. *et al.* Trailers Transporting Oranges to Processing Plants Move Asian Citrus Psyllids. *Florida Ento.* **93**, 33–38 (2010).

36. Lopes, S. A. *et al.* Graft Transmission Efficiencies and Multiplication of 'Candidatus Liberibacter americanus' and 'Ca. Liberibacter asiaticus' in Citrus Plants. *Phytopathology* **99**, 301–306 (2009).

37. Lee, R. F. & Bar-Joseph, M. Graft-transmissible diseases of citrus. in *Virus and Virus-like Diseases of Major Crops in Developing Countries* (eds. Loebenstein, G. & Thottappilly, G.) 607–639 (Springer Netherlands, 2003). doi:10.1007/978-94-007-0791-7_24.

38. Coletta-Filho, H. D., Daugherty, M. P., Ferreira, C. & Lopes, J. R. S. Temporal Progression of ' *Candidatus* Liberibacter asiaticus' Infection in Citrus and Acquisition Efficiency by *Diaphorina citri*. *Phytopathology* **104**, 416–421 (2014).

39. Lee, J. A. *et al.* Asymptomatic spread of huanglongbing and implications for disease control. *PNAS* **112**, 7605–7610 (2015).

40. Ed Stover *et al.* Resistance and tolerance to Huanglongbing in citrus. *Acta Hortic.* **1065**, 899–903 (2015).

41. Ramadugu, C. *et al.* Long-Term Field Evaluation Reveals Huanglongbing Resistance in Citrus Relatives. *Plant Disease* **100**, 1858–1869 (2016).

42. Dala-Paula, B. M. *et al.* Active taste compounds in juice from oranges symptomatic for Huanglongbing (HLB) citrus greening disease. *LWT* **91**, 518–525 (2018).

43. Munir, S. *et al.* Huanglongbing Control: Perhaps the End of the Beginning. *Microb Ecol* **76**, 192–204 (2018).

44. Blaustein, R. A., Lorca, G. L. & Teplitski, M. Challenges for Managing Candidatus Liberibacter spp. (Huanglongbing Disease Pathogen): Current Control Measures and Future Directions. *Phytopathology* **108**, 424–435 (2017).

45. Bové, J. M. Huanglongbing or yellow shoot, a disease of Gondwanan origin: Will it destroy citrus worldwide? *Phytoparasitica* **42**, 579–583 (2014).

46. Hall, D. G., Gottwald, T. R., Stover, E. & Beattie, G. A. C. Evaluation of Management Programs for Protecting Young Citrus Plantings from Huanglongbing. *HortScience* **48**, 330–337 (2013).

47. Belasque Jr., J., Bassanezi, R. B., Ayres, A. J., Tachibana, A. & Bove, J. M. Lessons from Huanglongbing management in Sao Paulo State, Brazil. *Journal of Plant Pathology* **92**, 285–302 (2012).

48. Canales, E. *et al.* 'Candidatus Liberibacter asiaticus', Causal Agent of Citrus Huanglongbing, Is Reduced by Treatment with Brassinosteroids. *PLOS ONE* **11**, e0146223 (2016).

49. Hoffman, M. T. *et al.* Heat treatment eliminates 'Candidatus Liberibacter asiaticus' from infected citrus trees under controlled conditions. *Phytopathology* **103**, 15–22 (2013).

50. Hu, J., Jiang, J. & Wang, N. Control of Citrus Huanglongbing via Trunk Injection of Plant Defense Activators and Antibiotics. *Phytopathology* **108**, 186–195 (2018).

51. Gottwald, T. R., Graham, J. H., Irey, M. S., McCollum, T. G. & Wood, B. W. Inconsequential effect of nutritional treatments on huanglongbing control, fruit quality, bacterial titer and disease progress. *Crop Protection* **36**, 73–82 (2012).

52. Milosavljević, I., Schall, K., Hoddle, C., Morgan, D. & Hoddle, M. Biocontrol program targets Asian citrus psyllid in California's urban areas. *California Agriculture* **71**, 169–177 (2017).

53. Hoddle, M. S. & Pandey, R. Host Range Testing of Tamarixia radiata (Hymenoptera: Eulophidae) Sourced from the Punjab of Pakistan for Classical Biological Control of Diaphorina citri (Hemiptera: Liviidae: Euphyllurinae: Diaphorinini) in California. *J Econ Entomol* **107**, 125–136 (2014).

54. Li, W., Hartung, J. S. & Levy, L. Quantitative real-time PCR for detection and identification of Candidatus Liberibacter species associated with citrus huanglongbing. *J. Microbiol. Methods* **66**, 104–115 (2006).

55. Li, W., Li, D., Twieg, E., Hartung, J. S. & Levy, L. Optimized Quantification of Unculturable Candidatus Liberibacter Spp. in Host Plants Using Real-Time PCR. *Plant Disease* **92**, 854–861 (2008).

56. Tatineni, S. *et al.* In Planta Distribution of ' *Candidatus* Liberibacter asiaticus' as Revealed by Polymerase Chain Reaction (PCR) and Real-Time PCR. *Phytopathology* **98**, 592–599 (2008).

57. Ding, F., Duan, Y., Paul, C., Brlansky, R. H. & Hartung, J. S. Localization and Distribution of 'Candidatus Liberibacter asiaticus' in Citrus and Periwinkle by Direct Tissue Blot Immuno Assay with an Anti-OmpA Polyclonal Antibody. *PLoS One* **10**, (2015).

58. Dutt, M., Barthe, G., Irey, M. & Grosser, J. Transgenic Citrus Expressing an Arabidopsis NPR1 Gene Exhibit Enhanced Resistance against Huanglongbing (HLB; Citrus Greening). *PLOS ONE* **10**, e0137134 (2015).

59. Huot, B., Yao, J., Montgomery, B. L. & He, S. Y. Growth–Defense Tradeoffs in Plants: A Balancing Act to Optimize Fitness. *Molecular Plant* **7**, 1267–1287 (2014).

60. Zhang, S. *et al.* Regulation of citrus DMR6 via RNA interference and CRISPR/Cas9-mediated gene editing to improve Huanglongbing tolerance. in (APSNET, 2018).

61. Gmitter, F. G., Chen, C., Nageswara Rao, M. & Soneji, J. R. Citrus Fruits. in *Fruits and Nuts* (ed. Kole, C.) 265–279 (Springer Berlin Heidelberg, 2007). doi:10.1007/978-3-540-34533-6_14.

62. Deng, H. *et al.* Phloem Regeneration Is a Mechanism for Huanglongbing-Tolerance of "Bearss" Lemon and "LB8-9" Sugar Belle® Mandarin. *Front. Plant Sci.* **10**, 277 (2019).

63. Ledford, H. Geneticists enlist engineered virus and CRISPR to battle citrus disease. *Nature* **545**, 277–278 (2017).

64. Toruño, T. Y., Stergiopoulos, I. & Coaker, G. Plant-Pathogen Effectors: Cellular Probes Interfering with Plant Defenses in Spatial and Temporal Manners. *Annu Rev Phytopathol* **54**, 419–441 (2016).

65. Zipfel, C. Pattern-recognition receptors in plant innate immunity. *Curr. Opin. Immunol.* **20**, 10–16 (2008).

66. Boller, T. & Felix, G. A renaissance of elicitors: perception of microbe-associated molecular patterns and danger signals by pattern-recognition receptors. *Annu Rev Plant Biol* **60**, 379–406 (2009).

67. Ma, W. & Guttman, D. S. Evolution of prokaryotic and eukaryotic virulence effectors. *Curr. Opin. Plant Biol.* **11**, 412–419 (2008).

68. Baggs, E., Dagdas, G. & Krasileva, K. V. NLR diversity, helpers and integrated domains: making sense of the NLR IDentity. *Curr. Opin. Plant Biol.* **38**, 59–67 (2017).

69. Jones, J. D. G. & Dangl, J. L. The plant immune system. *Nature* **444**, 323–329 (2006).

70. Torto-Alalibo, T. *et al.* Common and contrasting themes in host cell-targeted effectors from bacterial, fungal, oomycete and nematode plant symbionts described using the Gene Ontology. *BMC Microbiology* **9**, S3 (2009).

71. Dou, D. & Zhou, J.-M. Phytopathogen effectors subverting host immunity: different foes, similar battleground. *Cell Host Microbe* **12**, 484–495 (2012).

72. Durrant, W. E. & Dong, X. Systemic acquired resistance. *Annu Rev Phytopathol* **42**, 185–209 (2004).

73. Wang, Y., Tyler, B. M. & Wang, Y. Defense and Counterdefense During Plant-Pathogenic Oomycete Infection. *Annual Review of Microbiology* **73**, 667–696 (2019).

74. Thomma, B. P. H. J., Nürnberger, T. & Joosten, M. H. A. J. Of PAMPs and Effectors: The Blurred PTI-ETI Dichotomy. *The Plant Cell* **23**, 4–15 (2011).

75. Pritchard, L. & Birch, P. R. The zigzag model of plant-microbe interactions: is it time to move on? *Mol Plant Pathol* **15**, 865–870 (2014).

76. Zou, H. *et al.* The Destructive Citrus Pathogen, ‘Candidatus Liberibacter asiaticus’ Encodes a Functional Flagellin Characteristic of a Pathogen-Associated Molecular Pattern. *PLOS ONE* **7**, e46447 (2012).

77. Duan, Y. *et al.* Complete genome sequence of citrus huanglongbing bacterium, ‘Candidatus Liberibacter asiaticus’ obtained through metagenomics. *Mol. Plant Microbe Interact.* **22**, 1011–1020 (2009).

78. Shi, Q. *et al.* Identification of Gene Candidates Associated with Huanglongbing Tolerance, Using 'Candidatus Liberibacter asiaticus' Flagellin 22 as a Proxy to Challenge Citrus. *MPMI* **31**, 200–211 (2017).

79. Bendix, C. & Lewis, J. D. The enemy within: phloem-limited pathogens. *Mol. Plant Pathol.* **19**, 238–254 (2018).

80. Aritua, V., Achor, D., Gmitter, F. G., Albrigo, G. & Wang, N. Transcriptional and Microscopic Analyses of Citrus Stem and Root Responses to Candidatus Liberibacter asiaticus Infection. *PLoS ONE* **8**, e73742 (2013).

81. Kim, J.-S., Sagaram, U. S., Burns, J. K., Li, J.-L. & Wang, N. Response of Sweet Orange (*Citrus sinensis*) to ' *Candidatus* Liberibacter asiaticus' Infection: Microscopy and Microarray Analyses. *Phytopathology* **99**, 50–57 (2009).

82. Folimonova, S. Y. & Achor, D. S. Early Events of Citrus Greening (Huanglongbing) Disease Development at the Ultrastructural Level. *Phytopathology* **100**, 949–958 (2010).

83. Etxeberria, E., Gonzalez, P., Achor, D. & Albrigo, G. Anatomical distribution of abnormally high levels of starch in HLB-affected Valencia orange trees. *Physiological and Molecular Plant Pathology* **74**, 76–83 (2009).

84. Jain, M., Fleites, L. A. & Gabriel, D. W. Prophage-Encoded Peroxidase in 'Candidatus Liberibacter asiaticus' Is a Secreted Effector That Suppresses Plant Defenses. *MPMI* **28**, 1330–1337 (2015).

85. Albrecht, U. & Bowman, K. D. Gene expression in Citrus sinensis (L.) Osbeck following infection with the bacterial pathogen Candidatus Liberibacter asiaticus causing Huanglongbing in Florida. *Plant Science* **175**, 291–306 (2008).

86. Nwugo, C. C., Duan, Y. & Lin, H. Study on Citrus Response to Huanglongbing Highlights a Down-Regulation of Defense-Related Proteins in Lemon Plants Upon 'Ca. Liberibacter asiaticus' Infection. *PLoS ONE* **8**, e67442 (2013).

87. Costa, T. R. D. *et al.* Secretion systems in Gram-negative bacteria: structural and mechanistic insights. *Nat. Rev. Microbiol.* **13**, 343–359 (2015).

88. Troisfontaines, P. & Cornelis, G. R. Type III secretion: more systems than you think. *Physiology (Bethesda)* **20**, 326–339 (2005).

89. Cunnac, S. *et al.* Genetic disassembly and combinatorial reassembly identify a minimal functional repertoire of type III effectors in Pseudomonas syringae. *Proc Natl Acad Sci U S A* **108**, 2975–2980 (2011).

90. Feng, F. & Zhou, J.-M. Plant-bacterial pathogen interactions mediated by type III effectors. *Curr. Opin. Plant Biol.* **15**, 469–476 (2012).

91. Cong, Q., Kinch, L. N., Kim, B.-H. & Grishin, N. V. Predictive Sequence Analysis of the Candidatus Liberibacter asiaticus Proteome. *PLOS ONE* **7**, e41071 (2012).

92. Yan, Q. *et al.* Global gene expression changes in Candidatus Liberibacter asiaticus during the transmission in distinct hosts between plant and insect. *Molecular Plant Pathology* **14**, 391–404 (2013).

93. Green, E. R. & Mecsas, J. Bacterial Secretion Systems – An overview. *Microbiol Spectr* **4**, (2016).

94. Natale, P., Brüser, T. & Driessen, A. J. M. Sec- and Tat-mediated protein secretion across the bacterial cytoplasmic membrane--distinct translocases and mechanisms. *Biochim. Biophys. Acta* **1778**, 1735–1756 (2008).

95. Sugio, A. *et al.* Diverse Targets of Phytoplasma Effectors: From Plant Development to Defense Against Insects. *Annual Review of Phytopathology* **49**, 175–195 (2011a).

96. Sugio, A., Kingdom, H. N., MacLean, A. M., Grieve, V. M. & Hogenhout, S. A. Phytoplasma protein effector SAP11 enhances insect vector reproduction by manipulating plant development and defense hormone biosynthesis. *Proceedings of the National Academy of Sciences* **108**, E1254–E1263 (2011b).

97. Hoshi, A. *et al.* A unique virulence factor for proliferation and dwarfism in plants identified from a phytopathogenic bacterium. *Proceedings of the National Academy of Sciences* **106**, 6416–6421 (2009).

98. MacLean, A. M. *et al.* Phytoplasma Effector SAP54 Induces Indeterminate Leaf-Like Flower Development in Arabidopsis Plants. *Plant Physiol.* **157**, 831–841 (2011).

99. Prasad, S., Xu, J., Zhang, Y. & Wang, N. SEC-Translocon Dependent Extracytoplasmic Proteins of Candidatus Liberibacter asiaticus. *Front. Microbiol.* **7**, (2016).

100. Pagliaccia, D. *et al.* A Pathogen Secreted Protein as a Detection Marker for Citrus Huanglongbing. *Front. Microbiol.* **8**, 2041 (2017).

101. Imlau, A., Truernit, E. & Sauer, N. Cell-to-Cell and Long-Distance Trafficking of the Green Fluorescent Protein in the Phloem and Symplastic Unloading of the Protein into Sink Tissues. *The Plant Cell* **11**, 309–322 (1999).

Chapter I

Development of antibody-based detection for the Huanglongbing-associated bacterium using *Candidatus* Liberibacter asiaticus Sec-delivered effectors

ABSTRACT

Since a cure is not available for Huanglongbing (HLB), a key step in disease management is to restrict the spread of the associated pathogen by identifying and removing infected trees. However, uneven distribution of *Candidatus* Liberibacter asiaticus (*C*Las) cells and long latency periods for symptom development create challenges for detection. Therefore, we implemented the use of *C*Las Sec-delivered effector (SDE) proteins as biomarkers to develop serological-based detection strategies. SDEs are secreted out of *C*Las cells into the citrus phloem and are smaller in size than bacterial cells themselves, thus can presumably distribute throughout host tissues. Additionally, serological-based detection assays have many benefits including, low cost, simplicity, and throughput. In this chapter, I discuss my role in a collaborative effort to develop different antibody-based detection platforms for *C*Las using SDEs as biomarkers.

Polyclonal antisera were generated against the biomarkers SDE1 and SDE2, which are unique to *C*Las and exhibit high expression *in planta*. I found the antisera to have high binding affinity to the respective antigens *in vitro* and *in planta*. I purified the antibodies from the antisera mixtures for their application to different detection platforms including direct tissue imprints, enzyme-linked immunosorbent assays (ELISAs), and field-deployable nanosensors. In addition, I further optimized the anti-SDE1 antibodies by affinity purification against tag-free-SDE1 protein, as opposed to the HIS-tagged

SDE1, to better simulate the native protein form that would be found in *C*Las-infected citrus. Results concluded that both SDE1 and SDE2 have potential as biomarkers for detection of the presence of *C*Las in a tree. Further development of such novel detection technologies will greatly aid in HLB disease management.

INTRODUCTION

Current CLas detection and HLB diagnosis status

As HLB is prevalent globally [1–6], and has spread across the US in the past decade [7–9], disease detection is critical. In particular, rapid and accurate, early detection of *C*Las-infected trees is needed to maintain exclusion of the disease and reduce inoculum pressure in infected areas [10,11]. This is extremely important in California, where infection is still localized to a few counties. However, detection of *C*Las-infected trees and subsequent HLB diagnosis has proven challenging for many researchers in the field. The symptoms of HLB are easily confused with those caused by other diseases or nutrient deficiencies [12–14]. In addition, symptom development has a variable latency, ranging from months to years [10,13]. Therefore, symptoms-based diagnoses are unreliable and often too late to have an effect on HLB management.

The current "gold-standard" for *C*Las detection is the use of quantitative polymerase chain reaction (qPCR)-based assays targeting *C*Las DNA [15,16], yet these assays require the presence of the bacterial cells in the citrus tissue sampled for a positive diagnosis. This is an issue because *C*Las cells are typically unevenly distributed throughout citrus tissues; thus, the outcome of PCR-based detection is greatly affected by sampling [17–19]. Due to this obstacle, researchers are exploring detection methods based on the host's response to *C*Las, including assays based on citrus volatile organic

compounds, metabolites, starch accumulation, and microbial communities [20–24]. However, such methods fail to detect the associated-pathogen or pathogen molecules directly, which could lead to false diagnoses if other pathogens or environmental conditions cause the same or similar responses in the host.

Advantages of serological-based detection for CLas

Serological assays detecting protein biomarkers are widely used in disease diagnosis for plant and animal diseases, and for the identification of food-borne pathogens [25–28]. Compared to PCR-based methods, antibody-based detection assays are in general faster and more cost-efficient since they do not typically require expensive lab equipment or detailed nucleic acid extraction procedures [29,30]. For instance, PCR-based detection methods require DNA/RNA extraction from citrus tissue followed by use of a thermocycler [15,31]. Thus, processing thousands of samples, with the current qPCR method remains challenging [30]. However, it should be noted that modified PCR-based methods are being explored in citrus and in psyllids, aiming to make the assay more applicable for in-field usage [32,33] and more specific [34]. Detection using antibodies developed against a *C*Las outer membrane protein (OmpA) has been explored via direct tissue blot immunoassay [19,35]. Yet, biomarkers developed against *C*Las cell surface components would encounter the same issues with uneven cell distribution as do PCR-based techniques. Antibody-based detection via direct tissue blot immunoassay has been developed for other phloem-limited citrus pathogens including, citrus tristeza virus (CTV) [36], and *Spiroplasma citri* [37]. These methods illustrate that antibodies generated against robust pathogen biomarkers can be employed towards various serological platforms with different advantages.

Sec-delivered effectors (SDEs) as CLas detection biomarkers

*C*Las encodes all the components necessary for the general Sec secretion pathway which secretes proteins carrying a specific N-terminal secretion signal [38,39]. Sec-delivered effectors (SDEs) are secreted into the periplasmic space, and thereafter potentially out of bacterial cells into their extracellular environment [40–42]. Thus, in the case of *C*Las-infection, these proteins would be directly secreted into the citrus phloem (sieve elements). After secretion from *C*Las cells, SDEs could be disseminated with the transportation flow in the phloem and therefore have increased distribution in infected trees. Such movement has been previously characterized for SDEs of Phytoplasmas, which are also phloem-limited, insect-transmitted, bacterial pathogens [43–47]. It is hypothesized that SDEs may travel to neighboring cells via plasmodesmata since the size exclusion limits of plasmodesmata in most cells vary from 10 kDa to 50 kDa [48], and the sizes of both Phytoplasma and *C*Las SDEs fall within or even below this range. Effectors are vital for the virulence of pathogens. Many cause host modifications allowing pathogen colonization; thus, their expression can be exhibited at early infection stages [49,50]. Altogether, the use of SDEs as biomarkers for *C*Las detection provides a novel strategy which detects pathogen components, rather than cells and/or host responses, potentially during the early infection stages.

CLas SDE biomarker discovery

Previous research in our lab mined the *C*Las psy62 genome (GenBank No. CP001677.5) for proteins with an N-terminal signal peptide sequence as potential Sec-delivered effectors (SDEs) [51]. From this analysis, genes with transmembrane helix domains or homologs in other bacteria were excluded to remove membrane bound

proteins and to select for secreted biomarkers unique to *C*Las, respectively. Expression analysis of the candidates using semi-quantitative (reverse transcription) RT-PCR found *CLIBASIA_05315* and *CLIBASIA_03230* (hereon *SDE1* and *SDE2*) to be expressed in *C*Las-infected tissues of different citrus species (**Figure Va**). Transcriptome analysis conducted in collaboration with Dr. Nian Wang's lab (University of Florida) revealed that *SDE1* is upregulated ~10-folds (**Figure Vb**) and *SDE2* is upregulated ~3.5-folds in *C*Las-infected citrus vs. psyllids [39,51]. In addition, *SDE1* was found to be expressed in asymptomatic tissues from *C*Las-infected citrus, reiterating its potential as an early detection biomarker [51].

From work done in collaboration with Dr. Gitta Coaker's lab (University of California, Davis) we also found SDE1 and SDE2 to be part of a "core" set of SDEs, that are present in several *C*Las isolates including; TX2351, Ischi, SGCA5, HHCA, UCHHA, YCPsy, A4, Gxpsy, FLC2, FL17, and Psy62 (Thapa et. al. *in prep*). Furthermore, SDE1 and SDE2 are small proteins (each ~15kDa), which increases their potential for movement through the phloem sieve elements and from cell-to-cell via plasmodesmata [43,48]. This natural movement should allow for an even distribution of the proteins throughout infected trees which increases biomarker availability for detection.

RESULTS

Antibody generation for CLas biomarkers

Upon secretion from the cell, Sec-delivered proteins exhibit removal of their N-terminal signal peptides; therefore, upon secretion from *C*Las, SDE1 and SDE2 "full-length" proteins would not contain their signal peptide sequences. *SDE1* and *SDE2* gene sequences without their N-terminal signal peptides were cloned into the plasmid vectors pET28a and pET14b, respectively, with N-terminal, 6xHIS-tags. These sequences were considered full-length (**Table 1.1**). The recombinant proteins were then expressed in *Escherichia coli* and purified by binding of the HIS-tag to a nickel-agarose affinity column. The purified SDE1 and SDE2 proteins were sent for generation of polyclonal antisera via rabbit-injection (Robert Sargent, Ramona, CA). In addition, two short peptide epitopes for both SDE1 and SDE2 were selected to generate additional polyclonal antisera via rabbit-injection (**Table 1.1**) (Genemed Synthesis, San Antonio, TX).

In vitro evaluations of antisera generated against CLas biomarkers

The antibodies generated against the full-length and antigenic peptides of SDE1 and SDE2 were provided as crude rabbit antisera with multiple bleeds per rabbit injected. To confirm each bleed had affinity to the corresponding SDE biomarker, I performed enzyme-linked immunosorbent assay (ELISA) and Western blotting. From the ELISA evaluations, I found that the antisera at different dilutions can bind to the respective SDE1 or SDE2 antigens (**Figure 1.1 - 1.3**). This was true for all antisera bleeds tested. Sometimes antisera from one rabbit would exhibit more affinity to the corresponding SDE proteins compared to antisera from another rabbit (**Figure 1.3**). This result could be due to individual rabbit immune responses to the injected antigen (SDE

protein). Rabbits with stronger immune responses generated sera with more antibody titer, which was assessed by the antigen binding of crude antisera in a dilution series (**Figure 1.3**, for example antisera bleeds from rabbit 1 vs. rabbit 2).

Western blotting confirmed that antisera generated against SDE1, SDE2, or peptides could still bind full-length SDE1 or SDE2 protein expressed in *E. coli*, but did not bind proteins in *E. coli* cells containing empty vector controls (**Figure 1.4**). Note that anti-SDE1-peptide-1 was not tested due to failure to perform in preliminary direct citrus-tissue imprint assays. Results are shown for a representative bleed from each type of antiserum; however, all bleeds exhibited similar Western blot results to their subsequent antigens. Based on these evaluations, antiserum bleeds with the highest affinity to their subsequent *C*Las SDE biomarkers were selected for further antibody purification.

In planta evaluations of antisera generated against CLas biomarkers

To verify that antibodies within the antisera could detect the SDEs *in planta,* I introduced the constructs pEG103::SDE1-GFP and pEG103::SDE2-GFP into *Agrobacterium tumefacians* and transiently expressed the fusion proteins in *Nicotiana benthamiana* leaves via *Agro*-infiltration. I extracted total proteins from the infiltrated leaf tissue and detected the SDEs by Western blotting using the anti-SDE1-full-length or anti-SDE2-full-length antisera (**Figure 1.5a, b**). SDE1- and SDE2-GFP fusion proteins could be detected, confirming binding of the antisera *in planta*. Tissue extracted from *N. benthamiana* plants *Agro*-infiltrated with pEG103::EV was used as a negative control and had some background binding, as indicated by the non-specific band at ~72kDa (**Figure 1.5a, b**). This non-specific band was seen throughout the *N. benthamiana* plant

samples when using crude antisera but was reduced when using purified anti-SDE1-full-length antibodies (**Figure 1.5c**).

To assess binding in citrus, anti-SDE1-full-length and anti-SDE1-peptide-2 purified antibodies were evaluated for binding to SDE1 protein “spiked” into healthy citrus extract. I incubated HIS-SDE1 purified protein with extracts from healthy citrus tissues and subjected the mixtures to Western blotting. Results found that anti- SDE1-full-length and anti-SDE1-peptide-2 detected “spiked” SDE1 protein at different dilutions in healthy citrus extract with minimal interference. This is represented by a band at the expected molecular weight (~20kDa) in spiked samples, and the lack of the same band in healthy citrus extract alone (**Figure 1.6a**). Note that anti-peptide-2 antibody exhibits a different non-specific band in healthy citrus. This assay was repeated with the purified anti-SDE1-full-length antibody using the extracts from different citrus species (**Figure 1.6b**). Use of the purified antibody as opposed to the antisera reduced non-specific binding, as shown by the lack of background bands in the samples with healthy citrus extracts alone (**Figure 1.6a, b**).

Table 1.1 – Amino acid sequences and predicted sizes of SDE biomarkers used for antibody generation.

Biomarker Name	Full-length or peptide	Amino acid sequence used for antibody generation	Amino acid region	Predicted size (kDa)
SDE1	Full-length	*GSSFGCCGEFKKKASSPRIHMRPF*TKSSPYNNSVSN TVNNTPRVPDVSEMNSSRGSAPQSHVNVSSPHYKHE YSSSSA**SSSTHASPPPHFEQKHIS**RTRIDSSPPP**GHID PHPDHIRNTLALHRKM**LEQS	24-154	14.31
	Peptide 1 (Genemed)	**SSSTHASPPPHFEQKHIS**	103-120	NA
	Peptide 2 (Genemed)	**GHIDPHPDHIRNTLALHRKM**	131-150	NA
SDE2	Full-length	*LLTKKIES**DTDSRHEKATISL**SAHDKEGS*KHTMNAEFS VPKNDEKYTISSLTKKIESDTDFRREKATISLSAHDKE**G SKHTMNAEFSVPKND**EKYTISACASDDKGNKSTLCVE CPSPSTPGQYDLNHCAECENTTSKGLCP	21-162	15.63
	Peptide 1 (Genemed)	**DTDSRHEKATISLSAHDKEGS**	29-49	NA
	Peptide 2 (Genemed)	**GSKHTMNAEFSVPKND**	67-82	NA

Amino acids in italics are predicted signal peptides (Signal P 4.0) and amino acids in bold are peptide sequences.

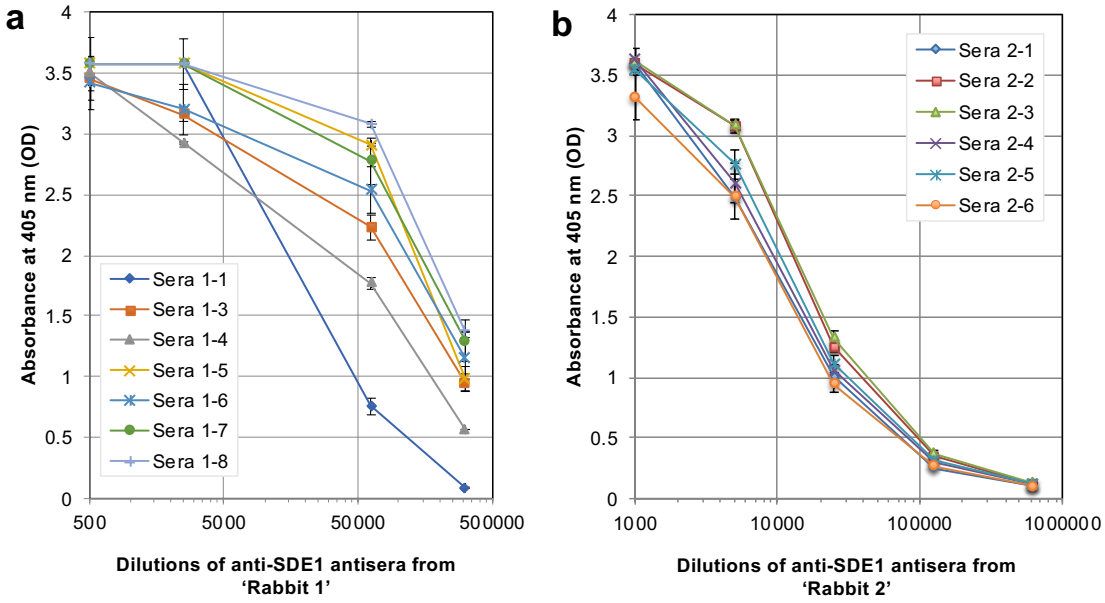

Figure 1.1 - Evaluations of anti-SDE1-full-length antisera using Enzyme-linked immunosorbent assay (ELISA). a) Representative anti-SDE1-full-length antisera bleeds from Rabbit 1 **b)** and Rabbit 2. Plates were coated with 200ng/mL of SDE1 antigen. Antisera dilution concentrations are represented on the x-axis in logarithmic scale, and absorbance values are on the y-axis. Error bars represent Standard Deviation, assays were performed in triplicates.

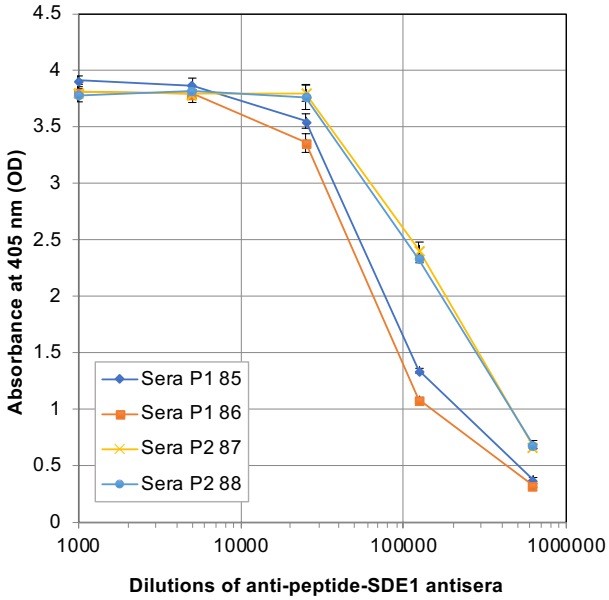

Figure 1.2- Evaluations of anti-SDE1-peptide-1 and anti-SDE1-peptide-2 antisera using ELISA. Representative antisera bleeds for anti-SDE1-peptide-1 (P1, Rabbit 85 and 86) and anti-SDE1-peptide-2 (P2, Rabbit 87 and 88) are shown. Plates were coated with 200ng/mL of SDE1 antigen. Antisera dilution concentrations are represented on the x-axis in logarithmic scale, and absorbance values are on the y-axis. Error bars represent Standard Deviation, assays were performed in triplicates.

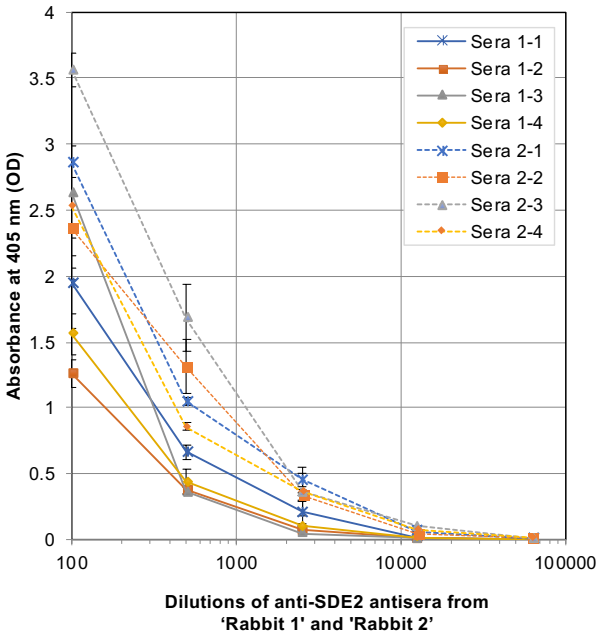

Figure 1.3 - Evaluations of anti-SDE2-full-length antisera using ELISA.
Representative anti-SDE2-full-length antisera bleeds from Rabbit 1 (solid lines) and Rabbit 2 (dotted lines) are shown. Plates were coated with 200ng/mL of SDE2 antigen. Antisera dilution concentrations are represented on the x-axis in logarithmic scale, and absorbance values are on the y-axis. Error bars represent Standard Deviation, assays were performed in triplicates.

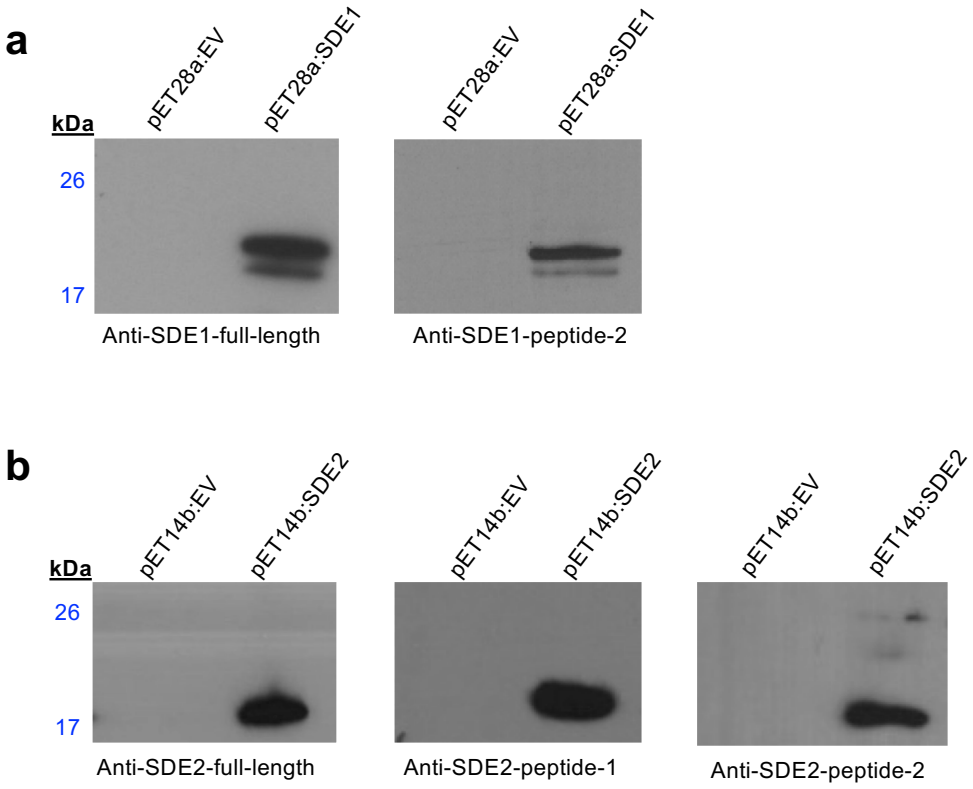

Figure 1.4 - Western blot evaluations of anti-SDE1 and anti-SDE2 antisera. a) Representative bleeds of anti-SDE1-full-length and -peptide-2 antisera. Wells were loaded with *E. coli* cells expressing pET28a::empty vector (EV) or pET28a::SDE1. **b)** Representative bleeds of anti-SDE2-full-length, -peptide-1, and -peptide-2 antisera. Wells were loaded with *E. coli* cells expressing pET14a::empty vector (EV) or pET14a::SDE2.

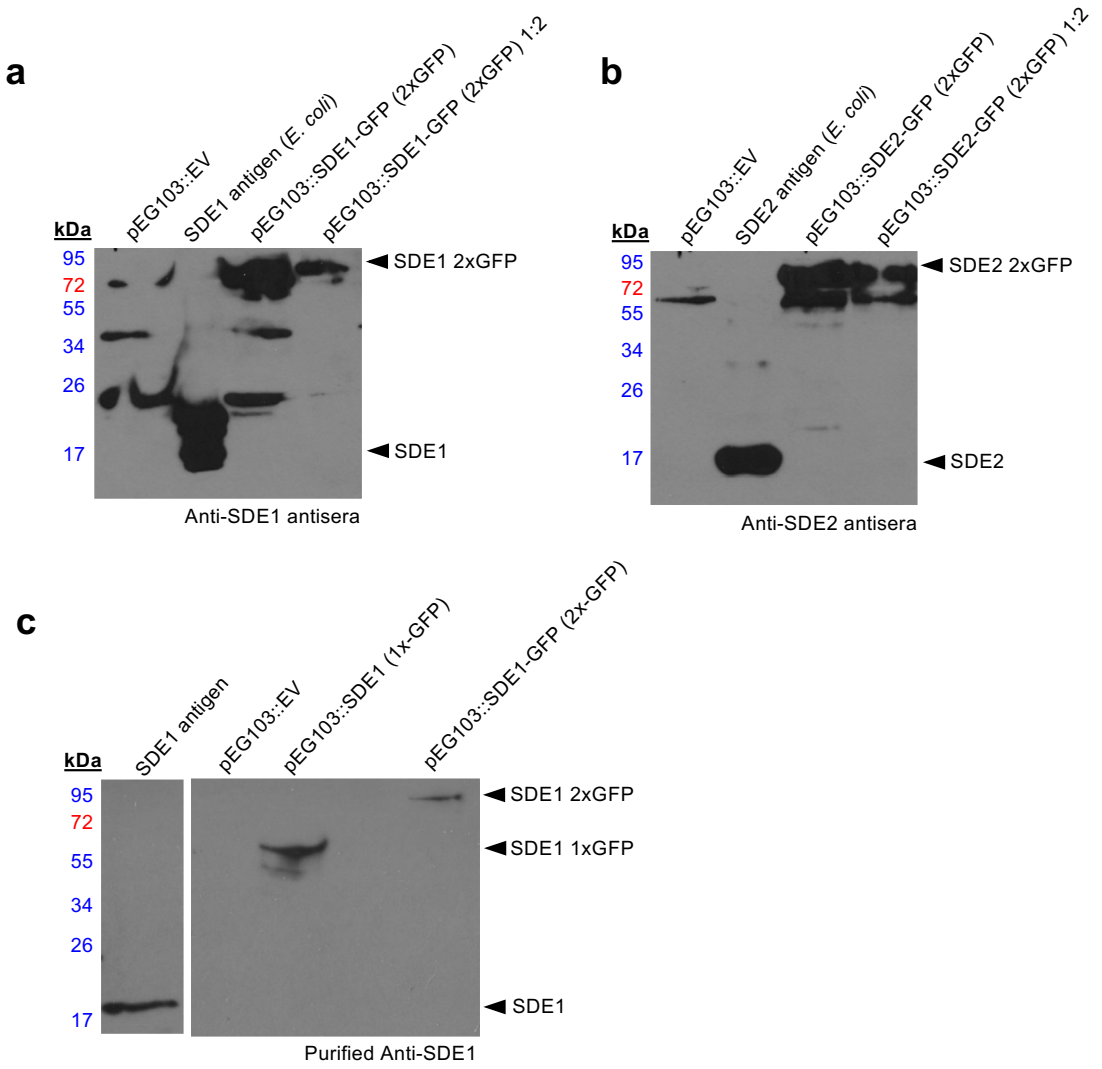

Figure 1.5 - Detection of SDE1 and SDE2-GFP fusion proteins *in planta* via transient expression in *Nicotiana benthamiana*. SDE1 or SDE2 containing either 1x or 2x GFP tags were transiently expressed in *N. bethanmiana* leaves through *Agro*-infiltration. Total proteins were extracted and detected by Western blotting using **a)** anti-SDE1-full-length antisera, **b)** anti-SDE2-full-length antisera, and **c)** anti-SDE1-full-length purified antibody. SDE1 and SDE2 antigen and pEG103::EV (empty vector) were used as controls.1:2 represents a 1 in 2 dilution of the sample. Arrowheads indicate sizes of annotated fusion proteins. GFP = green fluorescent protein.

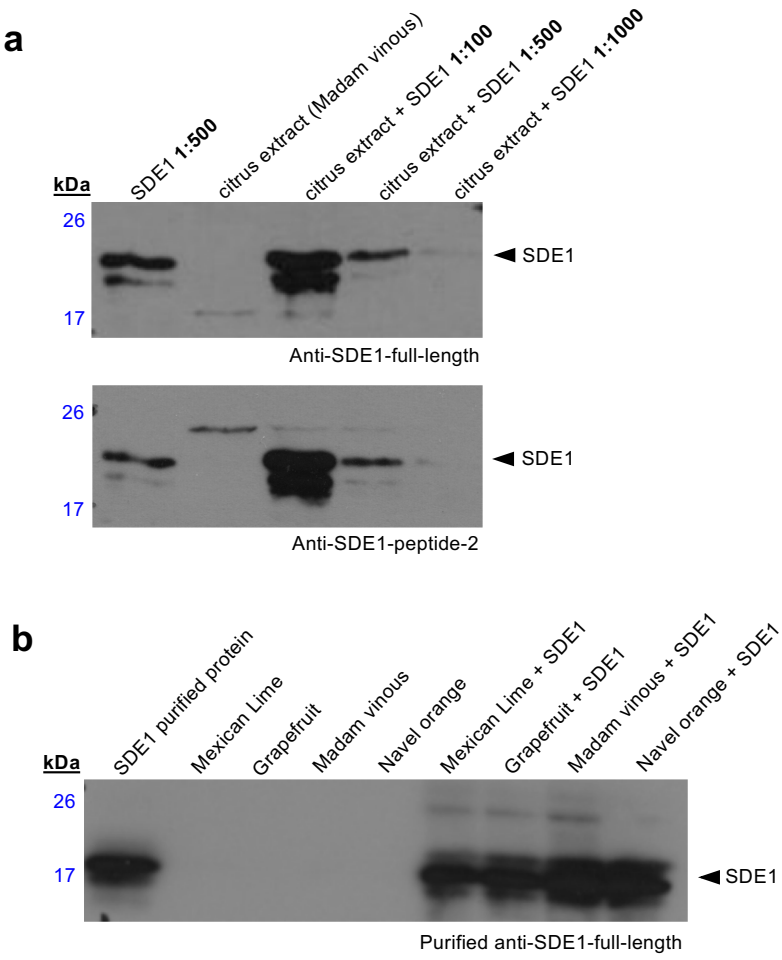

Figure 1.6 - Detection of SDE1 *in planta* by spiking into citrus tissue extract. a) Anti-SDE1-full-length antisera or anti-SDE1-peptide-2 antisera were used to detect SDE1 purified protein alone or spiked into healthy citrus extract from *Citrus sinensis* Madam Vinous, dilutions of spiked SDE1 protein are represented. **b)** Purified anti-SDE1-full-length antibody was used to detect SDE1 purified protein alone or spiked into healthy citrus extract from a range of citrus species. Arrowheads indicate the expected size of SDE1 protein.

Purification of anti-SDE antibodies

In order to purify the polyclonal antisera for downstream application, I worked in collaboration with Dr. Ashok Mulchandani's lab in the Department of Chemical and Environmental Engineering (University of California, Riverside) to perform affinity-based column chromatography. For the antisera purification, I first purified a large amount of full-length HIS-SDE1 and HIS-SDE2 recombinant proteins to be used as the affinity proteins. I immobilized these proteins to AminoLink coupling resins and then incubated them with their respective polyclonal antisera. High affinity antibodies in the antisera mixtures were allowed to bind to their respective antigens (**Figure 1.7**). Unbound, or low affinity antibodies, were washed out of the mixture and the remaining high affinity antibodies were eluted though the column flow. This affinity-based purification was performed for anti-SDE1-full-length, anti-SDE1-peptide-2, and anti-SDE2-full-length antisera. These three antisera were chosen for antibody purification based on results from the *in vitro* and *in planta* antisera evaluations and the preliminary tests using the different serological detection platforms. The purified antibodies were validated for binding to their respective purified antigens by ELISA.

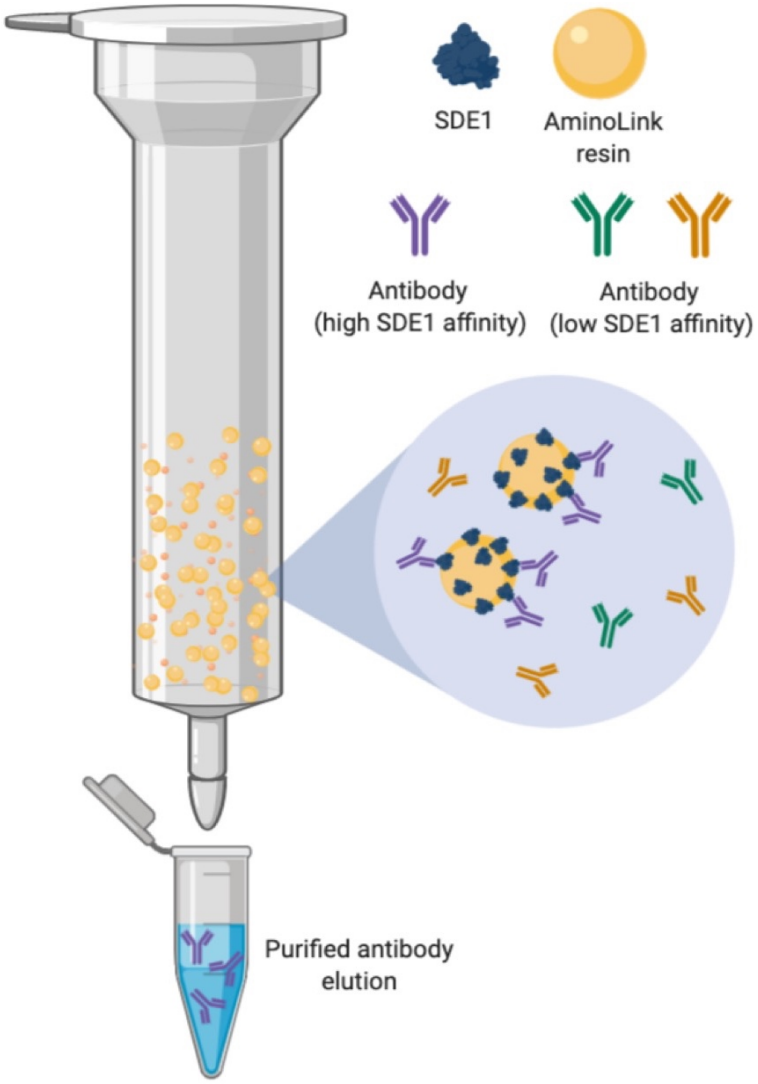

Figure 1.7 - Diagram of affinity-based column chromatography purification of anti-SDE antisera. SDE1 antigen and antisera are represented in the diagram. SDE proteins purified from *E. coli* are conjugated to AminoLink resins and packed into the gravity flow column. Antisera generated against the respective SDEs is incubated with the SDE-bound resin, antibodies with high affinity to their respective SDE antigen (purple) bind to the SDE-bound resin, while low affinity antibodies (green and orange) are washed out of the column. The antibodies with high affinity are eluted and collected for use. Illustration drawn with BioRender. Images are not to scale.

Generation of tag-free SDE1 and anti-tag-free-SDE1 antibodies

Application of the purified anti-SDE antibodies to different detection platforms using citrus-tissues found anti-SDE1-full-length antibody to be the most promising. Therefore, I focused my efforts on the SDE1 biomarker and anti-SDE1-full-length antibody. In this regard, I optimized the anti-SDE1 antibody purification to be against a more “native” form of SDE1 with the hope that these antibody populations may bind more effectively to SDE1 in *C*Las-infected citrus tissues. To better mimic the native SDE1 protein, I generated tag-free-SDE1 and implemented it in the affinity-based antibody purification. This enhancement should have also remove antibodies with affinity to the N-terminal HIS-tag of the recombinant protein.

To generate tag-free SDE1, I re-cloned the full-length *SDE1* gene into the plasmid vector pRSF-Duet, which contains an N-terminal 6xHIS-SUMO tag. I first purified the recombinant HIS-SUMO-SDE1 proteins using nickel resins (**Figure 1.8a**). Then, I cleaved the HIS-SUMO-SDE1 proteins with ubiquitin-like-specific protease 1 (ULP1), a SUMO protease, which cleaves between SUMO and SDE1 (**Figure 1.8b, c**). After cleavage, I separated the products by capturing the HIS-SUMO proteins on a new nickel column and eluting out tag-free-SDE1 proteins (**Figure 1.8b, c**). The tag-free-SDE1 biomarker proteins were then used for immobilization to the AminoLink resins and purification of the anti-SDE1-full-length antisera (**Figure 1.7**), generating anti-tag-free-SDE1 antibodies. These antibodies were then applied to the different *C*Las detection platforms.

Further optimization of SDE1 native form via periplasmic-expressed SDE1

In addition to attempts made with the tag-free-SDE1 protein to generate a more "native" protein form, I also worked to generate periplasmic-expressed SDE1 protein. During Sec-secretion, proteins must pass through the periplasmic space of Gram-negative bacteria, therefore periplasmic-expressed SDEs may better replicate the native folding and/or structure of *C*Las SDEs. To test this hypothesis, I cloned the SDE1 sequence with two different signal peptides predicted to secrete proteins to the periplasm; 1) the gene III (gIII) signal peptide from bacteriophage [52,53], and 2) the SDE1 native signal peptide. Each had a 6xHIS tag placed at either the C-terminus or the N-terminus, between the signal peptide and protein sequence (**Figure 1.9a**).

These constructs were transformed into *E. coli* and grown in cell culture for inducible protein expression (**Figure 1.9b**). The induced cultures were subjected to osmotic shock to obtain periplasmic extracts, and then run on SDS-PAGE followed by Coomassie staining to observe total protein. SDS-PAGE and Coomassie staining of periplasmic extracts (supernatants) did not result in observation of SDE1 protein, however SDE1 protein was observed in cell pellets (**Figure 1.19c**). Periplasmic extracts of another protein (the citrus PLCP, SAG12-63, used as a control) did yield observable protein levels via SDS-PAGE and Coomassie staining indicating the proteins secreted into the periplasm (**Figure 1.19c**). Observation of the SDE1 periplasmic extracts with Western blotting resulted in detection of the C-terminal HIS-tagged SDE1 proteins, which was likely at a very low titer since it could not be visualized with SDS-PAGE alone (**Figure 1.9d**). It should be noted that the N-terminally tagged SDE1 proteins (gIII-HIS-SDE1 and Native-HIS-SDE1) could not be detected in the periplasmic extract via SDS-PAGE and Coomassie stain or Western blotting using anti-HIS antibody. Therefore, it is

unlikely they are secreted to the periplasmic space. Post Sec-secretion, Sec-delivered proteins should have their signal peptides cleaved [40], which would expose the 6xHIS tag for detection by the anti-HIS antibody (**Figure 1.9d**). Therefore, we hypothesize that the N-terminal HIS-tag being sandwiched between the signal peptide and SDE1 could disrupt the cleavage process during Sec secretion.

It is possible that the protein we observed within the periplasmic extracts via Western blotting could be remnants of dead or lysed cell debris. Yet, filtering of the periplasmic extracts did not result in loss of this protein. Culture media was also checked for SDE1 protein via Western blotting to assure the proteins were not secreted completely outside of the cells, but SDE1 was not detected in culture media. Thus, we were not able to confidently decipher if the SDE1 protein produced were in the periplasm, with Sec secretion signals cleaved, or still within the cell cytoplasm. Furthermore, high titers of this protein within the periplasmic extract would likely not be attainable since the proteins could not be visualized in periplasmic extracts via SDS-PAGE and Coomassie staining, only with Western blotting, which can detect proteins even at very low concentrations.

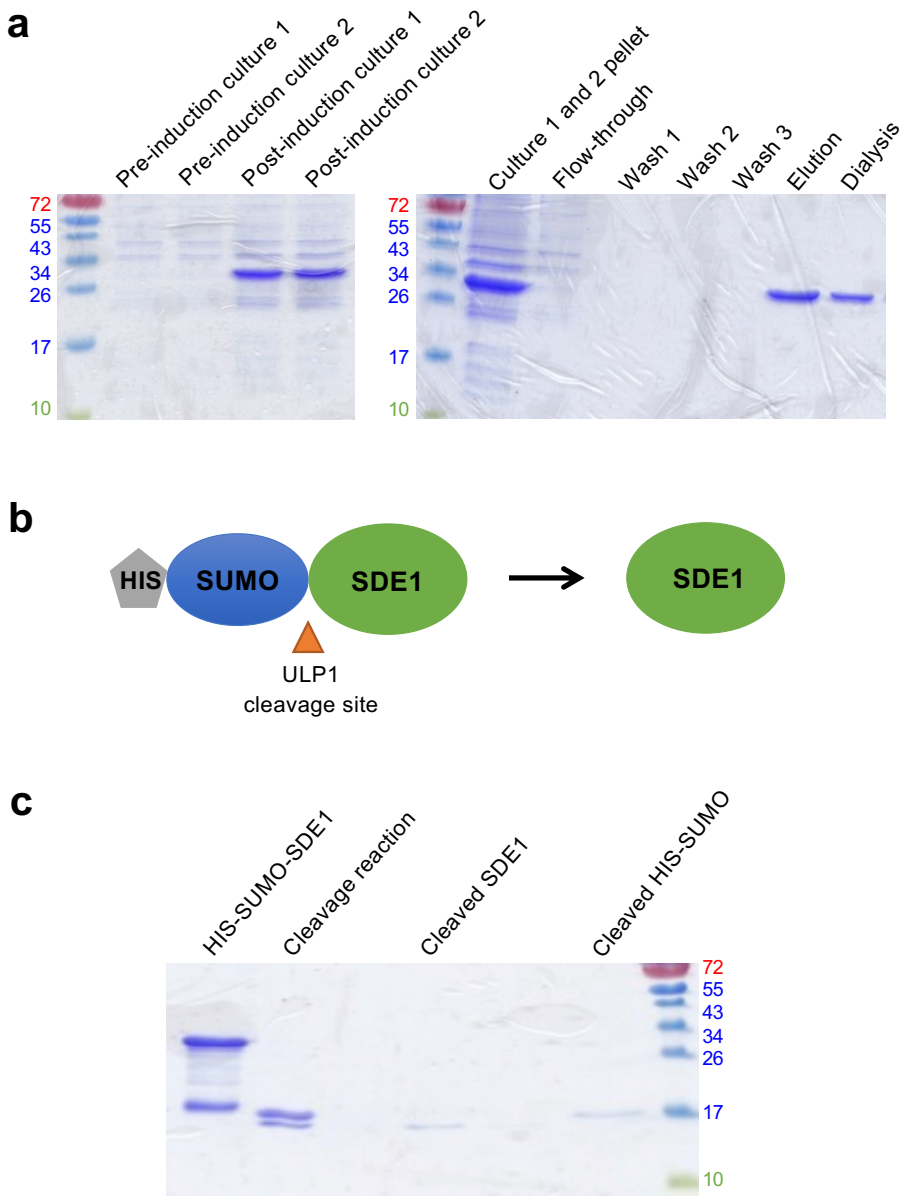

Figure 1.8 - Purification of SDE1 tag-free antigen. a) SDS-PAGE illustrating the steps of HIS-SUMO-SDE1 recombinant protein purification from *E. coli* cell culture. Cultures were induced for protein expression with IPTG, and the recombinant proteins were bound to nickel resins via HIS-tag affinity, all other residues were washed out of the column before elution of the HIS-SUMO-SDE1 protein. The purified proteins were then dialyzed overnight for buffer exchange. **b)** Diagram representing the cleavage of HIS-SUMO-SDE1 protein to release SDE1 tag-free protein. ULP1 was used to cleave the recombinant proteins. **c)** SDS-PAGE of the protein products before and after cleavage and the separated cleavage products. SDE1 tag-free is the lower band seen in the digestion reaction, HIS-SUMO is the higher band.

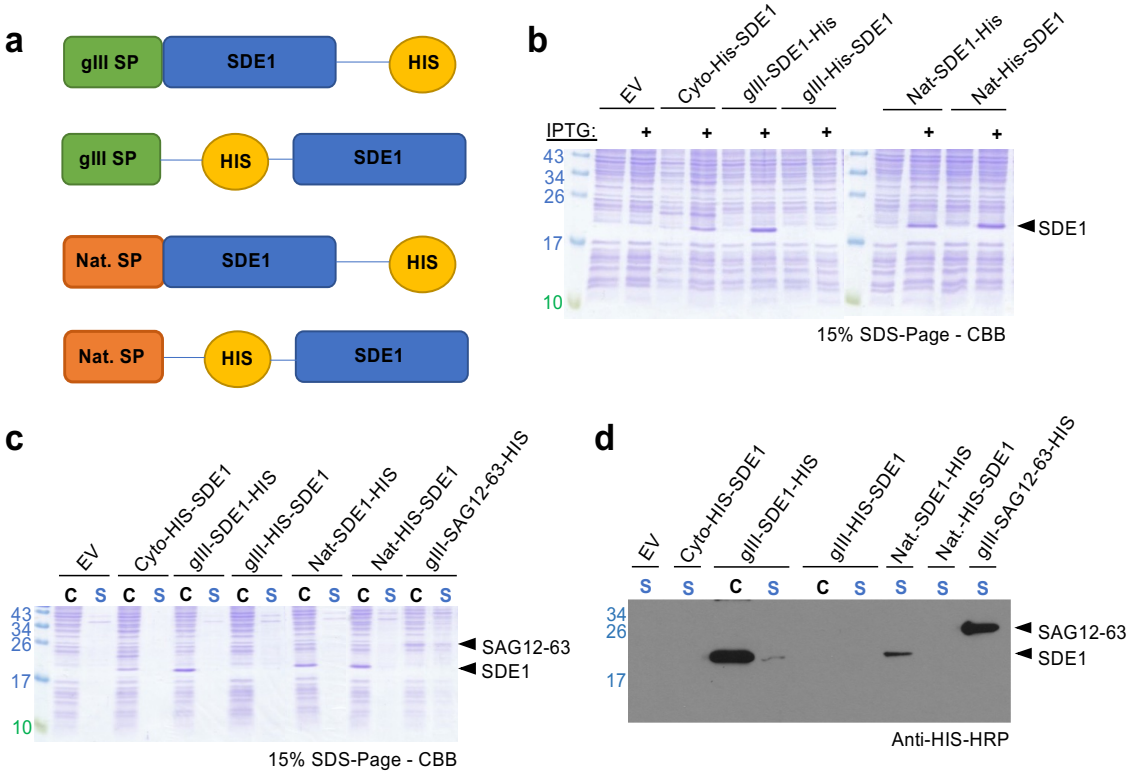

Figure 1.9 - Periplasmic expressed SDE1. a) Diagram illustrating the different signal peptides (gIII SP and native *C*Las SDE1, Nat. SP) and HIS-tag orientations (N-terminal and C-terminal) used to secrete SDE1 to the *E. coli* periplasm. **b)** Coomassie brilliant blue (CBB) stained SDS-PAGE showing the induction of SDE1 protein expression via addition of IPTG to *E. coli* culture for each of the four constructs generated. Cells containing EV (empty vector) and uninduced cells were used as negative controls. **c)** CBB stained SDS-PAGE of cell pellets (C) and periplasmic supernatants (S). Cyto-HIS-SDE1 does not have a signal peptide and therefore produces SDE1 in the cytoplasm. gIII-SAG12-63-HIS is another protein that had successful secretion to the periplasm and was used as a positive control. **d)** Western blot of a selection of the supernatants and pellets from the SDS-PAGE in c) using anti-HIS-HRP conjugated antibody.

CONCLUSIONS AND DISCUSSION

Urgent need for novel CLas detection strategies

With the looming HLB crisis it is imperative that disease management strategies include accurate, timely, and robust diagnosis of infected trees. Each undiagnosed tree serves as a reservoir for *C*Las populations, contributing to spread of the associated-pathogen and disease expansion. The use of *C*Las SDEs as biomarkers for identification of infected trees presents a novel strategy to overcome the challenges faced by other methods, such as nucleic acid-based detection and symptom-based diagnosis, which have been found prone to false negatives and mis-diagnoses [16,17]. Serological-based detection strategies can be high-throughput, cost-effective, and applied to a variety of platforms [29], many of which growers can use themselves. In addition, detection of *C*Las SDEs relies on the pathogen components, as opposed to the host's response, reducing possible mis-diagnosis due to the presence of other pathogens and/or abiotic stresses. Thus, antibody-based detection of *C*Las using SDEs as the detection biomarkers offers an economic approach that complements the current qPCR-based methods. As such, various anti-SDE antibody platforms could be implemented as a screening method for growers and inspectors, followed by sample collection and submission for the standard qPCR detection method to accelerate the rate of diagnosis and enhance HLB management programs.

Application of the anti-CLas SDE antibodies to serological detection technologies

The evaluation and purification of the anti-SDE antibodies was the initial step towards their application and end-goal use on different serological detection platforms. Compared to crude antisera, purified antibodies can remove cross reactivity to non-

specific antigens, as seen with the *in planta* evaluations (**Figure 1.5 and 1.6**), as well as allow for further conjugation with molecules (such as biotin) to enhance signal intensity [54]. In addition, polyclonal antibodies affinity-purified against a specific antigen represent a population with high binding affinity to that particular antigen. In comparison to polyclonal antibodies purified by protein A/G, which represent a mixed population since the purification is based on affinity to the heavy chain constant (Fc) of the IgG vs. the specific antigen [55,56]. Thus, the affinity-purified antibodies were utilized in the development of various serological-based detection platforms for *C*Las.

The anti-SDE, affinity-purified antibodies generated in this chapter were applied to different detection platforms including direct citrus-tissue imprint assay and indirect ELISA [51], which provided both qualitative and quantitative high-throughput forms of *C*Las SDE detection in citrus tissues. Continued improvement of this protocol is ongoing in our lab and now implements the use of a competitive ELISA format to increase sensitivity, and a sandwich ELISA format, to allow the use of multiple antibodies and thus increase specificity. In addition, the anti-SDE affinity-purified antibodies were fixed to field deployable nanosensors [57]. Nanosensor test runs show detection of the SDE1 biomarker in phosphate buffer and spiked into citrus tissue extracts, illustrating its potential as another *C*Las detection platform

Attempts at monoclonal antibody generation

In addition to the polyclonal antibodies, several attempts were made to generate monoclonal antibodies against the SDE1 biomarker. In order to do so, I purified the tag-free SDE1 protein and sent them to both Genscript (China) and Arigo biolaboratories (Taiwan) for monoclonal antibody production.

At Genscript, there was success with monoclonal antibody generation; however, comparison of the monoclonal anti-SDE1 antibodies to the purified, polyclonal anti-SDE1 antibodies found they did not show greater affinity to native SDE1 antigen in *C*Las-infected tissues. At Arigo, the monoclonal antibody candidates were screened against SDE1 expressed *in planta* in order to select for antibodies that may have better affinity to native SDE1. For the *in planta* screening, SDE1 protein was transiently expressed in *N. benthamiana* and the extracts were tested against the different monoclonal antibodies using ELISA. We found one monoclonal line with binding affinity to the *N. benthamiana* expressed SDE1. However, again this line did not exceed the sensitivity of the anti-SDE1 polyclonal when tested on *C*Las-infected citrus.

After attempts at traditional monoclonal antibody generation via mouse injection were repeatedly unsuccessful, we began working in collaboration with Dr. Xin Ge lab (Department of Chemical and Environmental Engineering, University of California, Riverside) to generate monoclonal antibodies against SDE1 using phage-display. Dr. Ge's lab has generated a library of synthetic, monoclonal antibodies by sequence diversification of variable immunoglobulin regions, which bind different antigen epitopes [58,59]. The library contains over 10^9 antibody-presenting, M13 bacteriophage, which are engineered to "display" a single-chain variable fragment (scFv) antibody outside their protein coat, and thus can be screened for affinity against a desired antigen. However, despite numerous attempts at screening the phage-display antibody library, we were unable to obtain an antibody with high affinity for the SDE1 biomarker. These efforts are ongoing.

Future implications for SDEs as CLas biomarkers

With the growing knowledge on *C*Las biology and gene expression in the host, new and improved biomarkers can continue to be selected based on their specificity to *C*Las and abundance in infected tissues. To improve the use of SDEs as *C*Las biomarkers in serological-based detection it would be beneficial to utilize different expression systems. For instance, other *C*Las secreted proteins or SDEs with biomarker potential could be expressed in the bacterial periplasmic space or *in planta* to better mimic the native protein forms that would be found in *C*Las-infected tissues. In this way, antibodies generated against one's protein would be more likely to capture the native form in infected tissues.

We attempted to secrete SDE1 protein to the *E. coli* periplasm using both the SDE1 native signal peptide and the bacteriophage-derived gIII signal peptide [52,53]. While SDE1 protein was expressed, secretion of the protein to the periplasm in a high abundance was not confirmed (**Figure 1.9**). Periplasmic expression could be a limiting technique when trying to generate a large volume of proteins (around one milligram needed for antibody generation). However, enhancement of the system could be done by exploring different signal peptides, promoter, or organisms [60,61]. In addition, "Sec" secretion might be better modeled in another system more closely related to *C*Las (i.e. *Liberibacter cresens*).

Expression of *C*Las biomarker proteins *in planta* is another possibility for enhancing detection of native *C*Las protein forms. This could be done by screening antibodies against proteins expressed 1) transiently in *N. benthamiana* or other model organisms, 2) transiently in citrus [62,63], or 3) natively in *C*Las-infected tissues. However, unless these proteins are adequately purified from the plant tissues, they cannot be

directly injected into animals for antibody generation due to their low purity and the high abundance of plant proteins (i.e. creating an antibody with too much background binding in the plant host).

MATERIALS AND METHODS

Microbial strains and plasmids

Escherichia coli strains DH5α and BL21 were grown in Luria-Bertani (LB) medium supplemented with kanamycin at 50 μg/mL at 37°C. A full list of vectors and strains used in this chapter are listed in Table A.1. Expression of SDE proteins was controlled by the T7 promoter which was induced with the addition of 0.2uM IPTG overnight at 16°C. Cell cultures were checked for SDE expression via SDS-PAGE and cell pellets were saved and frozen for protein purification.

Agrobacterium tumefaciens strain GV3101 was grown in LB medium supplemented with kanamycin at 50 μg/mL, rifampicin at 50 μg/mL, or gentamycin at 50 μg/mL at 30°C. GV3101 was transformed with pEG103::SDE1-GFP or pEG103::SDE2-GFP via free-thaw method [64] and used for transient protein expression in *Nicotiana benthamiana* by *Agro*-infiltration.

Plant materials and growth conditions for the in planta evaluations

Nicotiana benthamiana plants were geminated and grown in a conditioned growth room at 22°C with a 12/12 light/dark regime. Plants with fully expanded adult leaves were used for *Agro*-infiltration with the *Agrobacterium* strain GV3101 containing the SDE-GFP-expressing constructs. Proteins were extracted from leaf tissue after 48hrs by grinding the tissue in liquid nitrogen and re-suspending it in 2x Laemmli buffer [65] for evaluation via Western blotting.

Healthy citrus for the *in planta* “spiking” evaluation was kindly provided by Dr. Georgios Vidalakis at the Citrus Clonal Protection Program (CCPP). For the assay, tissue was ground with liquid nitrogen and re-suspended in 1xPBS buffer (pH 7.4).

Supernatants were obtained from the re-suspension by centrifugation and used as the healthy citrus extract, which was then mixed with different concentrations of SDE1 purified protein. These samples were combined with 2x Laemmli buffer and evaluated via Western blotting.

Protein purification

Recombinant proteins were purified from *E. coli* pellets by cell lysis via re-suspension of the cells in Buffer A (50mM Tris, 0.15M NaCl, 25mM imidazole, pH 8.0) followed by sonication. Cell lysates were then incubated with HIS60 Superflow nickel resins (Clontech, Mountain View, CA) allowing the HIS-tag on the recombinant proteins to bind. The resins were washed with Buffer A to remove unspecific proteins and cell debris. Then the HIS-SDE-bound proteins were eluted with Buffer B (50mM Tris, 0.5M NaCl, 250mM imidazole, pH 8.0). The eluted proteins were dialyzed overnight with 1xPBS buffer (pH 7.4), then quantified via Bradford assay, and stored with glycerol at -80°C for use.

For tag-free protein purification, HIS-SUMO-SDE1 proteins were first purified as described above, followed by cleavage of HIS-SUMO from SDE1 via SUMO protease. The HIS-SUMO proteins were then re-bound to fresh nickel-agarose resins and tag-free SDE1 proteins were eluted out of the column via gravity flow with Buffer A, while HIS-SUMO proteins remained bound to resins.

Affinity-based column chromatography

HIS-SDE1, tag-free SDE1, or SDE2 recombinant proteins were covalently immobilized to AminoLink coupling resins (ThermoFisher, Waltham, MA) in coupling

buffer (0.1M sodium phosphate, 0.15M NaCl, pH 7.2) with 50mM Cyanoborohydride overnight at 4°C. Remaining active sites were blocked with quenching buffer (1M Tris-HCl, pH 7.4) and non-coupled proteins were washed from the column with wash buffer (1M NaCl).

Once the affinity columns were prepared, the subsequent antisera were diluted in 1xPBS buffer (pH 7.4) and incubated with their respective SDE-bound AminoLink resins for 30min at room temperature to allow for affinity binding. The columns were washed with 1xPBS buffer (pH 7.4) to remove lower affinity antibodies and other antisera components. The high affinity antibodies were then eluted with 0.1M Glycine (pH 3.0), followed by immediate neutralization in an equal volume of 1M Phosphate buffer (pH 9.0). The eluted antibodies were dialyzed to 1xPBS (pH 7.4) overnight, quantified with Bradford assay, and stored with glycerol at -80°C for use.

Enzyme-linked immunosorbent assay (ELISA)

Indirect ELISA for the antisera evaluation was performed by coating 96-well ELISA plates (Immulon, 2 HB Flat Bottom Micro Titer Plates, ThermoFisher, Waltham, MA) with 200 ng/mL of SDE purified protein overnight at 4°C. Wells were manually washed with PBS-T (1xPBS buffer, pH 7.4, containing 0.1% Tween-20), then blocked with blocking buffer (1xPBS, pH 7.4, containing 3% w/v non-fat milk) at room temperature for 1hr. Wells were washed again and then incubated with different dilutions (1:1,000 to 1:1,000,000) of the various anti-SDE antisera bleeds prepared in blocking buffer at room temperature for 1hr. Plates were washed again and incubated with the goat-anti-rabbit IgG-horseradish peroxidase (HRP)-conjugated secondary antibody (Santa Cruz, Dallas, TX) diluted 1:5,000 in blocking buffer at room temperature for 1hr.

For signal detection, TMB-ELISA substrate solution (3,3',5,5'-tetramethyl benzidine) (ThermoFisher, Waltham, MA) or ABTS (2,2'-Azinobis [3-ethylbenzothiazoline-6-sulfonic acid]-diammonium salt) (ThermoFisher, Waltham, MA) was added to each well and incubated until color development (up to 15 min). 2 M Sulfuric acid (H_2SO_4) was added to stop the TMB reaction, no stop reaction for ABTS was required. The absorbance values were measured at 450 nm (for TMB) or 410 nm (for ABTS) using Tecan Plate Reader M200Pro. All samples were tested in triplicates.

Western blotting

For the Western blots, total proteins from *E. coli* cultures and plant tissues were prepared as described, 2x Laemmli buffer [65] was added to all protein extracts and samples were boiled for 5 min before separation by 12% or 15% polyacrylamide gels via SDS-PAGE. Gels were transferred to PVDF membrane paper and blocked with blocking buffer (1xTBS, pH 7.4, containing 3% w/v non-fat milk) at room temperature for 1hr, followed by incubation with the various anti-SDE antisera (1:1,000 dilution) or purified anti-SDE antibody (1:2,000 dilution). Membranes were then washed with TBS-T (1xTBS buffer, pH 7.4, containing 0.1% Tween-20) then incubated with the goat-anti-rabbit IgG-horseradish peroxidase (HRP)-conjugated secondary antibody (Santa Cruz, Dallas, TX) diluted 1:5000 in blocking buffer at room temperature for 1hr. Signals for antibody-bound proteins were detected with SuperSignal West Pico PLUS Chemiluminescent Substrate (ThermoFisher, Waltham, MA).

Osmotic shock for periplasmic extraction

DH5a BL21 cell cultures were grown and protein expression was induced as described above. For the periplasmic extraction, cell pellets of induced cultures were re-suspended in osmotic shock solution 1 (20 mM Tris-HCl, pH 8.0, 2.5 mM EDTA, 20% Sucrose) based on the sample OD_{600} and volume ($V_{Re\text{-}suspension}$ = (OD_{600} of sample/5.0) x V_{Sample}) then incubated on ice for 10 min. Samples were then centrifuged at 4°C and supernatants were discarded. The remaining pellets were then re-suspended in the osmotic shock buffer 2 (20 mM Tris-HCl, pH 8.0, 2.5 mM EDTA) and incubated on ice for another 10 min. The samples were again centrifuged at 4°C to separate the periplasmic fluid (supernatant). Supernatants and pellets were kept in separate tubes for evaluation via SDS-PAGE and Western blotting.

ACKNOWLEDGEMENTS

Special acknowledgements go to those who contributed to the research in this chapter. Big thanks go to Dr. Deborah Pagliaccia, Dr. Jinxia Shi, Dr. Agustina de Francesco, Eva Hawara, and Robert Lui for their roles in the both the preliminary work that stimulated this research and the application-based aspects including testing on the different detection platforms. I would also like to thank Dr. Ashok Mulchandani and Dr. Thien-Toan Tran (UC Riverside, Department of Chemical and Environmental Engineering) for their guidance in antibody purification and further application of these antibodies to the nanosensor platform. Dr. Jikui Song (UC Riverside, Department of Biochemistry) for vectors used in this chapter. And my undergraduate mentee Shellen Lee (UC Riverside) for her assistance with the periplasmic protein work.

REFERENCES

1. Gottwald, T. R. Current Epidemiological Understanding of Citrus Huanglongbing. *Annual Review of Phytopathology* **48**, 119–139 (2010).

2. Zheng, Z., Chen, J. & Deng, X. Historical Perspectives, Management, and Current Research of Citrus HLB in Guangdong Province of China, Where the Disease has been Endemic for Over a Hundred Years. *Phytopathology* **108**, 1224–1236 (2018).

3. Teixeira, D. do C. *et al.* 'Candidatus Liberibacter americanus', associated with citrus huanglongbing (greening disease) in São Paulo State, Brazil. *Int. J. Syst. Evol. Microbiol.* **55**, 1857–1862 (2005).

4. Coletta-Filho, H. D. *et al.* First Report of the Causal Agent of Huanglongbing ("Candidatus Liberibacter asiaticus") in Brazil. *Plant Disease* **88**, 1382–1382 (2004).

5. Faghihi, M. M., Salehi, M., Bagheri, A. & Izadpanah, K. First report of citrus huanglongbing disease on orange in Iran. *Plant Pathology* **58**, 793–793 (2009).

6. Manjunath, K. L. *et al.* First Report of the Citrus Huanglongbing Associated Bacterium 'Candidatus Liberibacter asiaticus' from Sweet Orange, Mexican Lime, and Asian Citrus Psyllid in Belize. *Plant Dis.* **94**, 781 (2010).

7. da Graça, J. V. *et al.* Huanglongbing in Texas: Report on the first detections in commercial citrus. *Journal of Citrus Pathology* **2**, (2015).

8. Kumagai, L. B. *et al.* First Report of Candidatus Liberibacter asiaticus Associated with Citrus Huanglongbing in California. *Plant Disease* **97**, 283–283 (2012).

9. Halbert, S. E., Manjunath, K., Ramadugu, C. & Lee, R. F. Incidence of Huanglongbing-Associated 'Candidatus Liberibacter Asiaticus' in Diaphorina citri (Hemiptera: Psyllidae) Collected from Plants for Sale in Florida. *flen* **95**, 617–624 (2012).

10. Grafton-Cardwell, E. E., Stelinski, L. L. & Stansly, P. A. Biology and Management of Asian Citrus Psyllid, Vector of the Huanglongbing Pathogens. *Annual Review of Entomology* **58**, 413–432 (2013).

11. da Graça, J. V. *et al.* Huanglongbing: An overview of a complex pathosystem ravaging the world's citrus: Citrus huanglongbing. *J. Integr. Plant Biol.* **58**, 373–387 (2016).

12. Bové, J. M. Huanglongbing: A Destructive, Newly-Emerging, Century-Old Disease of Citrus. *Journal of Plant Pathology* **88**, 7–37 (2006).

13. Shen, W. *et al.* Occurrence and in-grove distribution of citrus huanglongbing in north central Florida. *Journal of Plant Pathology* **95**, 361–371 (2013).

14. Gottwald, T., Da Graca, J. & Bassanezi, R. Citrus Huanglongbing: The Pathogen and Its Impact. *Plant Health Progress* (2007) doi:10.1094/PHP-2007-0906-01-RV.

15. Li, W., Hartung, J. S. & Levy, L. Quantitative real-time PCR for detection and identification of Candidatus Liberibacter species associated with citrus huanglongbing. *J. Microbiol. Methods* **66**, 104–115 (2006).

16. Irey, M. S., Gast, T. & Gottwald, T. R. Comparison of visual assessment and polymerase chain reaction assay testing to estimate the incidence of the Huanglongbing pathogen in commercial Florida citrus. *Proc. Fla. State Hort. Soc.* **119**, 89–93 (2006).

17. Tatineni, S. *et al.* In Planta Distribution of ' *Candidatus* Liberibacter asiaticus' as Revealed by Polymerase Chain Reaction (PCR) and Real-Time PCR. *Phytopathology* **98**, 592–599 (2008).

18. Li, W., Levy, L. & Hartung, J. S. Quantitative Distribution of ' *Candidatus* Liberibacter asiaticus' in Citrus Plants with Citrus Huanglongbing. *Phytopathology* **99**, 139–144 (2009).

19. Ding, F., Duan, Y., Paul, C., Brlansky, R. H. & Hartung, J. S. Localization and Distribution of 'Candidatus Liberibacter asiaticus' in Citrus and Periwinkle by Direct Tissue Blot Immuno Assay with an Anti-OmpA Polyclonal Antibody. *PLoS One* **10**, (2015).

20. Aksenov, A. A. *et al.* Detection of Huanglongbing Disease Using Differential Mobility Spectrometry. *Anal. Chem.* **86**, 2481–2488 (2014).

21. Chin, E. L., Mishchuk, D. O., Breksa, A. P. & Slupsky, C. M. Metabolite Signature of *Candidatus* Liberibacter asiaticus Infection in Two Citrus Varieties. *J. Agric. Food Chem.* **62**, 6585–6591 (2014).

22. Slisz, A. M., Breksa, A. P., Mishchuk, D. O., McCollum, G. & Slupsky, C. M. Metabolomic Analysis of Citrus Infection by '*Candidatus* Liberibacter' Reveals Insight into Pathogenicity. *J. Proteome Res.* **11**, 4223–4230 (2012).

23. Pourreza, A., Lee, W. S., Etxeberria, E. & Zhang, Y. Identification of Citrus Huanglongbing Disease at the Pre-Symptomatic Stage Using Polarized Imaging Technique. *IFAC-PapersOnLine* **49**, 110–115 (2016).

24. Yin, X., Kelly, K. N., Maharaj, N. N., Rolshausen, P. & Leveau, J. H. J. A microbiota-based approach to citrus tree health: in search of microbial biomarkers to pre-diagnose trees for HLB infection. *Citrograph* **9**, 58–63 (2018).

25. Byrne, B., Stack, E., Gilmartin, N. & O'Kennedy, R. Antibody-Based Sensors: Principles, Problems and Potential for Detection of Pathogens and Associated Toxins. *Sensors* **9**, 4407–4445 (2009).

26. van Slogteren, E. & van Slogteren, D. H. M. Serological Identification of Plant Viruses and Serological Diagnosis of Virus Diseases of Plants. *Annual Review of Microbiology* **11**, 149–164 (1957).

27. Schaad, N. W. Serological Identification of Plant Pathogenic Bacteria. *Annual Review of Phytopathology* **17**, 123–147 (1979).

28. Vidic, J., Manzano, M., Chang, C.-M. & Jaffrezic-Renault, N. Advanced biosensors for detection of pathogens related to livestock and poultry. *Vet Res* **48**, (2017).

29. Sankaran, S., Mishra, A., Ehsani, R. & Davis, C. A review of advanced techniques for detecting plant diseases. *Computers and Electronics in Agriculture* **72**, 1–13 (2010).

30. Arredondo Valdés, R. *et al.* A review of techniques for detecting Huanglongbing (greening) in citrus. *Can. J. Microbiol.* **62**, 803–811 (2016).

31. Li, W., Li, D., Twieg, E., Hartung, J. S. & Levy, L. Optimized Quantification of Unculturable Candidatus Liberibacter Spp. in Host Plants Using Real-Time PCR. *Plant Disease* **92**, 854–861 (2008).

32. Rigano, L. A. *et al.* Rapid and sensitive detection of Candidatus Liberibacter asiaticus by loop mediated isothermal amplification combined with a lateral flow dipstick. *BMC Microbiol* **14**, 86 (2014).

33. Keremane, M. L. *et al.* A rapid field detection system for citrus huanglongbing associated 'Candidatus Liberibacter asiaticus' from the psyllid vector, Diaphorina citri Kuwayama and its implications in disease management. *Crop Protection* **68**, 41–48 (2015).

34. Kogenaru, S. *et al.* Repertoire of novel sequence signatures for the detection of Candidatus Liberibacter asiaticus by quantitative real-time PCR. *BMC Microbiol* **14**, 39 (2014).

35. Ding, F., Duan, Y., Yuan, Q., Shao, J. & Hartung, J. S. Serological detection of 'Candidatus Liberibacter asiaticus' in citrus, and identification by GeLC-MS/MS of a chaperone protein responding to cellular pathogens. *Sci Rep* **6**, (2016).

36. Garnsey, S. M., Permar, T. A., Cambra, M. & Henderson, C. T. Direct tissue blot immunoassay (DTBIA) for detection of Citrus tristeza virus (CTV). *Proceedings of the 12th conference of the international organization of citrus virologist (IOCV)* **12**, 39–50 (1993).

37. Shi, J. *et al.* Novel Diagnosis for Citrus Stubborn Disease by Detection of a *Spiroplasma citri* -Secreted Protein. *Phytopathology* **104**, 188–195 (2014).

38. Cong, Q., Kinch, L. N., Kim, B.-H. & Grishin, N. V. Predictive Sequence Analysis of the Candidatus Liberibacter asiaticus Proteome. *PLOS ONE* **7**, e41071 (2012).

39. Yan, Q. *et al.* Global gene expression changes in Candidatus Liberibacter asiaticus during the transmission in distinct hosts between plant and insect. *Molecular Plant Pathology* **14**, 391–404 (2013).

40. Natale, P., Brüser, T. & Driessen, A. J. M. Sec- and Tat-mediated protein secretion across the bacterial cytoplasmic membrane--distinct translocases and mechanisms. *Biochim. Biophys. Acta* **1778**, 1735–1756 (2008).

41. Rapoport, T. A. Protein translocation across the eukaryotic endoplasmic reticulum and bacterial plasma membranes. *Nature* **450**, 663–669 (2007).

42. Costa, T. R. D. *et al.* Secretion systems in Gram-negative bacteria: structural and mechanistic insights. *Nat. Rev. Microbiol.* **13**, 343–359 (2015).

43. Sugio, A. *et al.* Diverse Targets of Phytoplasma Effectors: From Plant Development to Defense Against Insects. *Annual Review of Phytopathology* **49**, 175–195 (2011a).

44. Sugio, A., Kingdom, H. N., MacLean, A. M., Grieve, V. M. & Hogenhout, S. A. Phytoplasma protein effector SAP11 enhances insect vector reproduction by manipulating plant development and defense hormone biosynthesis. *Proceedings of the National Academy of Sciences* **108**, E1254–E1263 (2011b).

45. MacLean, A. M. *et al.* Phytoplasma Effector SAP54 Induces Indeterminate Leaf-Like Flower Development in Arabidopsis Plants. *Plant Physiol.* **157**, 831–841 (2011).

46. Hoshi, A. *et al.* A unique virulence factor for proliferation and dwarfism in plants identified from a phytopathogenic bacterium. *Proceedings of the National Academy of Sciences* **106**, 6416–6421 (2009).

47. Bai, X. *et al.* AY-WB Phytoplasma Secretes a Protein That Targets Plant Cell Nuclei. *MPMI* **22**, 18–30 (2008).

48. Imlau, A., Truernit, E. & Sauer, N. Cell-to-Cell and Long-Distance Trafficking of the Green Fluorescent Protein in the Phloem and Symplastic Unloading of the Protein into Sink Tissues. *The Plant Cell* **11**, 309–322 (1999).

49. Toruño, T. Y., Stergiopoulos, I. & Coaker, G. Plant-Pathogen Effectors: Cellular Probes Interfering with Plant Defenses in Spatial and Temporal Manners. *Annu Rev Phytopathol* **54**, 419–441 (2016).

50. Uhse, S. & Djamei, A. Effectors of plant-colonizing fungi and beyond. *PLOS Pathogens* **14**, e1006992 (2018).

51. Pagliaccia, D. *et al.* A Pathogen Secreted Protein as a Detection Marker for Citrus Huanglongbing. *Front. Microbiol.* **8**, 2041 (2017).

52. Boeke, J. D. & Model, P. A prokaryotic membrane anchor sequence: carboxyl terminus of bacteriophage f1 gene III protein retains it in the membrane. *Proc Natl Acad Sci U S A* **79**, 5200–5204 (1982).

53. Rapoza, M. P. & Webster, R. E. The filamentous bacteriophage assembly proteins require the bacterial SecA protein for correct localization to the membrane. *Journal of bacteriology* **175**, 1856–1859 (1993).

54. Bobrow, M. N., Harris, T. D., Shaughnessy, K. J. & Litt, G. J. Catalyzed reporter deposition, a novel method of signal amplification. Application to immunoassays. *J. Immunol. Methods* **125**, 279–285 (1989).

55. Zoller, M. & Matzku, S. Antigen and antibody purification by immunoadsorption: Elimination of non-biospecifically bound proteins. *Journal of Immunological Methods* **11**, 287–295 (1976).

56. O'Kennedy, R., Murphy, C. & Devine, T. Technology advancements in antibody purification. *ANTI* **6**, 17–32 (2016).

57. Tran, T.-T., Clark, K., Ma, W. & Mulchandani, A. Detection of a secreted protein biomarker for citrus Huanglongbing using a single-walled carbon nanotubes-based chemiresistive biosensor. *Biosensors and Bioelectronics* **147**, 111766 (2020).

58. Ge, X., Mazor, Y., Hunicke-Smith, S. P., Ellington, A. D. & Georgiou, G. Rapid construction and characterization of synthetic antibody libraries without DNA amplification. *Biotechnol. Bioeng.* **106**, 347–357 (2010).

59. Reddy, S. T. *et al.* Monoclonal antibodies isolated without screening by analyzing the variable-gene repertoire of plasma cells. *Nat. Biotechnol.* **28**, 965–969 (2010).

60. Baumgarten, T., Ytterberg, A. J., Zubarev, R. A. & Gier, J.-W. de. Optimizing Recombinant Protein Production in the Escherichia coli Periplasm Alleviates Stress. *Appl. Environ. Microbiol.* **84**, e00270-18 (2018).

61. Karyolaimos, A. *et al.* Enhancing Recombinant Protein Yields in the E. coli Periplasm by Combining Signal Peptide and Production Rate Screening. *Front. Microbiol.* **10**, (2019).

62. Jia, H. & Wang, N. Xcc-facilitated agroinfiltration of citrus leaves: a tool for rapid functional analysis of transgenes in citrus leaves. *Plant Cell Rep* **33**, 1993–2001 (2014).

63. Figueiredo, J. F. L. *et al.* Agrobacterium-mediated transient expression in citrus leaves: a rapid tool for gene expression and functional gene assay. *Plant Cell Rep* **30**, 1339–1345 (2011).

64. Höfgen, R. & Willmitzer, L. Storage of competent cells for Agrobacterium transformation. *Nucleic Acids Res* **16**, 9877 (1988).

65. Laemmli, U. K. Cleavage of Structural Proteins during the Assembly of the Head of Bacteriophage T4. *Nature* **227**, 680–685 (1970).

Chapter II

Elucidation of the molecular mechanisms behind Huanglongbing disease by determining and defining the host targets of *C*Las Sec-delivered effector 1 (SDE1)

Note: the contents of this chapter are adapted from Clark and Franco *et. al.* (2018) *Nature Communications*. 9:1718.

ABSTRACT

The citrus industry is facing an unprecedented challenge from Huanglongbing (HLB). All cultivars can be affected by the HLB-associated bacterium *Candidatus* Liberibacter asiaticus (*C*Las) and there is no known resistance. Insight into HLB pathogenesis is urgently needed in order to develop effective management strategies. In this chapter, I utilized the Sec-delivered effector 1 (SDE1), which is conserved in all *C*Las isolates, as a molecular probe to understand *C*Las virulence. My results indicated that SDE1 interacts with citrus papain-like cysteine proteases (PLCPs) and inhibits their protease activity. PLCPs are defense-inducible and exhibit increased protein accumulation in *C*Las-infected trees, suggesting a role in citrus defense responses. As a collaborative effort, we analyzed PLCP activity in field samples, revealing specific members that increase in abundance but remain unchanged in activity during infection. *SDE1*-expressing transgenic citrus also exhibit reduced PLCP activity. In addition, we found that *C*Las-infection of *SDE1*-expressing transgenic citrus resulted in more severe pathogen colonization relative to controls. Taken together, these data demonstrate that SDE1 inhibits the activity of citrus PLCPs, which are immune-related proteases that enhance defense responses in plants, likely to promote bacterial infection.

INTRODUCTION

Huanglongbing (HLB), or citrus greening disease, is currently considered the most destructive disease of citrus worldwide[1-5]. In the major citrus-growing areas including the US and Asia, the presumed causal agent of HLB is a gram-negative bacterium, *Candidatus* Liberibacter asiaticus (*C*Las). *C*Las is transmitted to citrus by the Asian citrus psyllid (ACP) during sap feeding, where it then colonizes the phloem sieve elements, eventually leading to disease symptoms. Infected trees exhibit leaf mottling, deformed and discolored fruits, premature fruit drop, and tree mortality[2]. In the US, Florida has lost over $7 billion in total industry output due to HLB from when it was first detected in 2005 to 2014[6,7].

Secreted proteins of pathogens, called effectors, play an essential role in bacterial virulence. Collectively, effectors aid infection by suppressing plant immunity and creating environments favorable for colonization and proliferation[8,9]. Many gram-negative bacteria 'inject' effectors directly into host cells through the type III secretion system[10]. In contrast, insect-transmitted bacteria, like *C*Las, often lack this specialized delivery machinery, but can utilize the general Sec secretion system to release effectors[11]. These Sec-delivered effectors (SDEs) carry an N-terminal secretion signal, allowing their export from pathogen cells into the extracellular space. The essential roles of SDEs in bacterial virulence are best illustrated by insect-transmitted, phloem-colonizing phytoplasmas, where expression of their individual SDEs in *Arabidopsis thaliana* leads to phenotypes that mimic disease symptoms[12,13]. Sequence analysis of the *C*Las genome revealed that it encodes all the components of the Sec secretion machinery[14]. In addition, 86 proteins were confirmed to possess a functional Sec-secretion signal, indicating that they could potentially be released by *C*Las into the

phloem during infection[15]. A few of these SDEs exhibited higher expression levels in citrus relative to expression in ACP[14,15], indicating that they may contribute to *C*Las colonization and/or disease progression in the plant host. However, our knowledge on the cellular function of *C*Las SDEs in both plant and insect hosts is lacking.

In this chapter I identified citrus host targets of the *C*Las effector, SDE1 (CLIBASIA_05315), and characterized SDE1 function upon interaction with said targets. SDE1 is conserved across *C*Las isolates with a typical Sec-dependent secretion signal[15,16,17]. The expression of *SDE1* is ~10-fold higher in citrus than in ACP[16] (**Figure 1.1b**), indicating a role for this effector in *C*Las colonization of plant hosts. *SDE1* is also highly expressed in asymptomatic tissues, suggesting a potential virulence function during early infection stages[16]. My results demonstrated that SDE1 interacts with multiple members of citrus papain-like cysteine proteases (PLCPs), which are known to regulate defense in *Arabidopsis* and solanaceous crops against bacterial, fungal, and oomycete pathogens[18,19]. Interestingly, SDE1 can directly inhibit PLCP activity *in vitro* and in transgenic citrus. Research done in collaboration with Dr. Gitta Coaker's lab found PLCP abundance is increased in *C*Las-infected citrus, likely as a defense response, subsequently PLCP activity is not always increased. Using *SDE1*-expressing transgenic citrus, we further show that SDE1 promoted *C*Las infection in citrus. Taken together, this research advances our understanding of HLB pathogenesis by identifying citrus targets of a conserved *C*Las effector, which could be exploited for HLB management.

RESULTS

SDE1 associates with citrus papain-like cysteine proteases

SDE1 is unique to *C*Las with no homologs in other organisms[16]. It is found in all sequenced *C*Las isolates from various geographic regions and its expression was detected from *C*Las-infected citrus including limes, sweet oranges, and grapefruits[15,16]. To understand the potential virulence function of SDE1 in citrus, an initial sequencing-based yeast-two-hybrid (Y2H) screening was performed, using a *Citrus sinensis* (L.) Osbeck cDNA library to identify candidate SDE1-interacting proteins (library generated and initial screening performed at Quintarabio, San Francisco, CA). From the screening, several candidates were selected (**Table 2.1**), of which, I further tested their interaction with SDE1 using pairwise Y2H assay. Of the six evaluated candidates, the *C. sinensis* protein annotated as 'xylem cysteine protease 1' (NCBI accession XM_006495158, previously GI# 568885285) was confirmed as an SDE1-interacting protein by pairwise Y2H (**Figure 2.1a**).

Xylem cysteine protease 1 is a member of the papain-like cysteine protease (PLCP) family. PLCPs share a conserved protease domain including a catalytic triad consisting of cysteine, histidine, and asparagine[19]. The canonical PLCPs have a pro-domain that must be autocatalytically processed for activity. The pre-proteases often contain an N-terminal signal peptide to ensure their entrance into the endomembrane system and subsequent function in the apoplast, vacuole, or lysosomes. Previous reports have shown that PLCPs contribute to plant defense during bacterial, oomycete, and fungal infection[19,20,21]. Search of the *C. sinensis* genome revealed 21 canonical PLCPs that can be classified into nine subfamilies based on their homology to the previously categorized *Arabidopsis thaliana* PLCPs[22] (**Figure 2.2**). Based on our

phylogenic analysis, XM_006495158 belongs to the SAG12 subfamily and is hereafter referred to as *Cs*SAG12-1.

Since PLCPs share a conserved catalytic domain, we examined whether SDE1 could also associate with PLCPs from other subfamilies. Therefore, I chose representatives from five additional PLCP subfamilies, *Cs*XCBP3 (orange1.1g012960), *Cs*RD21a (XM_006473212), *Cs*RD19 (orange1.1g017548), *Cs*AALP (XM_006474664), and *Cs*CTB (orange1.1g018568) to test for interaction with SDE1. Remarkably, all of them were able to interact with SDE1 in yeast (**Figure 2.1a**). Furthermore, a second member of the SAG12 subfamily, *Cs*SAG12-2 (XM_006470229), also interacted with SDE1 (**Figure 2.1a**). The observation that SDE1 interacts with members from multiple PLCP subfamilies suggests that it may associate with the conserved protease domain. Indeed, the protease domains of *Cs*SAG12-1, *Cs*SAG12-2, *Cs*RD21a, and *Cs*AALP are sufficient to mediate interaction with SDE1 in yeast (**Figure 2.1b**). In addition, SDE1 interacted with the protease domains of three other members from the SAG12 subfamily, i.e. *Cs*SAG12-3 (orange1.1g018958), *Cs*SAG12-4 (orange1.1g019063), and *Cc*SAG12-1 (Ciclev10005334, a PLCP from *C. clementina*) in yeast (**Figure 2.3**).

In order to determine if SDE1 can directly interact with citrus PLCPs, we conducted *in vitro* pull-down assays using recombinant proteins expressed and purified from *Escherichia coli*. The protease domains of the PLCPs were tagged with GST at the N-terminus and the recombinant proteins were incubated with HIS-tagged SDE1 in

Table 2.1 - Candidates identified from yeast-two-hybrid screening using SDE1 as the bait. Only “xylem cysteine proteinase 1” was confirmed positve using pairwise Y2H assay.

SDE1-interacting candidate	NCBI Sequence ID	Pairwise Y2H Positive
Diacylyglycerol (DAG) protein, chloroplastic	XM_006475194	No
E3 ubiquitin−protein ligase RNF12−B	XM_006489385	No
Putative E3 ubiquitin−protein ligase XBAT31	XM_006488247	No
Heavy−metal−associated domain−containing protein	XM_006467144	No
Calcyclin−binding protein	XM_006467400	No
Xylem cysteine proteinase 1	XM_006493578	Yes

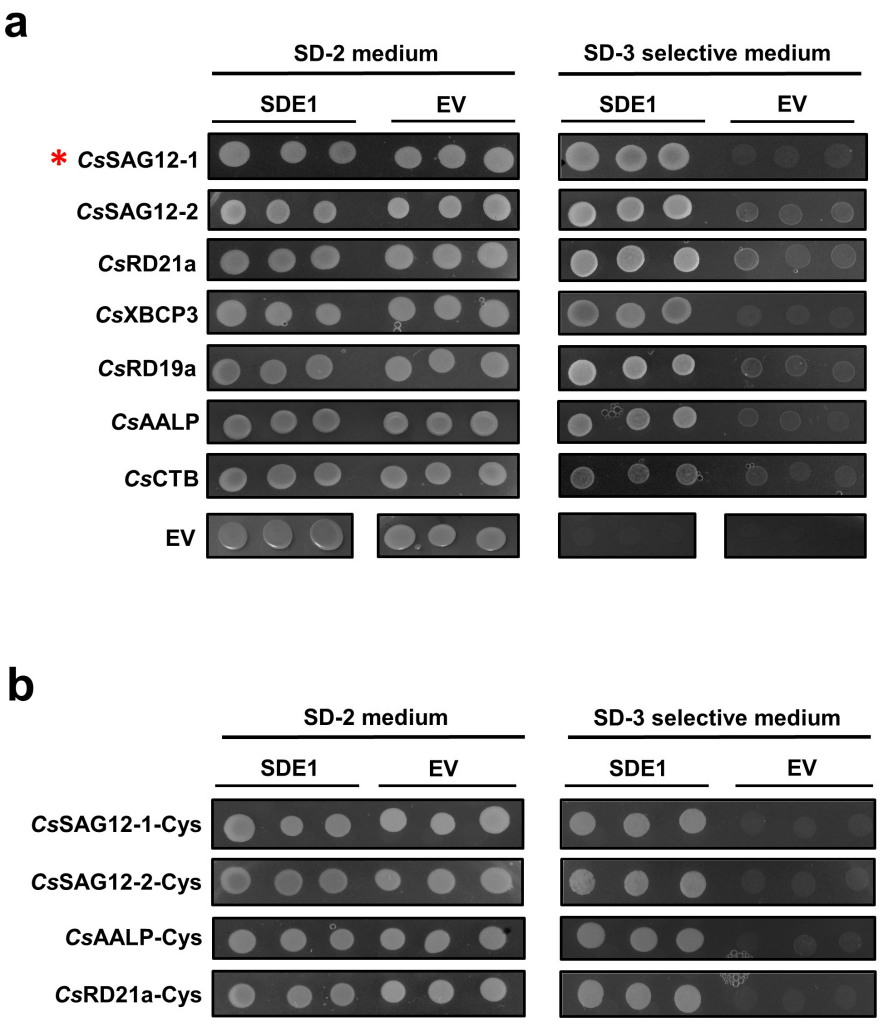

Figure 2.1 - SDE1 interacts with citrus papain-like cysteine proteases. a) Yeast-two-hybrid (Y2H) assays using the *C*Las effector SDE1 as the bait and full-length citrus papain-like cysteine proteases (*Cs*PLCPs), representing different subfamilies as the prey. SDE1 was cloned into the vector pGBKT7 and individual *Cs*PLCPs were cloned into the vector pGADT7. Growth of yeast cells on SD-3 selective media represents protein-protein interaction, growth of the same cells on SD-2 media confirms yeast transformation. Yeast transformed with the empty vectors served as negative controls. The initial PLCP found from Y2H screening (*Cs*SAG12-1, XM_006495158) is indicated with an asterisk (*). **b)** Y2H assay examining the interaction of SDE1 with the cysteine protease domain of *Cs*PLCPs.

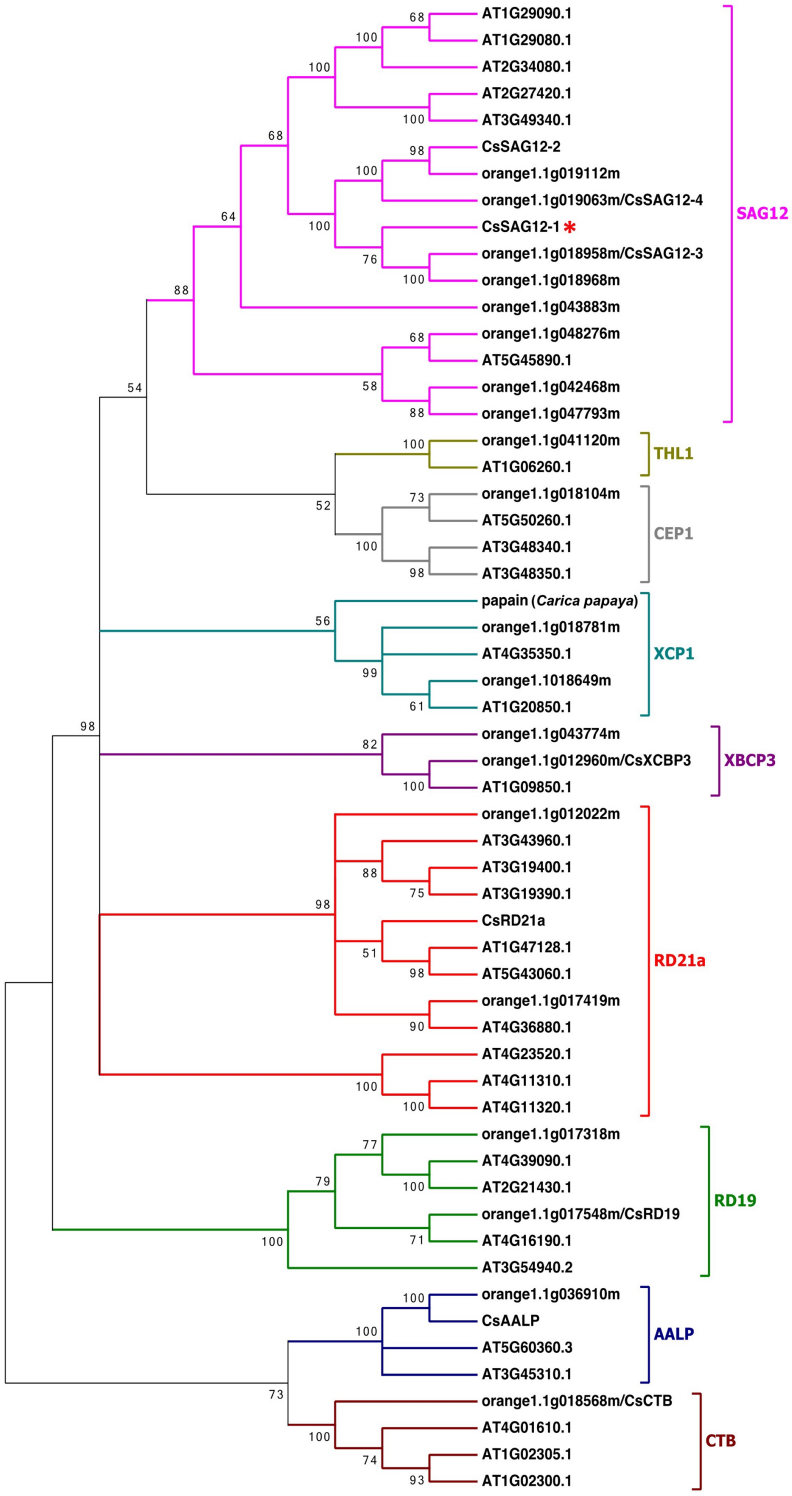
AT1G29090.1
AT1G29080.1
AT2G34080.1
AT2G27420.1
AT3G49340.1
CsSAG12-2
orange1.1g019112m
orange1.1g019063m/CsSAG12-4
CsSAG12-1 *
orange1.1g018958m/CsSAG12-3
orange1.1g018968m
orange1.1g043883m
orange1.1g048276m
AT5G45890.1
orange1.1g042468m
orange1.1g047793m
SAG12
orange1.1g041120m
AT1G06260.1
THL1
orange1.1g018104m
AT5G50260.1
AT3G48340.1
AT3G48350.1
CEP1
papain (Carica papaya)
orange1.1g018781m
AT4G35350.1
orange1.1018649m
AT1G20850.1
XCP1
orange1.1g043774m
orange1.1g012960m/CsXCBP3
AT1G09850.1
XBCP3
orange1.1g012022m
AT3G43960.1
AT3G19400.1
AT3G19390.1
CsRD21a
AT1G47128.1
AT5G43060.1
orange1.1g017419m
AT4G36880.1
AT4G23520.1
AT4G11310.1
AT4G11320.1
RD21a
orange1.1g017318m
AT4G39090.1
AT2G21430.1
orange1.1g017548m/CsRD19
AT4G16190.1
AT3G54940.2
RD19
orange1.1g036910m
CsAALP
AT5G60360.3
AT3G45310.1
AALP
orange1.1g018568m/CsCTB
AT4G01610.1
AT1G02305.1
AT1G02300.1
CTB

Figure 2.2 - Phylogeny and subfamily classification of canonical PLCPs in the *Citrus sinensis* (L.) Osbeck genome. The phylogenetic tree was made with MEGA6.06 (100 bootstrap replicates, Maximum Likelihood method, Jones-Taylor-Thornton model), using the *Arabidopsis thaliana* PLCP subfamily classification[22]. The asterisk (*) indicates the initially found *Cs*SAG12-1.

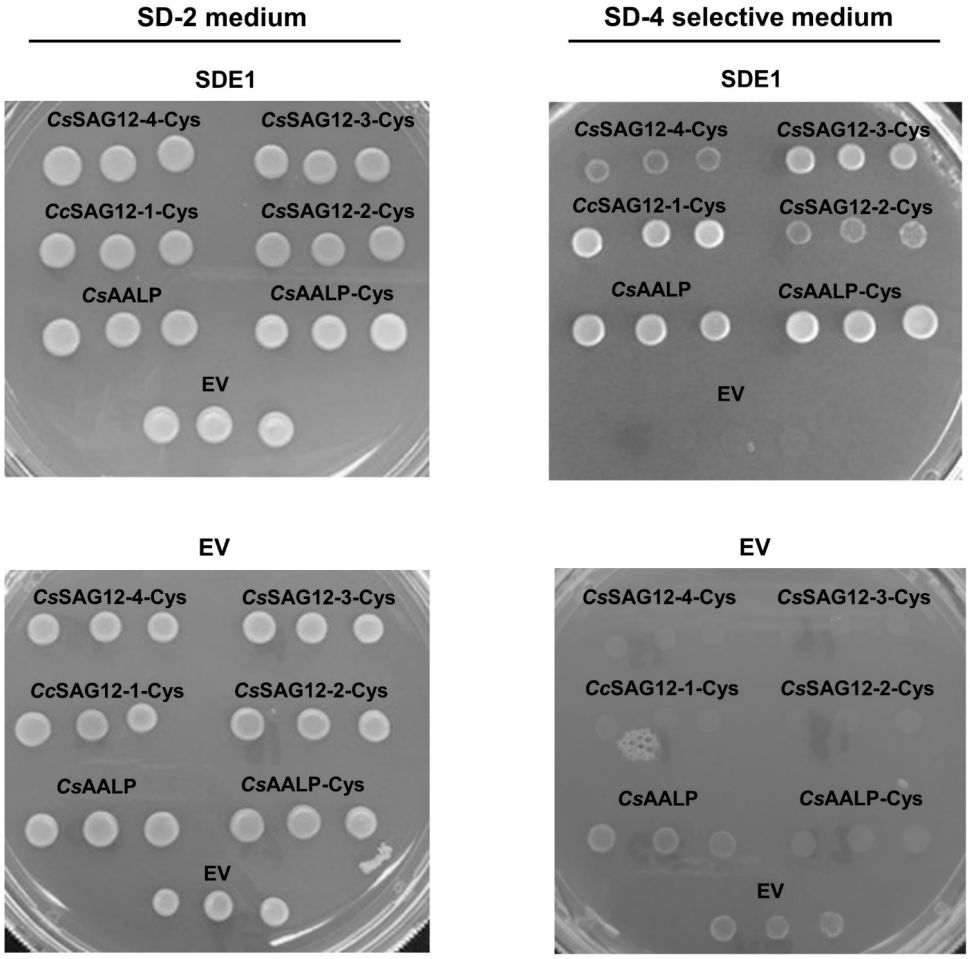

Figure 2.3 - SDE1 interacts with additional PLCPs from the SAG12 subfamily. Pairwise yeast-two-hybrid (Y2H) assay using SDE1 as bait and the cysteine protease domains of PLCPs (*Cs*SAG12-1, *Cs*SAG12-3, *Cc*SAG12-4) as the prey. Growth of yeast on SD-4 selective medium represents protein-protein interaction, growth of yeast on SD-2 medium confirms yeast transformation. Yeast cells transformed with pGBKT7 and pGADT7 empty vectors served as negative controls. *Cs*AALP (full-length) and *Cs*AALP-Cys (cysteine protease domain only) served as positive controls.

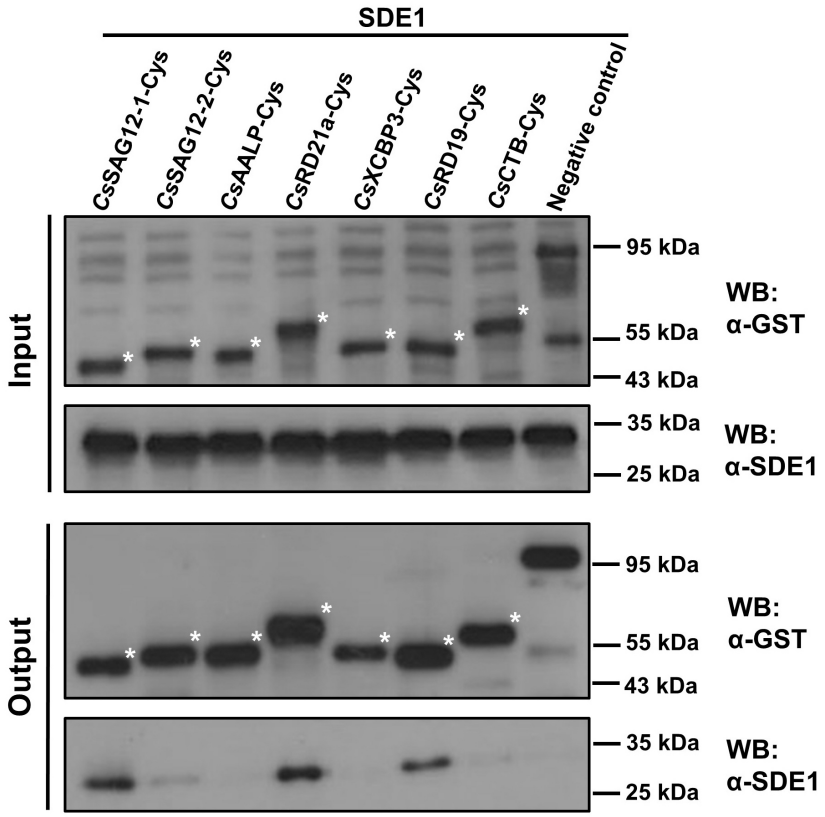

Figure 2.4 - SDE1 interacts with citrus papain-like cysteine proteases *in vitro*. *In vitro* pull-down assay using the GST-tagged cysteine protease domain of *Cs*PLCPs to immunoprecipitate SDE1 protein. Input and immunoprecipitated proteins (output) were visualized by Western blotting using anti-GST and anti-SDE1 antibodies. Asterisks (*) indicate the protein bands that correspond to individual *Cs*PLCPs. GST-tagged *Arabidopsis* Double-stranded DNA binding protein 4 (*At*DRB4) was used as a negative control.

excess. The protein complexes were immunoprecipitated using glutathione beads and enrichment of SDE1 was detected by Western blotting. Our results found that SDE1 co-precipitated with the protease domains of *Cs*SAG12-1, *Cs*SAG12-2, *Cs*RD19, and *Cs*RD21a (**Figure 2.4**). Although *Cs*AALP, *Cs*XCBP3, and *Cs*CTB were able to interact with SDE1 in yeast, these interactions were not detected in the *in vitro* pull-down assay. This could be, at least in part, due to the poor solubility of the recombinant GST-PLCP proteins when produced in *E. coli*. The cysteine residues within the protease domains have the potential to form disulfide bonds[19,22], which may have resulted in incorrect folding and/or low solubility of these normally secreted PLCPs when expressed in the cytoplasm. Another possibility is that the pull-down assay is more stringent (and thus, less sensitive) in monitoring particular SDE1-PLCP interactions than Y2H. Nonetheless, these experiments strongly suggest that SDE1 can interact with multiple PLCPs belonging to different subfamilies through the conserved cysteine protease domain.

SDE1 inhibits PLCP activity

Knowing SDE1 interacts with PLCPs through the protease domain, I next examined whether SDE1 could inhibit proteolytic activity. Several assays were used to measure the proteolytic activities of PLCPs in the presence of SDE1. In all these assays, the chemical inhibitor E-64, which forms a covalent bond with the catalytic cysteine of the PLCP protease domain, was used as a positive control[24].

First, I examined the inhibitory effect of SDE1 on the proteolytic activity of papain, a PLPC from papaya[22]. Fluorescein-labeled casein was used as a substrate which, upon cleavage by papain, releases a fluorescent signal that can be quantified using a fluorometer. My results found that SDE1 could inhibit substrate cleavage by papain in a

dose-dependent manner (**Figure 2.5a**). Using 100 and 500 nM purified SDE1 protein, the proteolytic activity of papain was decreased by 12% and 49%, respectively, when compared to papain alone. This inhibitory effect is significant, although weaker compared to that of E-64, which reduced protease activity at the same concentrations by about 68% and 85%. As a negative control, addition of BSA or another *C*Las effector, termed SDE2 (CLIBASIA_03230), did not reduce the protease activity of papain (**Figure 2.5a and 2.6**).

Next, I examined whether SDE1 binds near the catalytic site of PLCPs, if so, its interaction with PLCPs should be blocked by pre-incubation with E-64. To test this hypothesis, I conducted *in vitro* pull-down assays with or without E-64 using the protease domains of the citrus PLCPs, *Cs*SAG12-1 and *Cs*RD21a. A third PLCP was also included, resistance to *Cladosporium fulvum* 3 (RCR3), which is a member of the tomato SAG12 subfamily and is known to be inhibited by the Avr2 effector from the fungal pathogen *C. fulvum*[25]. The protease domains of these PLCPs were expressed in *E. coli* and enriched using GST affinity resins. PLCP-bound resins were pre-incubated with 200 μM E-64 and the enrichment of SDE1 with the resins was examined by Western blotting. Co-precipitation of SDE1 with all three PLCPs was reduced in the presence of E-64, suggesting that SDE1 binds near the catalytic cysteine bound by E-64, resulting in a steric hindrance around the active site (**Figure 2.7**). Since SDE1-PLCP interactions were not completely abolished by the addition of E-64, it is likely that SDE1 does not directly bind to the catalytic cysteine residue. Rather, SDE1 might block the catalytic cleft to prevent access to substrates, thus inhibiting proteolytic activity. Alternatively, the binding

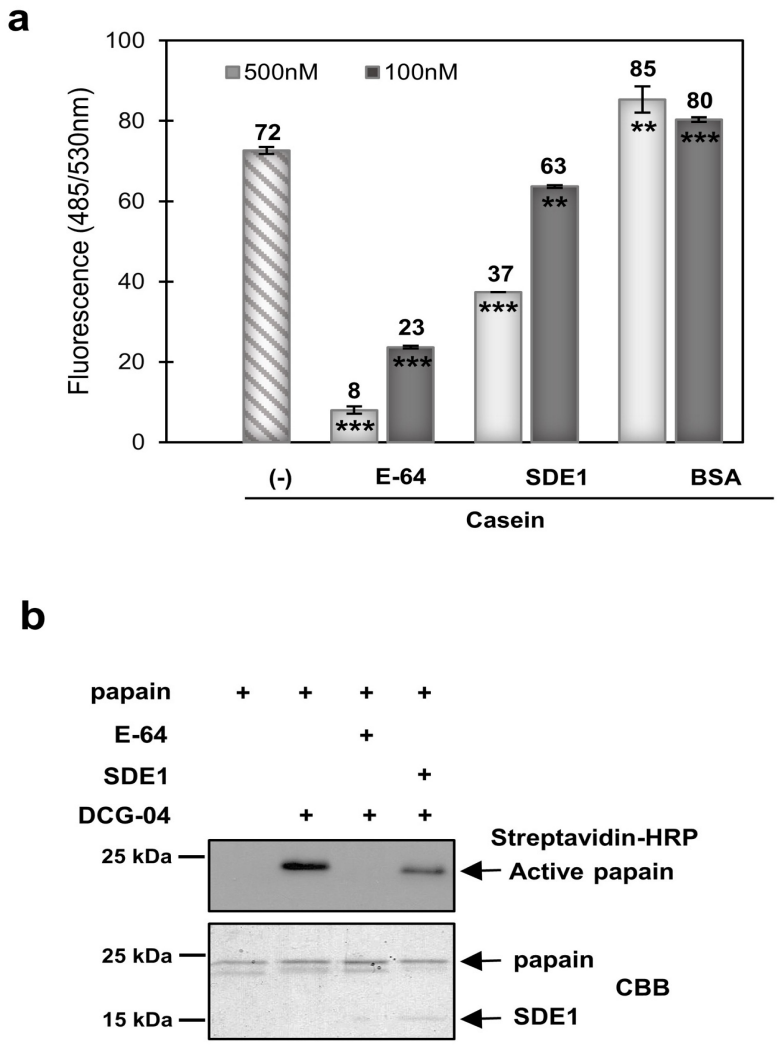

Figure 2.5 - SDE1 inhibits PLCP activity *in vitro*. **a**) Proteolytic activity of papain measured by digestion of a fluorescent casein substrate in the presence of E-64, purified SDE1 protein, or BSA (as a negative control). Fluorescence was measured at 485/530 nm excitation/emission. Mean ± standard deviation (n=3) is shown. Asterisks (*) indicate statistically significant differences based on the two-tailed Student's *t*-test. $p < 0.01$ = **, $p < 0.001$ = ***. **b**) Inhibitory effect of SDE1 on the protease activity of papain examined by activity-based protein profiling (ABPP). Active papain was labeled by DCG-04 in the presence of 10 μM E-64 or 1.6 μM purified SDE1 protein and detected using streptavidin conjugated with horseradish peroxidase (HRP).

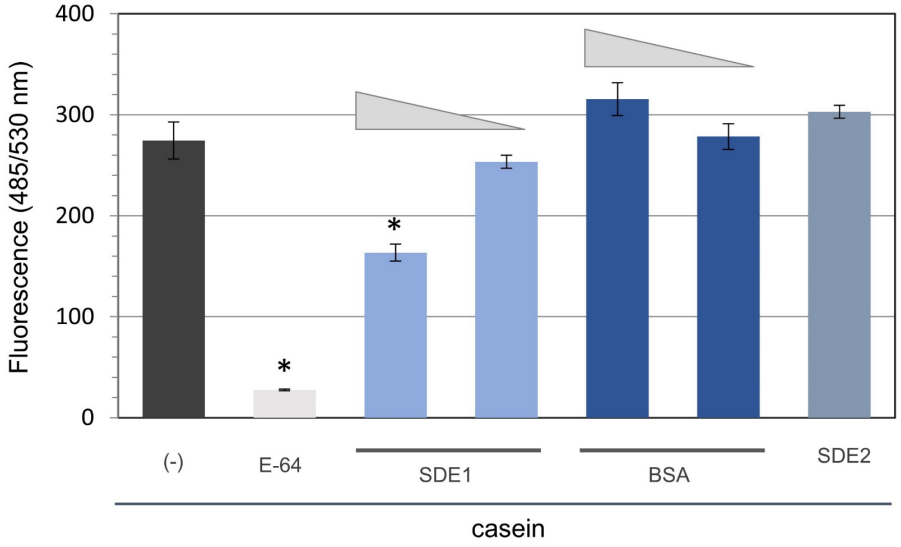

Figure 2.6- SDE1 but not SDE2 can inhibit the protease activity of papain. Proteolytic activity of papain measured by digestion of fluorescent casein substrates in the presence of 1 μM E-64, purified SDE1 (0.74 and 0.15 μM) or SDE2 (0.3 μM) protein (CLIBASIA_03230), and BSA (0.74 and 0.15 μM). Fluorescence was measured at 485 nm excitation over 530 nm emission. Values are average of duplicates with the Standard Deviation shown as the error bars. Statistical analysis was done using Student's two-tailed t-test and significant differences ($p < 0.05$) are labeled with asterisks (*).

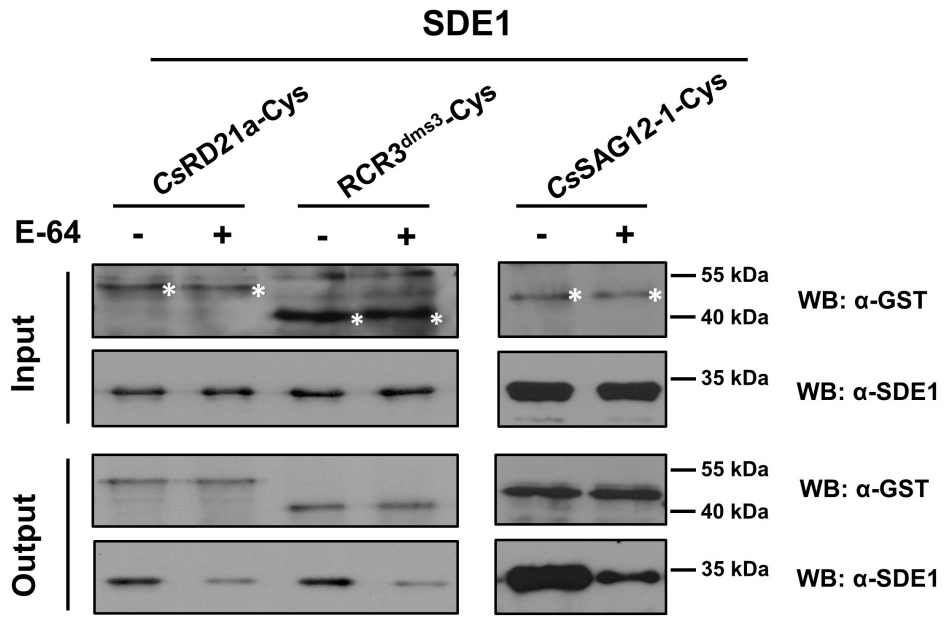

Figure 2.7 - E-64 inhibits the interaction of SDE1 with PLCPs *in vitro*. Proteins extracted from *E. coli*-expressing GST-tagged cysteine protease domains of *Cs*RD21a, *Cs*SAG12-1 or RCR3^{dms3} (from the wild potato species *Solanum demissum*) were pre-incubated with E-64. The enrichment of SDE1 on PLCP-bound resins was then examined by Western blotting using an anti-SDE1 antibody. Asterisks (*) indicate the protein bands corresponding to individual PLCPs.

of E-64 to the catalytic cysteine could result in conformational changes of the protease, and therefore, partially interfere with SDE1's interaction with the PLCPs.

Finally, I directly measured the protease activity of SDE1-interacting PLCPs using activity-based protein profiling (ABPP) where DCG-04, a biotinylated derivative of E-64, is used as a probe[24]. Since E-64 only binds to the active form of cysteine proteases, Western blots using streptavidin conjugated with horseradish peroxidase (HRP) can detect DCG-04-labled PLCPs via biotin, and the signal intensity reflects their activity level. First, I examined ABPP of papain in the presence of SDE1 or E-64. My results indicated that pre-incubation with SDE1 at 1.6 μM was able to reduce DGC-04 labeling by about 53%, demonstrating that SDE1 suppresses the protease activity of papain *in vitro* (**Figure 2.5b**). Pre-incubation of papain with E-64 (10 μM) completely abolished the DCG-04 labeling, which is consistent with the results from the *in vitro* protease activity assay using the fluorescein-labeled substrate.

I also conducted ABPP in a semi-*in vitro* assay using recombinant SDE1 protein purified from *E. coli* and PLCPs expressed in plant tissues. To this end, full-length *CsRD21a* was transiently expressed in *Nicotiana benthamiana* leaves (*CsRD21a* construct generated by Dr. Simon Schwizer). Using the native N-terminal secretion signal, *Cs*RD21a was secreted into the apoplast as shown by Coomassie brilliant blue (CBB) stain comparing control apoplastic fluids from wild-type *N. benthamiana* to those transiently expressing *Cs*RD21a (**Figure 2.8a**). *Cs*RD21a could be labeled by DCG-04, suggesting that it is an active enzyme. A reduction of *Cs*RD21a activity was observed with the addition of SDE1 in a dose-dependent manner using 0.8, 1.6, or 3.2 μM purified proteins (**Figure 2.8a**). We then determined whether SDE1 could inhibit other PLCPs in citrus. Total proteins were extracted from leaves of *C. sinensis* (L.) Osbeck. PLCP

accumulation was induced by spraying the leaves with 2 mM of the defense hormone salicylic acid (SA)[26], followed by total protein extraction and incubation with purified SDE1 protein. In this experiment, the labeled PLCPs were further concentrated using streptavidin beads. Immunoblots using streptavidin-HRP showed PLCP activity was greatly decreased after incubation with 120 nM SDE1, and completely inhibited with 25μM E-64 (**Figure 2.8b**). Together, these results demonstrate that SDE1 suppresses the protease activity of *Cs*RD21a and other citrus PLCPs natively in the plant cells.

To further demonstrate that PLCPs are the *in vivo* targets of SDE1 in citrus, transgenic seedlings of *Citrus paradisi* (L.) Macfad. (Duncan grapefruit) expressing *SDE1* were generated (without the N-terminal 1-24 amino acids which correspond to a secretion signal peptide) under the cauliflower mosaic virus *35S* promoter. Total protein extracts from leaf tissues of one-year-old seedlings were labeled with DCG-04 and the levels of active PLCPs were examined by Western blotting using streptavidin-HRP. My results show reduced PLCP activities in four independent *SDE1*-expressing lines (SDE1-5, SDE1-6, SDE1-8, and SDE1-9), relative to non-transgenic Duncan grapefruit controls (**Figure 2.8c**). I confirmed that these lines were indeed producing SDE1 proteins using Western blotting (**Figure 2.9**). In addition, the transgenic line SDE1-10 exhibited little to no SDE1 protein accumulation (**Figure 2.9**), which correlated with a lack of reduction in protease activity in this line (**Figure 2.8c**). Taken together, these data strongly suggest that SDE1 can inhibit the protease activity of PLCPs in citrus.

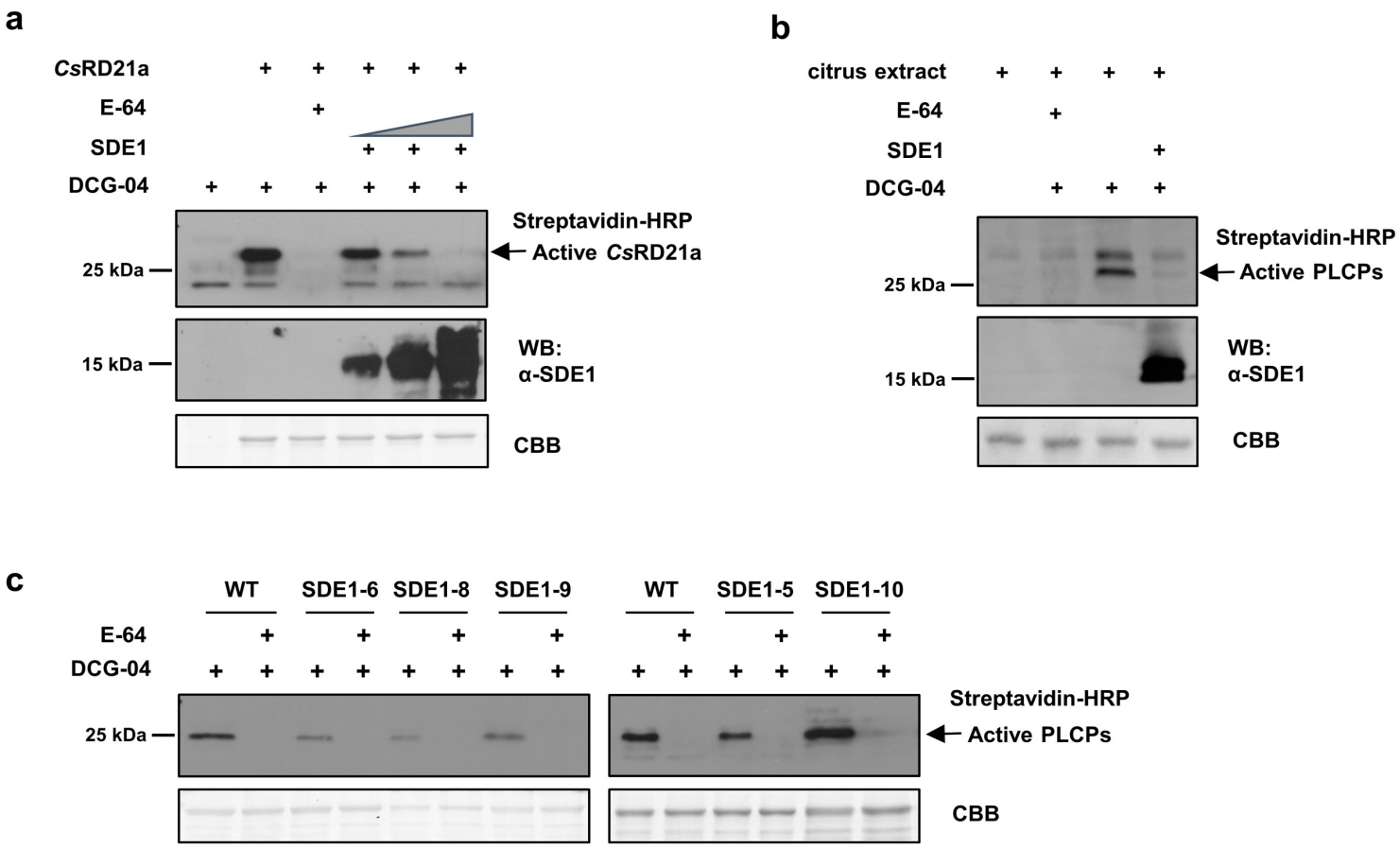
a
CsRD21a
E-64
SDE1
DCG-04
25 kDa
15 kDa
Streptavidin-HRP
Active CsRD21a
WB:
α-SDE1
CBB
b
citrus extract
E-64
SDE1
DCG-04
25 kDa
15 kDa
Streptavidin-HRP
Active PLCPs
WB:
α-SDE1
CBB
c
WT
SDE1-6
SDE1-8
SDE1-9
WT
SDE1-5
SDE1-10
E-64
DCG-04
25 kDa
Streptavidin-HRP
Active PLCPs
CBB

Figure 2.8 - SDE1 inhibits PLCP activity in plant cells. a) SDE1 inhibits the activity of *Cs*RD21a. *Cs*RD21a-Flag (with its N-terminal secretion signal) was expressed in *N. benthamiana*. Active protease in the apoplastic fluid was labeled via ABPP. ImageJ analysis of the signal intensity revealed approximately 9%, 62%, and 96% reduction of *Cs*RD21a activity in the presence of 0.8, 1.6, or 3.2 μM purified SDE1 protein, respectively. **b)** SDE1 inhibits PLCP activity in citrus. Total protein extracts from Navel orange (*C. sinensis*) leaves were labeled via ABPP in the presence of 120 nM purified SDE1 protein. Active proteases were enriched using streptavidin beads and detected using streptavidin-HRP conjugates. **c)** Transgenic grapefruit (Duncan) seedlings expressing *SDE1* exhibit reduced protease activity. Five individual lines were analyzed by ABPP. SDE1-10 does not have significant SDE1 protein accumulation and served as a negative control.

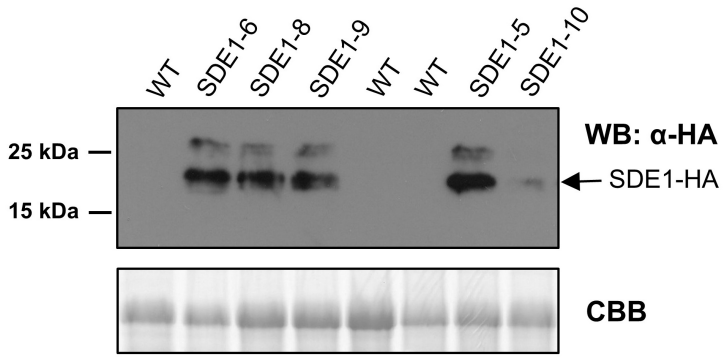

Figure 2.9 - SDE1 proteins accumulate in transgenic citrus. Transgenic and control citrus are in *Citrus paradisi* (L.) Macfadyen (Duncan grapefruit) background. Leaves from individual transgenic citrus lines (one-year-old seedlings) were ground with liquid nitrogen into powder and re-suspended in 2x Laemmli loading dye[50]. Samples were boiled for five minutes, then separated on a 12% protein gel for Western blotting. SDE1 proteins were detected by anti-HA antibody (Santa Cruz Biotechnology, CA). Gel stained with Coomassie brilliant blue (CBB) served as a loading control. Leaf tissue from wild-type (WT) grapefruit seedlings of the same age were included as controls. Transgenic plants generated by Dr. Zhiqian Pang, University of Florida.

Citrus PLCPs accumulate during CLas infection of citrus

Analysis of publicly available transcriptome data[28,29] found genes encoding *Cs*PLCPs of several subfamilies including, but not limited to, SAG12, RD21a, and AALP to be up-regulated during *C*Las-infection. These results indicate that citrus PLCPs accumulate during infection and may act as defense proteases in *C*Las-infected trees.

Since *C*Las is a phloem-colonizing bacterium, we assessed whether SDE1 and PLCPs could both be detected in the phloem sap of infected citrus trees at the protein level. For this purpose, we performed direct citrus-tissue imprint using anti-SDE1[16] or anti-AALP[30] antibodies, respectively. We monitored AALP as a representative of PLCPs in this experiment due to the availability of the antibody. Young stems from *C*Las-infected and non-infected (i.e. *C*Las-free) trees of *Citrus paradisi* (L.) Macfad. (Rio Red grapefruit) were freshly cut and imprinted onto nitrocellulose membranes, which were then incubated with either anti-SDE1 or anti-AALP. For the *C*Las-infected trees, I examined both symptomatic and asymptomatic tissues, which presumably represent late and early infection stages as suggested by the bacterial titers. My results show that while SDE1 was only present in the infected tissues, AALPs were detected from both healthy and infected tissues (**Figure 2.10**). However, the signals representing AALPs were stronger in the infected stems, both symptomatic and asymptomatic, compared to those from the healthy stems. This is consistent with the increased of PLCP gene expression revealed from the transcriptome data analysis. Furthermore, similar to SDE1, the AALP signals were mainly detected from the bark layers, which is enriched with phloem cells.

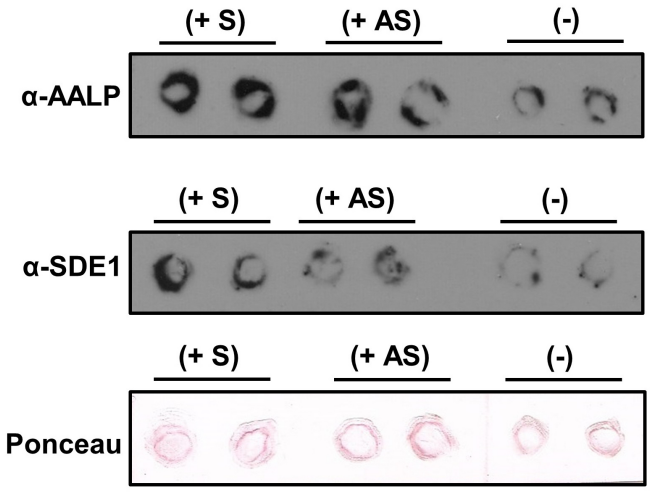

Figure 2.10 - *Cs*PLCPs accumulate during infection. Protein abundance of papain-like cysteine proteases (PLCPs) was determined in healthy (-) or *C*Las-infected (+) citrus branches using an anti-AALP antibody. Freshly cut stems were stamped onto nitrocellulose membranes and PLCPs and SDE1 were detected using Western blotting. The titer of *C*Las in each sample was evaluated by quantitative PCR with observed Ct values of 27.97 for symptomatic tissue (+ S), and not detected for asymptomatic tissue from the same infected tree (+ AS) or tissue from an uninfected tree (-). Ponceau-stained membrane was shown as a control.

SDE1 does not inhibit RCR3 activity in solanaceous plants

In tomato, inhibition of RCR3 activity by the *C. fulvum* effector Avr2 activates Cf-2-mediated immune responses, including programmed cell death, conferring resistance to the fungal pathogen[25]. SDE1 interacts with RCR3 *in vitro* (**Figure 2.7**). We therefore tested whether SDE1 can inhibit the activity of PLCPs from solanaceous plants. To do this, I performed ABPP using RCR3 from *Solanum pimpinellifolium* ($RCR3^{pim}$) and from the wild potato species *Solanum demissum* ($RCR3^{dms3}$)[38]. Unlike with *Cs*RD21a, SDE1 was unable to inhibit the activity of either $RCR3^{pim}$ or $RCR3^{dms3}$ proteins (**Figure 2.11**). These results indicate that the lack of Cf-2-mediated cell death in response to SDE1 is likely due to the inability of the *C*Las effector to inhibit the protease activity of RCR3 from these non-host plants and illustrates the host-specific function of SDE1.

SDE1 promotes CLas infection in citrus

To determine if SDE1 could promote bacterial infection we performed *C*Las graft inoculation on the different SDE1-expressing transgenic citrus lines (**Figure 2.9**) and non-transgenic grapefruit controls. Cycle threshold (Ct) values were taken monthly post-*C*Las graft inoculation. Comparison of Ct values found that SDE1-expressing transgenic lines exhibit lower Ct scores than infected controls, indicating the presence of SDE1 contributes to *C*Las growth in citrus (**Figure 2.12**). Lines SDE1-8 and SDE1-9, which exhibited reduced total active PLCP activity (**Figure 2.8c**) had particularly low Ct values and line SDE1-8 died four months post infection (**Table 2.2**), indicating SDE1 contributes to *C*Las virulence in these lines likely via inhibition of PLCP activity.

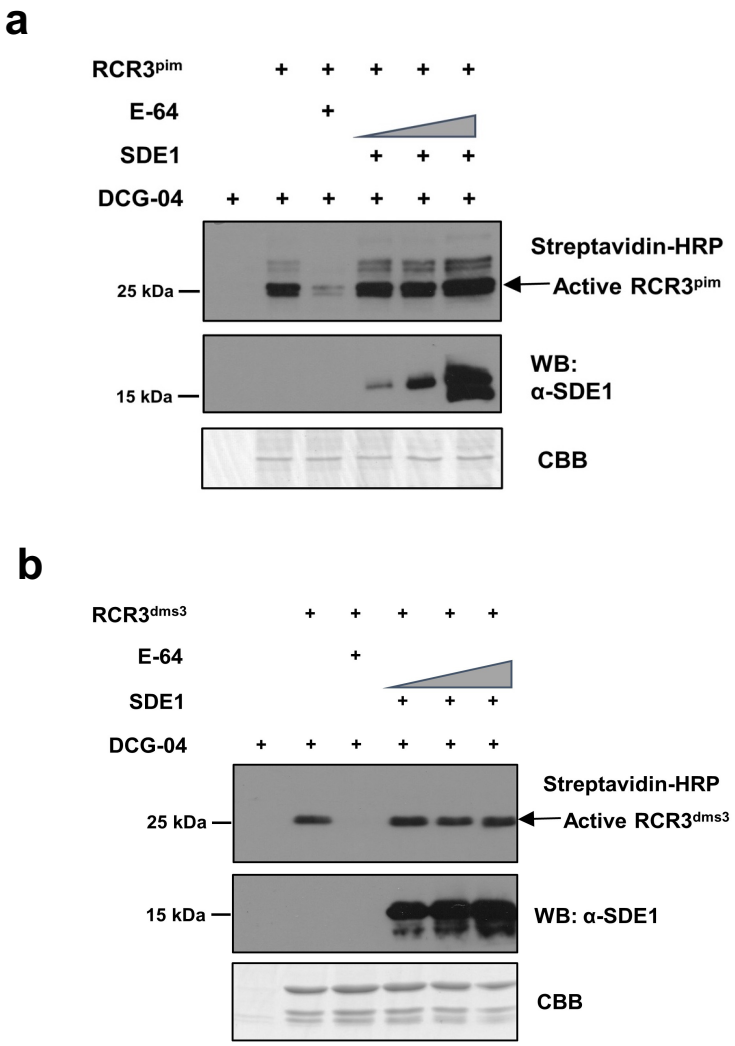

Figure 2.11 - SDE1 does not inhibit Solanaceous PLCP activity. a) SDE1 does not inhibit the activity of the *Solanum pimpinellifolium* PLCP, RCR3^{pim}. **b)** SDE1 does not inhibit the activity of the wild potato species *Solanum demissum* PLCP, RCR3^{dms3}. Full-length of RCR3^{pim}-HIS or RCR3^{dms3}-HIS were transiently expressed in *N. benthamiana* and secreted into the apoplast. Apoplastic fluid was extracted and the active protease was labeled via ABPP in the presence of 0.8, 1.6 or 3.2 µM of purified SDE1 protein. Coomassie brilliant blue (CBB) served as a loading control.

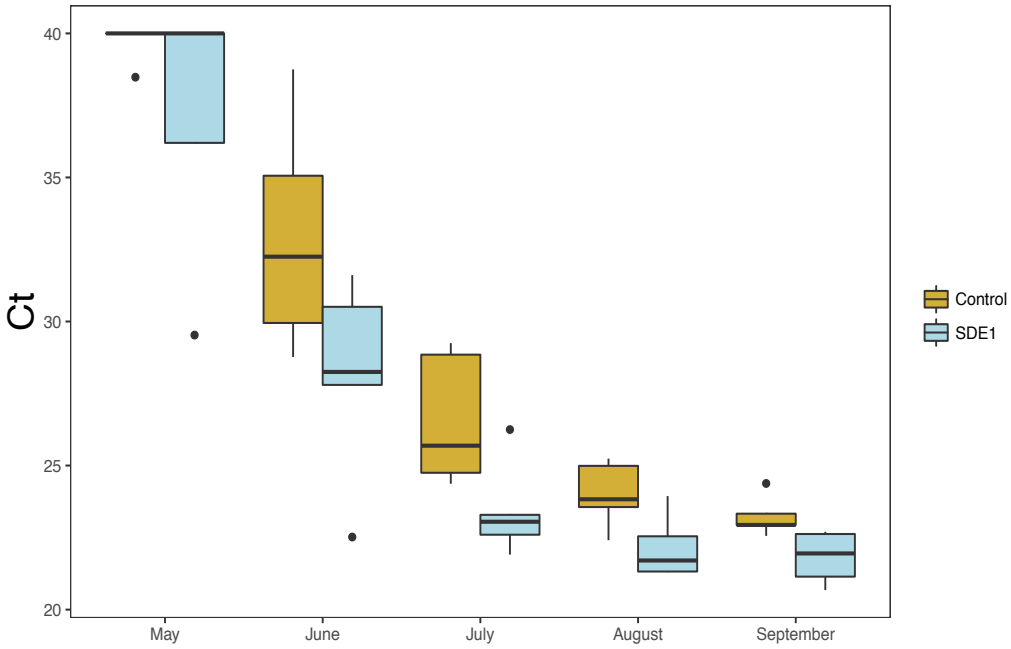

Figure 2.12 – *C*Las infected SDE1-expressing citrus plants have higher *C*Las titers relative to infected controls. SDE1-expressing transgenic lines and non-transgenic controls were graft inoculated with *C*Las in March and Ct values were measured monthly post-inoculation. Detectable Ct values were not observed until two months post graft inoculation. No amplification is represented as a Ct value of 40. Each group (SDE1 or control) contains five individual lines. Dots represent outliers. Line SDE1-8 died in August and was therefore removed from the dataset at that timepoint.

Table 2.2 – Cycle threshold (Ct) scores representing *C*Las titers in SDE1 transgenic and control citrus post graft inoculation. *C*Las *rplKAJL-rpoBC* (β-operon) region was used for qPCR detection. ± represents the standard deviation of triplicates.

SDE1 transgenic lines					
	19-May	**19-Jun**	**19-Jul**	**19-Aug**	**19-Sep**
SDE1-7	36.20±1.11	30.51±0.23	22.60±0.11	21.33±0.30	20.68±0.10
SDE1-8	29.53±1.08	22.52±0.17	21.91±0.03	Dead	Dead
SDE1-9	NA	27. 80±0.34	23.05±0.09	22.08±0.08	22.60±0.07
SDE1-12	NA	28. 25±0.29	23.29±0.05	21.30±0.04	21.30±0.05
SDE1-15	NA	31.61±0.51	26.25±0.17	23.94±0.34	22.70±0.10
Controls					
	19-May	**19-Jun**	**19-Jul**	**19-Aug**	**19-Sep**
Control-2	NA	28.77±0.05	24.75±0.07	23.56±0.19	22.94±0.39
Control-3	NA	29.95±0.51	25.69±0.15	23.82±0.07	23.33±0.45
Control-4	38.48±0.56	38.75±0.22	28.85±0.64	24.99±0.14	22.56±0.04
Control-5	NA	35.06±1.37	29.25±0.11	25.24±0.02	24.38±0.14
Control-6	NA	32.25±0.12	24.37±0.85	22.41±0.32	22.94±0.05

CONCLUSIONS AND DISCUSSION

The devastating impact of HLB on the citrus industry warrants immediate yet sustainable solutions, which we are only beginning to unveil. Advances in understanding the molecular interactions between *C*Las and citrus will provide the fundamental knowledge needed to develop robust HLB management techniques. In this chapter, I used the effector SDE1 as a molecular probe to reveal PLCPs as virulence targets of *C*Las in citrus, thereby providing one of the first mechanistic insights into HLB pathogenesis.

PLCPs have been reported to regulate plant immunity and contribute to defense against a broad range of pathogens including bacteria, fungi, and oomycetes[20,21,25,32]. For example, the SAG12 subfamily members, RCR3 and PIP1, in tomato species contribute to defense against the oomycete pathogen *Phytophthora infestans*[25,34]. Knocking out or silencing specific *PLCP* genes in *Arabidopsis*, tomato, and *N. benthamiana* resulted in increased susceptibly to various pathogens[19,35]. The mechanisms underlying PLCP-mediated defense could work on multiple levels. They may directly hydrolyze pathogen components; for example, growth inhibition by papain against the papaya pathogen *Phytophthora palmivora* was recently reported[36]. However, we did not observe an inhibitory effect of papain on bacterial growth in artificial media, suggesting that direct antimicrobial activity by PLCPs is highly specific[61]. It is possible that PLCPs contribute to the citrus response to *C*Las by regulating defense signaling. For example, it was proposed that PLCPs could cleave microbial or host peptides to elicit defense responses[19].

Bacterial, fungal, and oomycete pathogens as well as nematodes have all evolved effector proteins to suppress PLCP activities in order to promote

infection[20,21,25,32,37,38,39]. The *C. fulvum* effector Avr2 and the *Ustilago maydis* effector Pit2 play important roles during fungal infection of their respective plant hosts[40,41]. Similarly, Cip1 produced by the bacterial pathogen *P. syringae* is required for full virulence in *Solanum lycopersicum* Money-Maker (tomato) and *A. thaliana* through inhibition of C14 protease activity, a member of the RD21a subfamily of PLCPs[3232]. Cip1 is also Sec-secreted, indicating that it might similarly promote *C*Las infection in citrus. Indeed, we found that SDE1 can partially compliment Cip1 virulence during infection of *A. thaliana* via a *P. syringae* pv. *tomato* strain DC3000 *cip1* mutant[61]. Although PLCPs are a major hub of effector targets, none of these effectors share sequence similarities, suggesting that they have evolved independently (through convergent evolution) to interfere with the activities of this important group of defense regulators.

During pathogen recognition, PLCP abundance is usually increased alongside activity[31]. In collaboration with Dr. Gitta Coaker's lab at UC Davis, we performed mass spectrometry analysis on *C*Las-infected citrus in order to uncouple PLCP abundance and activity during *C*Las infection[61]. We found the abundance of *Cs*SAG12-1, *Cs*SAG12-3, and *Cs*SAG12-4 significantly increased in infected trees, whereas their activity remained unchanged. These results indicate certain SAG12 subfamily members are potentially involved in citrus defense responses and that their activities might be inhibited by *C*Las SDEs, including SDE1.

Phloem sieve tube elements are metabolically inactive and are supported by adjacent companion cells derived from the same mother cell[42]. PLCPs have been identified in phloem proteomic analyses of other plants, indicating that they could be directly secreted into sieve elements from adjacent companion cells[43,44]. In total, we detected increased accumulation of AALP, XBCP3, and SAG12 subfamily members in

*C*Las-infected citrus trees. We found that SDE1 associates with multiple citrus PLCPs in various subfamilies and there is a discordance between abundance and activity of three SAG12 members during *C*Las infection. SDE1 is potentially secreted into the phloem by *C*Las during infection, where it might act to suppress PLCP activity. SDE1 might also be able to move through the sieve elements and translocate into the companion cells via plasmodesmata to inhibit these important defense proteins (**Figure 2.13**). Further experiments are needed to investigate the mechanisms by which PLCPs contribute to citrus defense signaling and enhance immune responses to *C*Las.

The findings described in this work lay the foundation for the development of HLB-resistant germplasm through genetic manipulation. Our results showing that SDE1 does not inhibit RCR3 activity (**Figure 2.11**) and thus fails to trigger Cf-2-dependent cell death in tomato[61] illustrate the host specificity of pathogen effectors and raises the possibility of engineering a similar immune receptor pathway to elicit defense responses upon effector-mediated inhibition of citrus PLCPs. In addition, PLCPs themselves could be excellent targets for genetic modification. It has been shown that overexpression of a specific PLCP gene in *N. benthamiana* increased disease resistance to *P. infestans*[39]. CRISPR-based promoter editing to manipulate PLCP gene expression in a conditional manner in citrus is another approach that could lead to urgently needed HLB resistance or tolerance.

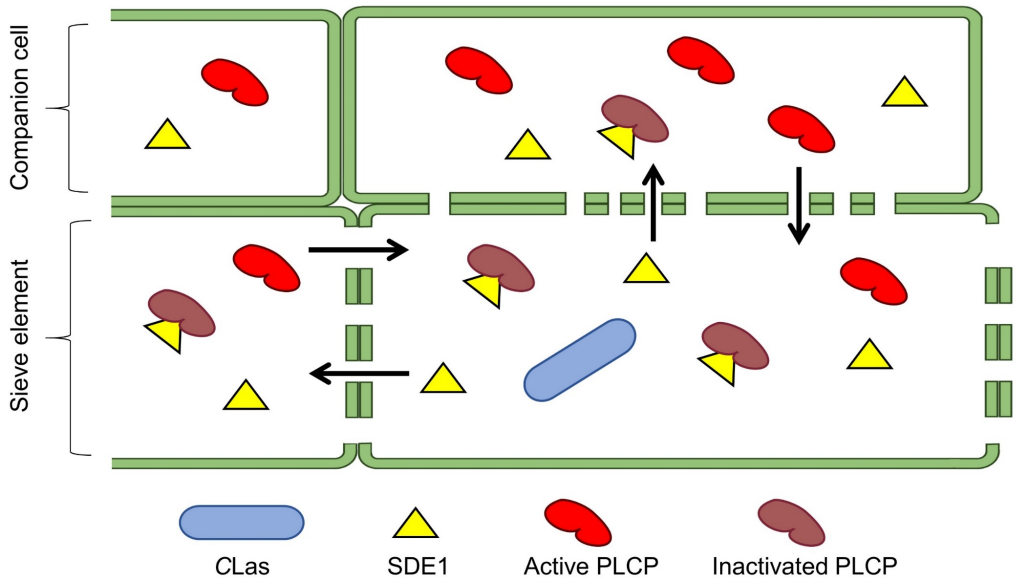

Figure 2.13 - A potential model of SDE1 and PLCP interaction in *C*Las-infected citrus. After infection, *C*Las proliferates in phloem sieve elements. Sieve elements are dependent upon adjacent, metabolically active companion cells. Citrus is able to perceive the bacterial pathogen and induce defense responses, including increased PLCP accumulation. These proteins may be directly delivered into the sieve elements through plasmodesmatal connections. *C*Las possesses the Sec secretion system and secretes multiple Sec-delivered effectors, including SDE1, which acts to inhibit the protease activity of PLCPs. SDE1 can move through the sieve elements and may be able to translocate into adjacent companion cells to suppress this PLCP-based defense responses and promote bacterial infection.

MATERIALS AND METHODS

Microbial strain growth

Escherichia coli strains DH5α, BL21, and SHuffle T7 (New England BioLabs, Ipswich, MA) were grown in Luria-Bertani (LB) medium supplemented with kanamycin at 50 µg/mL or ampicillin at 100 ug/mL at 37°C. Recombinant expression of proteins was controlled by the T7 promoter which was induced with the addition of 0.2uM IPTG overnight at 16°C. Cell cultures were checked for SDE or PLCP expression via SDS-PAGE and cell pellets were saved and frozen for protein purification and application to various *in vitro* and *in planta* assays described below. Vectors and strains used in this chapter are listed in Table A.2.

Agrobacterium tumefaciens strain GV3101 was grown in LB medium supplemented with kanamycin at 50 µg/mL at 30°C. Cultures were used for *Agro*-infiltration as described below.

Plant material and growth conditions

SDE1 transgenic citrus was generated via *Agrobacterium*-mediated transformation of grapefruit epicotyls[45]. Transgenic shoots were selected and micro-grafted onto one-month-old Carrizo citrange nucellar rootstocks. After one month in tissue culture the plants were potted in peat-based commercial potting medium and kept under greenhouse conditions. Citrus material for the imprint assay was from a commercial orchard in Donna, TX. See materials and methods for the citrus imprint assay.

Nicotiana benthamiana plants used for the *in planta* inhibition were geminated and grown in a conditioned growth room at stable 22°C with a 12/12 light/dark regime.

Plants with fully expanded adult leaves were used for *Agro*-infiltration with the *Agrobacterium* strain GV3101 containing the PLCP-HIS-expressing constructs. Proteins were extracted from leaf tissue after 48hrs by grinding the tissue in liquid nitrogen and re-suspending it in 2x Laemmli buffer[50] for evaluation via Western blotting.

Yeast-two-hybrid assays

A *Citrus sinensis* cDNA library was generated with total RNA extracted from healthy and *C*Las-infected tissues. The library was screened against SDE1 using a mating-based yeast-two-hybrid (Y2H) approach coupled with Illumina sequencing (performed by Quintarabio, CA). Sequences were analyzed by BLASTn using the NCBI database and top hits from *C. sinensis* were marked as potential SDE1-interacting proteins. Selected candidates from the Y2H screen were further tested using pairwise Y2H. The full-length cDNA of each potential SDE1 interactor was cloned into the pGADT7 prey vector (Clontech, Mountain View, CA) and transformed into yeast strain AH109 (Clontech, Mountain View, CA) containing *SDE1* in the bait plasmid pGBKT7. Transformation of the prey plasmids into AH109 containing pGBKT7 empty vector served as a negative control.

To test the interaction of SDE1 with PLCPs of various subfamilies, cDNA sequences of the PLCP representatives *Cs*SAG12-1, *Cs*SAG12-2, *Cs*RD21a, *Cs*RD19, *Cs*AALP, *Cs*XBCP3, and *Cs*CTB, excluding their signal peptides, were cloned into pGADT7 and expressed in AH109. Signal peptides were predicted using SignalP 4.1 (organism group 'Eukaryotes'; default D-cutoff values). For PLCP fragments encoding only the cysteine protease domain, full-length PLCP protein sequences were analyzed

by SMART[46,47] and sequences corresponding to the protease domains were cloned into pGADT7. The experiments were repeated at least three times with similar results.

Phylogenetic analysis of PLCPs

Protein sequences of 31 PLCP genes from *Arabidopsis thaliana*[22] and the annotated protein sequences from the entire sequenced genome of *C. sinensis* were downloaded from Phytozome (https://phytozome.jgi.doe.gov/pz/portal.html). Local BLASTp with an e-value of 1e-5 was used to search for PLCP homologs in *C. sinensis* using the *At*PLCPs as query. To confirm that the resultant *C. sinensis* sequences are indeed homologous to the queried *At*PLCPs, the BLASTp search was reversed. All PLCP protein sequences were aligned using MUSCLE v3.8.3[48]. MEGA v6.06[49] was used to construct the maximum likelihood phylogenetic tree using the James-Taylor-Thorthon model and a bootstrap value of 100.

In vitro pull-down assays

The protease domains of *Cs*SAG12-1, *Cs*SAG12-2, *Cs*RD21a, *Cs*RD19, *Cs*AALP, *Cs*XBCP3, and *Cs*CTB were cloned into the pGEX-4T2 vector (GE Healthcare, Chicago, IL) and SDE1 was cloned into pRSF-Duet vector (gift from Dr. Jikui Song, University of California, Riverside). Vectors were transformed into *E. coli* BL21 or SHuffle T7 competent cells (New England BioLabs, Ipswich, MA) for protein expression. Total proteins were extracted from *E. coli* expressing the PLCPs and incubated with 25 µL glutathione resins (Thermo Scientific, Waltham, MA) for 1 hr at 4ºC, followed by washing with TKET buffer (20 mM Tris-HCl, 200 mM KCl, 0.1 mM EDTA, 0.05% Triton X-100, pH 6.0). *SDE1*-expressing cell lysate was added to the PLCP-bound resins and

incubated for 3 hrs at 4ºC, followed by washing with TKET buffer to remove non-specifically bound proteins. Washed resins were boiled in Laemmli sample buffer[50] and the supernatants were used for gel electrophoresis and the subsequent immunoblotting. The enrichment of SDE1 proteins in PLCP-bound resins was detected using an anti-SDE1 antibody[16] followed by goat anti-rabbit-HRP (Santa Cruz, Dallas, TX). Levels of PLCPs were determined using anti-GST followed by goat anti-rabbit-HRP (Santa Cruz, Dallas, TX). After antibody incubation, the membranes were washed, and signals were developed using SuperSignal Chemiluminescent substrates (Thermo Scientific, Waltham, MA).

For the E-64 inhibition assay, glutathione resins with bound GST-tagged *Cs*SAG12-1, *Cs*RD21a, and RCR3[38] were incubated with either 200 μM E-64 as an inhibition treatment or TKET buffer as a control. Supernatant of *SDE1*-expressing cells was collected and incubated with the PLCP-bound resins for 3 hrs at 4ºC. The resins were washed and enrichment of SDE1 detected by electrophoresis and subsequent immunoblotting as described above. The experiments were repeated at least two times with similar results.

In vitro protease activity assay with papain

The EnzChek protease assay kit (Molecular Probes, Eugene, OR) was used to measure protease activity. Tag-free SDE1, E-64 (Sigma-Aldrich, St. Louis, MO), and BSA (Gold Biotechnologies, St. Louis, MO) at two different concentrations (100 and 500 nM) were mixed with papain (Sigma-Aldrich, St. Louis, MO) at 100 μg/mL and added to 96-well Immulon plates (Thermo Scientific, Waltham, MA) containing BODIPY FL casein substrate. Papain with MES buffer alone served as a no treatment control for proteolytic

activity and SDE2 (CLIBASIA_03230) at 300 nM served as an alternative *C*Las effector control. Reactions were allowed to perform for 1 hr at room temperature in the dark before fluorescence was measured using a Tecan Pro 2000 plate reader at 460/480 nm excitation/emission, with a gain value of 50. *P*-values were determined using a two-tailed student's *t*-test. SDE1 and SDE2 recombinant proteins were purified from *E. coli* using His60 Ni-NTA Superflow resins (Clontech, Mountain View, CA). The purified SDE1 proteins were cleaved with Ubiquitin-like-specific protease 1 (ULP1) to remove the His-SUMO tag, generating tag-free SDE1 proteins. The experiments were repeated at least three times with similar results.

Activity-based protein profiling (ABPP)

Papain (Sigma-Aldrich, St. Louis, MO), *Nicotiana benthamiana* apoplastic fluids, and total citrus leaf extracts were pretreated with either buffer control, E-64, or SDE1 recombinant proteins. Total leaf extracts from *SDE1*-expressing transgenic citrus lines were pretreated with either 100 μM E-64 or buffer control. After pretreatment, the samples were incubated with a final concentration of 2 μM DCG-04[24] for 4 hrs at room temperature, followed by precipitation with 100% ice-cold acetone. Samples were centrifuged at 12,000 x *g*, washed with 70% acetone, then centrifuged again. Precipitated products were re-suspended in 50 mM Tris buffer (pH 6.4) and either used directly for Western blotting using Streptavidin-HRP conjugates (Thermo Scientific, Waltham, MA) or further enriched on streptavidin magnetic beads (Thermo Scientific, Waltham, MA). For enrichment, samples were incubated with 25 μL streptavidin magnetic beads at room temperature for 1 hr, washed twice with 1% SDS, and eluted by heating for 5 min at 95ºC in Laemmli sample buffer with 13% β-mercaptoethanol[50]. The

labeled proteins were separated using SDS-PAGE and active proteases were visualized by Western blotting using Streptavidin-HRP conjugates (Thermo Scientific, Waltham, MA). The experiments were repeated two times with similar results.

Citrus imprint assay

Freshly cut stems of *C*Las-infected (both symptomatic and asymptomatic) Rio Red grapefruit trees from a commercial orchard in Donna, TX and non-infected (*C*Las-free) stems from grapefruit kept in a screen house were imprinted onto nitrocellulose membranes. *C*Las status was verified by qRT-PCR prior to imprinting. Imprinted membranes were then incubated with either anti-AALP (gift from Dr. Natasha Raikhel, University of California, Riverside) or anti-SDE1 antibodies[16] and the corresponding proteins were detected using goat anti-rabbit-HRP secondary antibodies (Santa Cruz, Dallas, TX) and SuperSignal West Pico PLUS Chemiluminescent Substrate (Thermo Scientific, Waltman, MA).The experiments were repeated two times with similar results.

Statistical data analysis

When comparing a test group to a control group, a two-sided Student's *t*-test was used. The significance values are reported as follows: (*) = $p < 0.05$, (**) = $p < 0.01$, and (***) = $p < 0.001$.

Antibodies and chemicals

Streptavidin-HRP used for ABPP of PLCPs was purchased from ThermoFisher (Cat No. 21130) and used in 1:1,000 dilution. Antibodies used in this study include Goat-anti-Rabbit IgG-HRP (Santa Cruz, Cat No. SC2004, used in 1:5,000 dilution), Anti-AALP

(anti-serum gifted from Dr. Natasha Raikel in Ref. 30, used in 1:1,000 dilution), Anti-SDE1 (polyclonal antibody generated in Ref. 16, used in 1:1,500 dilution), Anti-GST (Santa Cruz, Cat No. SC138, used in 1:2000 dilution), Anti-HA high affinity (Roche, Cat No. 11867423001, used in 1:1,500 dilution), Goat-anti-Rat IgG-HRP (Santa Cruz, Cat No. SC2065, used in 1:5,000 dilution).

ACKNOWLEDGEMENTS

Special acknowledgements go towards those who contributed to the research presented in this chapter. Largely to Dr. Simon Schwizer (University of California, Riverside) for assistance with generation of several of the clones used and experiments performed. Dr. Liping Zeng (UC Riverside) for assistance with the phylogenetic tree and transcriptomic analysis. Drs. Zhiqian Pang and Nian Wang (University of Florida, Lake Alfred) for generation of the *SDE1* transgenic citrus lines and *C*Las infection. Jessica Franco and Dr. Gitta Coaker (UC Davis) for the Mass Spec analysis which greatly contributed to the conclusions of this work. And, Eva Hawara (UC Riverside) for the infection assay using the surrogate system *P. syringae* and Arabidopsis, which also greatly contributed to the conclusions of this work. I also thank Drs. Suomeng Dong (Nanjing Agricultural University, China), Jikui Song (UC Riverside), and Natasha Raikhel (UC Riverside) for providing vectors or antibodies. And my undergraduate mentee Thomas Forest (UC Riverside) for his assistance with the experiments.

REFERENCES

1. Bové, J. M. Huanglongbing: a destructive, newly-emerging, century-old disease of citrus. *Journal of Plant Pathology* **88**, 7-37 (2006).

2. da Graça, J. V. *et al.* Huanglongbing: An overview of a complex pathosystem ravaging the world's citrus. *Journal of Integrative Plant Biology* **58**, 373-387 (2016).

3. Gottwald, T. R. Current epidemiological understanding of citrus Huanglongbing. *Annual Review of Phytopathology* **48**, 119-139 (2010).

4. Wang, N. & Trivedi, P. Citrus Huanglongbing: a newly relevant disease presents unprecedented challenges. *Phytopathology* **103**, 652-665 (2013).

5. Wang, N. *et al.* The *Candidatus* Liberibacter–host interface: insights into pathogenesis mechanisms and disease control. *Annual Review of Phytopathology* **55**, 451-482 (2017).

6. Spreen, T.H. & Hodges, A.W. Economic impacts of citrus greening (HLB) in Florida, 2006/07-2010/11, http://ufdc.ufl.edu/IR00005615/00001 (2012).

7. Spreen, T.H. *et. al.* An economic assesment of the impact of Huanglongbing on citrus tree plantings in Florida. *HortScience* **49**, 1052-1055 (2014).

8. Toruño, T. Y., Stergiopoulos, I. & Coaker, G. Plant-pathogen effectors: cellular probes interfering with plant defenses in spatial and temporal manners. *Annual Review of Phytopathology* **54**, 419-441 (2016).

9. Dodds, P. N. & Rathjen, J. P. Plant immunity: towards an integrated view of plant–pathogen interactions. *Nature Reviews Genetics* **11**, 539-548 (2010).

10. Feng, F. & Zhou, J.-M. Plant–bacterial pathogen interactions mediated by type III effectors. *Current Opinion in Plant Biology* **15**, 469-476 (2012).

11. Sugio, A. *et al.* Diverse targets of phytoplasma effectors: from plant development to defense against insects. *Annual Review of Phytopathology* **49**, 175-195 (2011).

12. MacLean, A. M. *et al.* Phytoplasma effector SAP54 induces indeterminate leaf-like flower development in *Arabidopsis* plants. *Plant Physiology* **157**, 831-841 (2011).

13. Hoshi, A. *et al.* A unique virulence factor for proliferation and dwarfism in plants identified from a phytopathogenic bacterium. *Proceedings of the National Academy of Sciences* **106**, 6416-6421 (2009).

14. Yan, Q. *et al.* Global gene expression changes in *Candidatus* Liberibacter asiaticus during the transmission in distinct hosts between plant and insect. *Molecular Plant Pathology* **14**, 391-404 (2013).

15. Prasad, S., Xu, J., Zhang, Y. & Wang, N. SEC-translocon dependent extracytoplasmic proteins of *Candidatus* Liberibacter asiaticus. *Frontiers in Microbiology* **7**, 1989 (2016).

16. Pagliaccia, D. *et al.* A pathogen secreted protein as a detection marker for citrus Huanglongbing. *Frontiers in Microbiology* **8**, 2041 (2017).

17. Pitino, M., Armstrong, C. M., Cano, L. M. & Duan, Y. Transient expression of *Candidatus* Liberibacter asiaticus effector induces cell death in *Nicotiana benthamiana*. *Frontiers in Plant Science* **7**, 982 (2016).

18. Jashni, M., Mehrabi, R., Collemare, J., Mesarich, C. & de Wit, P. The battle in the apoplast: further insights into the roles of proteases and their inhibitors in plant-pathogen interactions. *Frontiers in Plant Science* **6**, 584 (2015).

19. Misas-Villamil, J. C., Hoorn, R. A. & Doehlemann, G. Papain-like cysteine proteases as hubs in plant immunity. *New Phytologist* **212**, 902-907 (2016).

20. Ilyas, M. *et al.* Functional divergence of two secreted immune proteases of tomato. *Current Biology* **25**, 2300-2306 (2015).

21. Lozano-Torres, J. L. *et al.* Dual disease resistance mediated by the immune receptor Cf-2 in tomato requires a common virulence target of a fungus and a nematode. *Proceedings of the National Academy of Sciences* **109**, 10119-10124 (2012).

22. Richau, K. H. *et al.* Subclassification and biochemical analysis of plant papain-like cysteine proteases displays subfamily-specific characteristics. *Plant Physiology* **158**, 1583-1599 (2012).

23. Than, M. E. *et al.* The 2.0 Å crystal structure and substrate specificity of the KDEL-tailed cysteine endopeptidase functioning in programmed cell death of *Ricinus communis* endosperm. *J Mol Biol* **336**, 1103-1116 (2004).

24. Powers, J. C., Asgian, J. L., Ekici, Ö. D. & James, K. E. Irreversible inhibitors of serine, cysteine, and threonine proteases. *Chemical Reviews* **102**, 4639-4750 (2002).

25. Rooney, H. C. *et al. Cladosporium* Avr2 inhibits tomato Rcr3 protease required for Cf-2-dependent disease resistance. *Science* **308**, 1783-1786 (2005).

26. Chen, Z., Zheng, Z., Huang, J., Lai, Z. & Fan, B. Biosynthesis of salicylic acid in plants. *Plant Signaling & Behavior* **4**, 493-496 (2009).

27. Piazza, A. *et al.* The dual nature of trehalose in citrus canker disease: a virulence factor for *Xanthomonas citri* subsp. *citri* and a trigger for plant defence responses. *Journal of Experimental Botany* **66**, 2795-2811 (2015).

28. Martinelli, F. *et al.* Transcriptome profiling of citrus fruit response to Huanglongbing disease. *PLoS One* **7**, e38039 (2012).

29. Kim, J.-S., Sagaram, U. S., Burns, J. K., Li, J.-L. & Wang, N. Response of sweet orange (*Citrus sinensis*) to '*Candidatus* Liberibacter asiaticus' infection: microscopy and microarray analyses. *Phytopathology* **99**, 50-57 (2009).

30. Ahmed, S. U. *et al.* The plant vacuolar sorting receptor *At*ELP is involved in transport of NH_2-terminal propeptide-containing vacuolar proteins in *Arabidopsis thaliana*. *The Journal of Cell Biology* **149**, 1335-1344 (2000).

31. Sueldo, D. *et al.* Dynamic hydrolase activities precede hypersensitive tissue collapse in tomato seedlings. *New Phytologist* **203**, 913-925 (2014).

32. Shindo, T. *et al.* Screen of non-annotated small secreted proteins of *Pseudomonas syringae* reveals a virulence factor that inhibits tomato immune proteases. *PLoS Pathogens* **12**, e1005874 (2016).

33. Jiang, S. *et al.* Bacterial effector activates jasmonate signaling by directly targeting JAZ transcriptional repressors. *PLoS Pathogens* **9**, e1003715 (2013).

34. Kaschani, F. *et al.* An effector-targeted protease contributes to defense against *Phytophthora infestans* and is under diversifying selection in natural hosts. *Plant Physiology* **154**, 1794-1804 (2010).

35. Shindo, T., Misas-Villamil, J. C., Hörger, A. C., Song, J. & van der Hoorn, R. A. A role in immunity for *Arabidopsis* cysteine protease RD21, the ortholog of the tomato immune protease C14. *PLoS One* **7**, e29317 (2012).

36. Gumtow, R., Wu, D., Uchida, J. & Tian, M. A *Phytophthora palmivora* extracellular cystatin-like protease inhibitor targets papain to contribute to virulence on papaya. *Molecular Plant-Microbe Interactions* **31**, 363-373 (2017).

37. Tian, M. *et al.* A *Phytophthora infestans* cystatin-like protein targets a novel tomato papain-like apoplastic protease. *Plant Physiology* **143**, 364-377 (2007).

38. Dong, S. *et al.* Effector specialization in a lineage of the Irish potato famine pathogen. *Science* **343**, 552-555 (2014).

39. Bozkurt, T. O. *et al. Phytophthora infestans* effector AVRblb2 prevents secretion of a plant immune protease at the haustorial interface. *Proceedings of the National Academy of Sciences* **108**, 20832-20837 (2011).

40. van Esse, H. P. *et al.* The *Cladosporium fulvum* virulence protein Avr2 inhibits host proteases required for basal defense. *Plant Cell* **20**, 1948-1963 (2008).

41. Mueller, A. N., Ziemann, S., Treitschke, S., Assmann, D. & Doehlemann, G. Compatibility in the *Ustilago maydis*-maize interaction requires inhibition of host cysteine proteases by the fungal effector Pit2. *PLoS Pathogens* **9**, e1003177 (2013).

42. Bové, J. & Garnier, M. Phloem- and xylem-restricted plant pathogenic bacteria. *Plant Science* **164**, 423-438 (2003).

43. Lopez-Cobollo, R. M., Filippis, I., Bennett, M. H. & Turnbull, C. G. Comparative proteomics of cucurbit phloem indicates both unique and shared sets of proteins. *The Plant Journal* **88**, 633-647 (2016).

44. Hu, C. *et al.* Proteomics and metabolomics analyses reveal the cucurbit sieve tube system as a complex metabolic space. *The Plant Journal* **87**, 442-454 (2016).

45. Orbović, V. & Grosser, J. W. in *Agrobacterium Protocols: Volume 2* (ed Kan Wang) 245-257 (Springer New York, 2015).

46. Schultz, J., Milpetz, F., Bork, P. & Ponting, C. P. SMART, a simple modular architecture research tool: identification of signaling domains. *Proceedings of the National Academy of Sciences* **95**, 5857-5864 (1998).

47. Letunic, I., Doerks, T. & Bork, P. SMART: recent updates, new developments and status in 2015. *Nucleic Acids Research* **43**, D257-D260 (2014).

48. Edgar, R. C. MUSCLE: a multiple sequence alignment method with reduced time and space complexity. *BMC Bioinformatics* **5**, 113 (2004).

49. Tamura, K., Stecher, G., Peterson, D., Filipski, A. & Kumar, S. MEGA6: Molecular Evolutionary Genetics Analysis version 6.0. *Molecular Biology and Evolution* **30**, 2725-2729 (2013).

50. Laemmli, U. K. Cleavage of structural proteins during the assembly of the head of bacteriophage T4. *Nature* **227**, 680-685 (1970).

51. Morgan, J. K. *et al.* Improved real-time PCR detection of '*Candidatus* Liberibacter asiaticus' from citrus and psyllid hosts by targeting the intragenic tandem-repeats of its prophage genes. *Molecular and Cellular Probes* **26**, 90-98 (2012).

52. Yadeta, K. A. *et al.* An extracellular cysteine-rich protein kinase associates with a membrane immune complex and is required for cell death. *Plant Physiology*, pp. 01404 (2016).

53. Cox, J. & Mann, M. MaxQuant enables high peptide identification rates, individualized ppb-range mass accuracies and proteome-wide protein quantification. *Nature Biotechnology* **26**, 1367-1372 (2008).

54. Cox, J. *et al.* Andromeda: a peptide search engine integrated into the MaxQuant environment. *Journal of Proteome Research* **10**, 1794-1805 (2011).

55. Cox, J. *et al.* Accurate proteome-wide label-free quantification by delayed normalization and maximal peptide ratio extraction, termed MaxLFQ. *Molecular & Cellular Proteomics* **9**, 2513-26 (2014).

56. Vizcaino, J. A. *et al.* The PRoteomics IDEntifications (PRIDE) database and associated tools: status in 2013. *Nucleic Acids Research* **41**, D1063-D1069 (2013).

57. Tyanova, S. *et al.* The Perseus computational platform for comprehensive analysis of (prote)omics data. *Nat Methods* **13**, 731-740 (2016).

58. Pieper, U. *et al.* MODBASE, a database of annotated comparative protein structure models, and associated resources. *Nucleic Acids Research* **32**, D217-D222 (2004).

59. Pettersen, E. F. *et al.* UCSF Chimera—a visualization system for exploratory research and analysis. *Journal of Computational Chemistry* **25**, 1605-1612 (2004).

60. Morgan, R.L. *et al.* Catalytic domain of the diversified Pseudomonas syringae type III effector HopZ1 determines the allelic specificity in plant hosts. *Molecular Microbiology* **2**, 437-55 (2010).

61. Clark, K. and Franco, J.Y. *et. al.* An effector from the Huanglongbing-associated pathogen targets citrus proteases. *Nature Communications* **9**, 1718 (2018).

Chapter III

Functional characterization of *Candidatus* Liberibacter asiaticus (*C*Las) Sec-delivered effector 1 (SDE1) in plants

ABSTRACT

Sec delivered effector 1 (SDE1), an effector from the Huanglongbing (HLB)-associated bacterium, *Candidatus* Liberibacter asiaticus (*C*Las), was previously characterized as an inhibitor of defense-related, papain-like cysteine proteases (PLCPs) *in vitro* and *in planta*. Furthermore, SDE1 promoted infection of *Arabidopsis thaliana* by *Pseudomonas syringae*, and of citrus by *C*Las graft-inoculation, likely through its inhibitory activity of PLCPs. In this chapter, I further investigated the virulence function of SDE1 in plants. Using transgenic *A. thaliana*, I found expression of SDE1 protein caused severe yellowing in mature leaves, reminiscent of *C*Las-infection symptoms and accelerated leaf senescence. Induction of senescence signatures including increased expression of the senescence-associated gene, senescence 1 (*AtSEN1*), and the production of reactive oxygen species (ROS) was apparent in SDE1-expressing lines. SDE1-induced yellowing symptoms and *AtSEN1* gene expression was more severe in older leaves, suggesting this effect is age-associated.

SDE1 expression in *Citrus paradisi* (L.) Macfadyen (Duncan grapefruit) also induced premature yellowing symptoms after *C*Las infection. In addition to defense, PLCPs are also major players in plant developmental and stress-induced senescence. *PLCP*s and senescence-associated genes (*SAG*s) in *SDE1* transgenic citrus with *C*Las-infection showed minimal but, altered gene expression. Taken together with the result that *SDE1*-expressing citrus plants are hypersusceptible to *C*Las infection, these

findings suggest that SDE1-induced premature senescence could be a virulence strategy of *C*Las through an SDE1-PLCP mediated interaction or other mechanism that remains to be explored.

INTRODUCTION

Sec-delivered effector 1 (SDE1) is a virulence factor of CLas

Candidatus Liberibacter asiaticus (*C*Las), the associated agent of Huanglongbing (HLB) encodes a Sec dependent secretion system, which is predicted to secrete Sec-delivered effectors (SDEs) [1–3]. Previously, Sec-delivered effector 1 (SDE1) was shown to interact with papain-like cysteine proteases (PLCPs) and inhibit their protease activity *in vitro* and in plants [4]. This inhibitory activity could be a virulence mechanism of *C*Las during colonization in citrus and HLB progression. Consistent with this hypothesis, SDE1 expression in citrus leads to higher susceptibility to *C*Las (**Chapter 2, Figure 2.12**). PLCPs are key players in protein proteolysis and involved in several physiological processes including germination, development, programmed cell death, immunity, stress, and senescence [5,6]. In particular, several PLCPs are known to participate in leaf senescence [7]. *Arabidopsis thaliana* senescence-associated gene 12 (*AtSAG12*) shows senescence-correlated expression patterns [8,9] and PLCPs from the AALP and RD21 subfamilies have also been reported to play major roles in dark-induced senescence [10].

HLB symptomatic leaves are visually similar to leaves with nutritional deficiencies, including micronutrients such as zinc, iron, and manganese [11]. Based on this observation, supplementation of nutrients to diseased trees has been implemented to prolong tree productivity and reduce symptoms [12–14]. Under low nutrient conditions or stress, initiation of senescence via proteolysis and distribution of nutrients to other

tissues can be a survival strategy in plants [15]. Indeed, *C*Las-infection has been reported to cause changes in nutrient reabsorption in citrus [16]. These yellowing symptoms are also visually similar to senescing leaves, therefore we hypothesized that HLB leaf yellowing may be connected to premature leaf senescence. Transient expression of truncated SDE1 was previously shown to induce chlorosis in *Nicotiana benthamiana*, suggesting SDE1 itself may contribute to HLB symptoms [17]. Therefore, it is possible that by affecting PLCP activities, SDE1 could manipulate the senescence process in plants.

Mechanisms of cellular senescence in plants

Senescence is an altruistic form of programmed cell death that allows for re-allocation of nutrients from aging/senescing tissues to developing parts of the plant [18–20]. As such, the senescence process is tightly regulated by transcriptional and post-transcriptional levels in addition to being temporally and spatially dynamic [21]. Leaves entering a senescent state lose their photosynthetic capabilities from the breakdown of chloroplasts, changing in color from green to yellow, while the mitochondria and nucleus remain intact until the final stages of senescence [18,20]. Molecular signatures of the early senescence process include lipid peroxidation and membrane leakiness, typically accompanied by reactive oxygen species (ROS), metabolic changes such as hydrolysis of macromolecules, and induction of transcription factors in the NAC and WRKY families [18,20,22]. Senescence-associated genes (*SAG*s) consist of proteinases, nucleases, lipases, transporters, and transcription factors associated with macromolecule degradation, detoxification of oxidative stress, and/or defense signaling [21,23–25]. However, the whole molecular process behind leaf senescence is lacking.

Senescence in disease progression

While it should seem logical that necrotrophic pathogens would be in favor of promoting cell death, and that biotrophic pathogens would want it delayed [26], the relationship between senescence-mediated death and disease is not completely clear. Senescence and pathogen defense response have many overlapping components including hormones, transcription factors, and downstream response genes [27–29]. Salicylic acid (SA) and jasmonic acid (JA) are major defense hormones in plants [30] that also contribute to senescence [31–33]. Senescence is thought to be SA-dependent and SA levels increase with leaf age, triggering expression of *SAG*s [33]. In addition, external application of JA results in premature senescence in *A. thaliana* [34].

Upregulation of *SAG*s has been reported in *C*Las-infected citrus [35,36]. For example, the senescence-related gene (*SRG1*) and several WRKY transcription factors known to be contribute to senescence signaling in *A. thaliana* were up-regulated in leaves of *C*Las-infected citrus [36]. In addition, the dark-inducible, senescence 1 (*SEN1*) gene, and cold-circadian rhythm-RNA binding (CCR)-like senescence-associated gene have been found up-regulated in fruit post *C*Las-infection [35]. Some *PLCPs* including *SAGs* are up-regulated in *C*Las-infected citrus and in an SA-dependent manner [4,37,38]. On the other hand, *A. thaliana vitamin c-1* (*vtc1*) mutants show higher *SAG* transcripts, in addition to levels of SA, which is associated with their resistance to *Peronospora parasitica* and *Pseudomonas syringae* [39]. *At*SAG12 homologs were also shown to contribute to defense in tomato [40,41]. These examples indicate that SAGs play a dual role in both plant senescence and pathogen defense. However, an established involvement of senescence induction with *C*Las-infection has not been explored.

RESULTS

Sec-delivered effector 1 (SDE1) induces yellowing in *Arabidopsis thaliana* leaves

To investigate SDE1 function *in planta*, I generated transgenic plants of *A. thaliana* ecotype Columbia (Col-0) that express *SDE1* (without the signal peptide amino acid 24-154**, Chapter 1, Table 1**) under a Dexamethasone (Dex)-inducible promoter [42]. Induction of SDE1 protein expression was confirmed in individual transgenic lines from 24 hours post Dex application during a three-week period by western blotting. I observed consistent expression of SDE1 in leaves throughout the three-week period. Approximately one-week post Dex induction, yellowing symptoms appeared in mature leaves with SDE1 expression (**Figure 3.1**). Dex-treated wild-type (Col-0) leaves or leaves of transgenic lines without SDE1 expression (line 3-1) did not exhibit yellowing. Yellowing symptoms were observed both via individual leaf induction (**Figure 3.1 and 3.2a**) and whole plant induction (**Figure 3.2b**). Initial yellowing symptoms were found on older or more mature rosette leaves (**Figure 3.1a**) and, in general, were more severe in older plants (**Figure 3.1b**). Since yellowing did not develop until one-week post SDE1 expression and the symptoms severity increased with leaf age, we hypothesized the yellowing phenotype was related to leaf senescence.

SDE1 expression in *A. thaliana* initiates cellular senescence

To measure the induction of cellular senescence in adult leaves, I performed quantitative PCR (qPCR) for the senescence marker senescence 1 (*AtSEN1*), which is a dark-inducible, senescence-related gene. *AtSEN1* exhibited increased gene expression in two independent SDE1-expressing lines (line 2-4 and line 5-2) at 24- and 30-hours

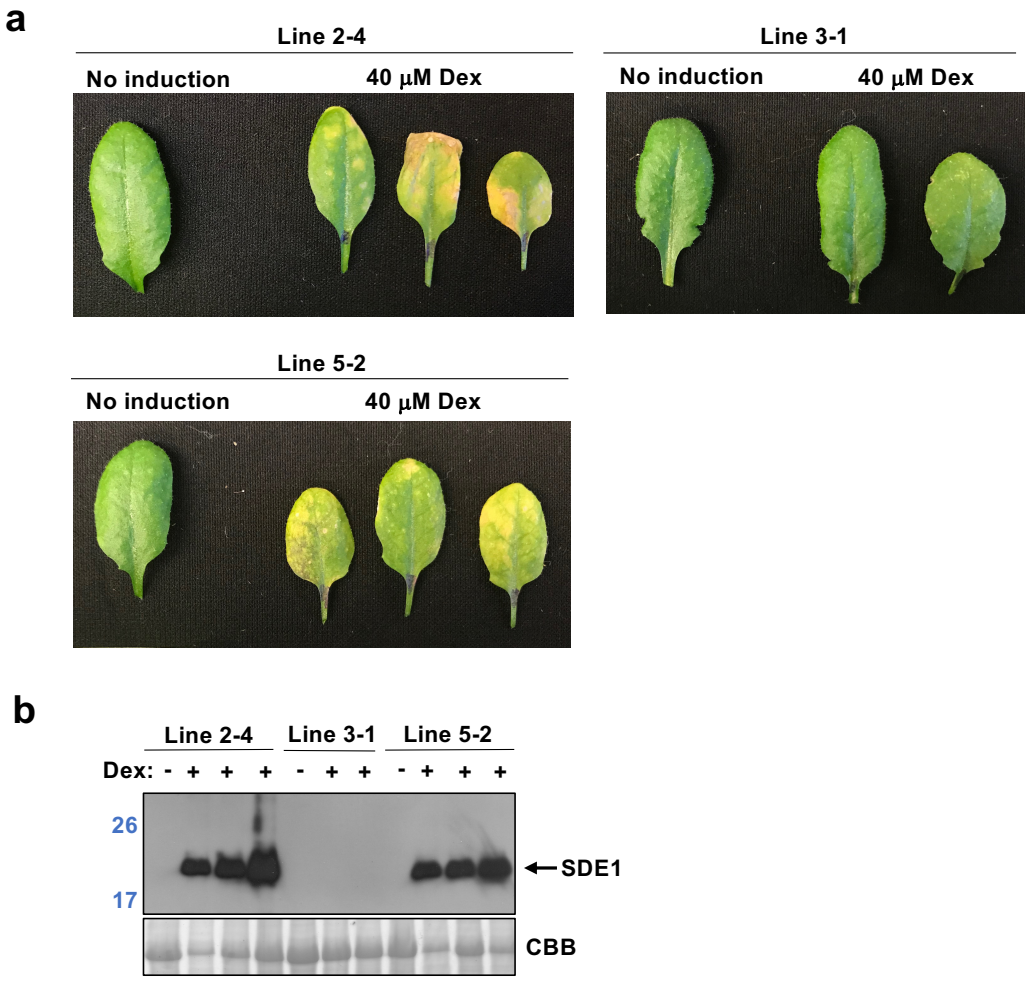

Figure 3.1 – Sec-delivered effector 1 (SDE1) expression in *Arabidopsis thaliana* induces yellowing. a) Induction of SDE1 protein expression in transgenic *A. thaliana* ecotype Columbia (Col-0) lines via Dexamethasone (Dex)-inducible promoter resulted in yellowing symptoms approximately one-week post Dex treatment. Yellowing is seen in leaves of the different transgenic lines treated with 40 μM Dex only when SDE1 protein expression is present. Individual leaves were swabbed for Dex treatment. **b)** Western blot showing FLAG-SDE1 recombinant protein levels from the leaves pictured in (a), note that line 3-1 does not have SDE1 protein expression in mature leaves and does not exhibit yellowing symptoms. Coomassie brilliant blue (CBB) stain is shown for total protein loading. Plus signs (+) indicate leaves that were Dex treated, minus signs (-) indicate leaves that were not treated.

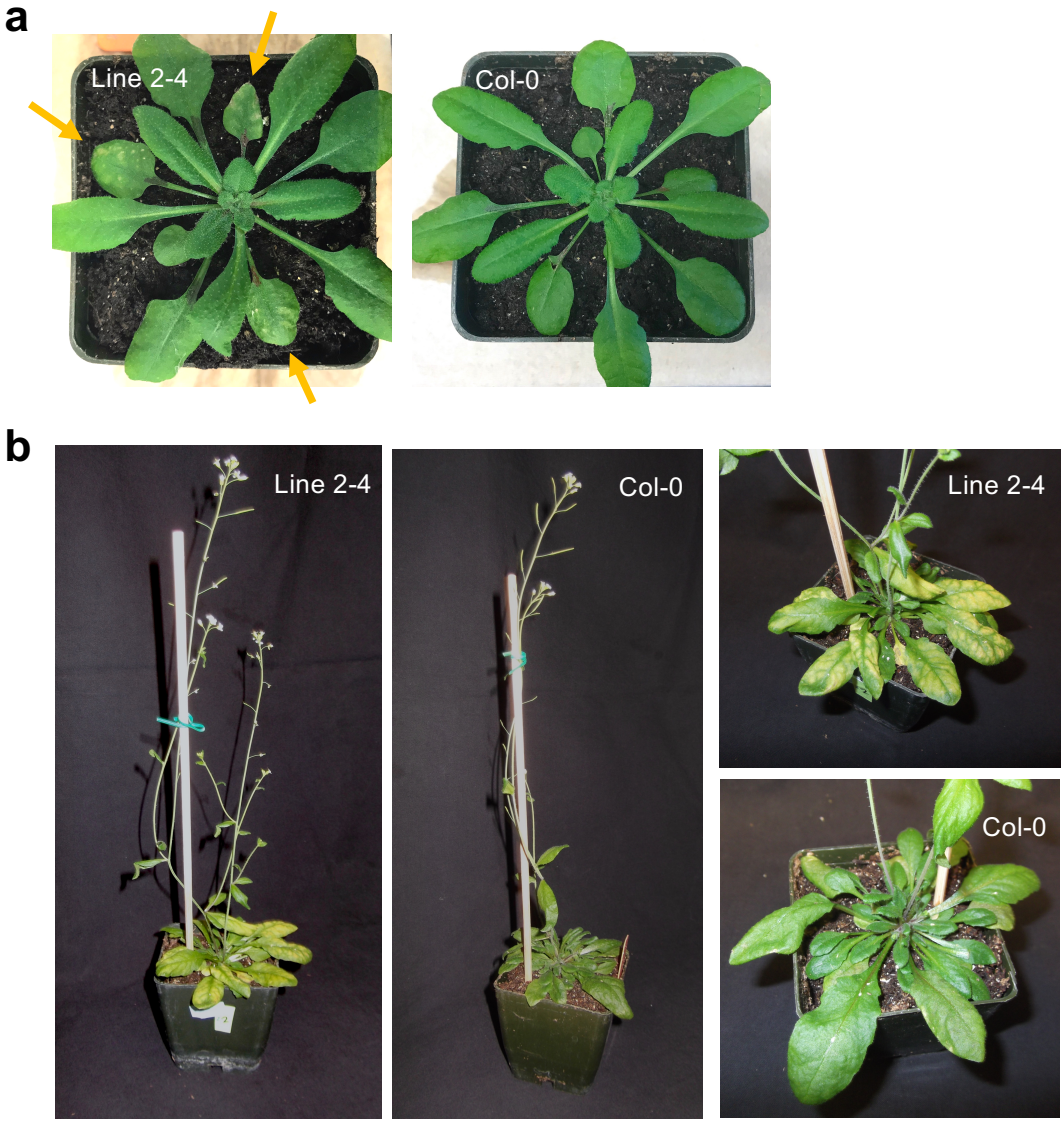

Figure 3.2 – SDE1-induced yellowing symptoms initiate and are more severe in older leaves of *A. thaliana* plants. a) Yellowing symptoms occur first on older rosette leaves (indicated with orange arrows). Four-week-old plants were treated with 40 μM Dexamethasone (Dex) by swabbing individual leaves (treated leaves are marked on stems). Pictures were taken five-days post Dex treatment. Line 2-4 is SDE1-expressing and Col-0 is wild-type control. **b)** Yellowing symptoms on whole plants spray treated with 40 μM Dex to induce *SDE1* expression. Plants are eight weeks old, later life stage as indicated by stalks and flowers, demonstrating symptom severity in older leaves. Pictures taken approximately 14 days post Dex treatment.

post SDE1 induction. Note that there were no yellowing symptoms at this time, so the induction of *AtSEN1* may indicate the initiation of a senescence process (**Figure 3.3**). While line 3-1, which has no SDE1 protein expression or yellowing in leaves in mature leaves, did not show the same trend (**Figure 3.1 and 3.3**), demonstrating *AtSEN1* induction was related to SDE1 protein levels. Dark-induced senescent leaves were used as a positive control as they are known to exhibit high *AtSEN1* expression (**Figure 3.3**).

I also assessed senescence gene expression in seedlings. On the contrary to adult plants, *AtSEN1* expression in Dex-treated transgenic seedlings was similar to wildtype Col-0 and did not indicate a pattern reflective of SDE1 protein levels (**Figure 3.4**). This is interesting because seedlings do not exhibit SDE1-inducded yellowing, which further indicates an age-dependency for symptom development.

Generation of reactive oxygen species (ROS) is another signature associated with the promotion of senescence [20,43]. Therefore, I next measured ROS accumulation in Dex-induced *SDE1* transgenic leaves using 3,3'-diaminobenzidine (DAB) staining. When oxidized by hydrogen peroxide (H_2O_2), DAB forms brown precipitates, which can be visualized in de-colorized leaves. Lines that express SDE1 protein accumulated these precipitates, representing the presence and localization of hydrogen peroxide in the leaf (**Figure 3.5**). Formation of DAB precipitates could be seen as early as 1- and 4-days post Dex induction of *SDE1*, but was more prominent with time, as seen in leaves from 10- and 14-days post Dex (**Figure 3.5a and b**). Precipitates were not observed or observed at a very low level in Dex-treated, Col-0 leaves. DAB precipitates also correlated with leaf yellowing symptoms as seen in lines 2-4 and 5-2 at 10- and 14-days post Dex treatment (**Figure 3.5a and b**). Illustrating that ROS accumulation increases over time and with SDE1-induced yellowing.

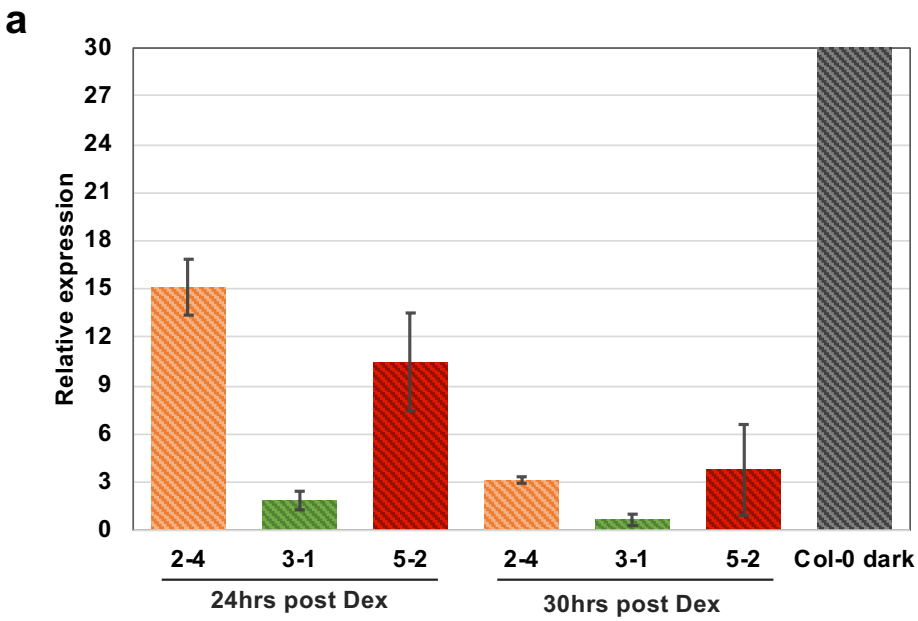

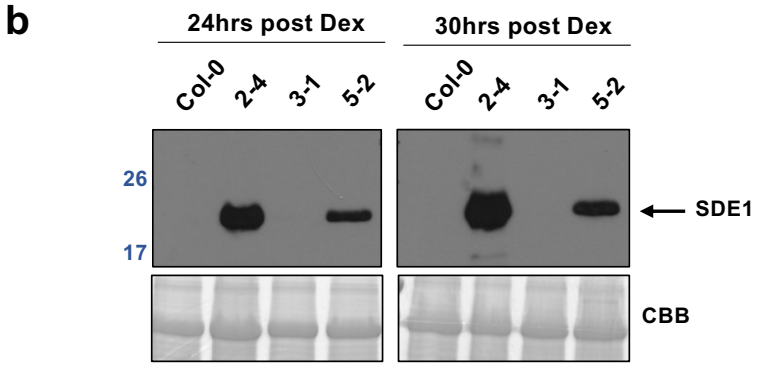

Figure 3.3 –*A. thaliana* SDE1-expressing leaves have up-regulated gene expression of the senescence marker, *AtSEN1*. a) Relative gene expression levels of *AtSEN1* in Dexamethasone (Dex)-treated; *SDE1*-transgenic leaves compared to Dex-treated Col-0 (wild-type) leaves (relative expression calculated as $2^{-\Delta\Delta Ct}$). Leaves were collected at two different timepoints post treatment (24hrs and 30hrs). Col-0 dark-treated leaves are a control for the *AtSEN1* marker and were collected after 48hrs in the dark. Two to three leaves were collected per sample. Data represents two different biological repeats. Error bars represent standard deviation of the relative expression for the biological repeats. **b)** Western blot showing FLAG-SDE1 recombinant protein expression from leaves used in one of the biological replicates from graph in (a). Coomassie brilliant blue (CBB) represents loading control.

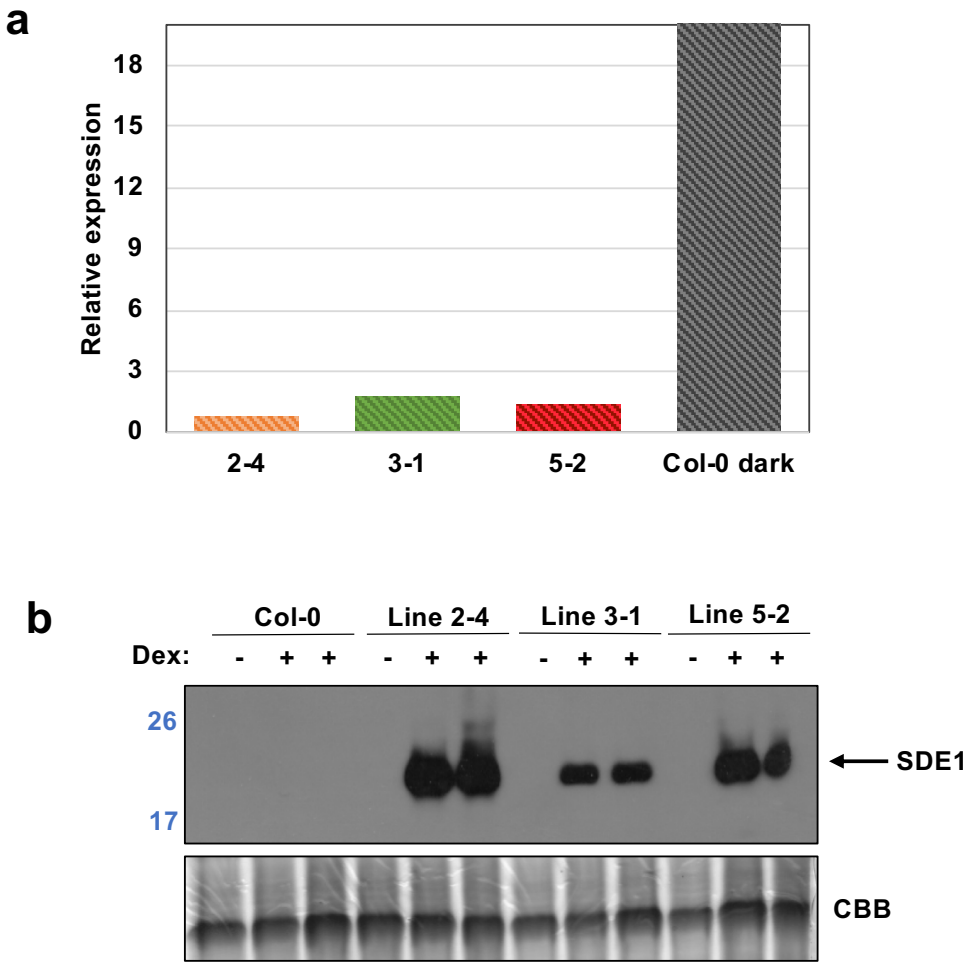

Figure 3.4 – *A. thaliana* SDE1-expressing seedlings showed minimal *AtSEN1* gene expression. a) Relative expression levels of *AtSEN1* in Dexamethasone (Dex)-treated; *SDE1*-transgenic seedlings compared to Dex-treated Col-0 (wild-type) seedlings (relative expression calculated as $2^{-\Delta\Delta Ct}$). Seedlings were collected 24 hours post treatment, approximately 20 seedlings were pooled. Col-0 dark-treated control is from mature leaves. **b)** Western blot showing corresponding FLAG-SDE1 recombinant protein expression for seedlings assayed in (a). Plus signs (+) represent seedlings that received Dex-treatment, minus signs (-) represent seedlings without Dex treatment. Coomassie brilliant blue (CBB) represents loading control.

a

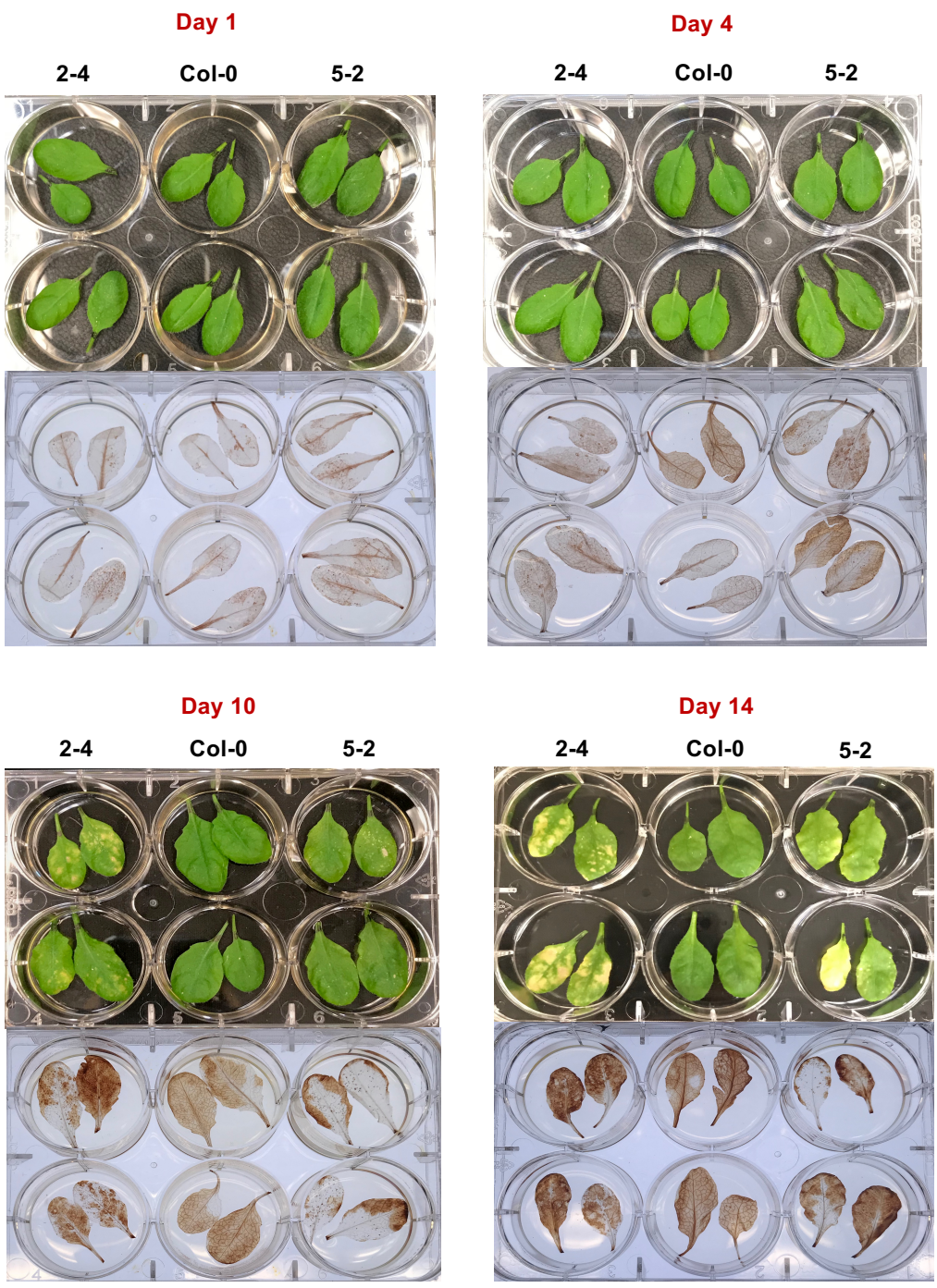
Day 1
2-4
Col-0
5-2
Day 4
2-4
Col-0
5-2
Day 10
2-4
Col-0
5-2
Day 14
2-4
Col-0
5-2

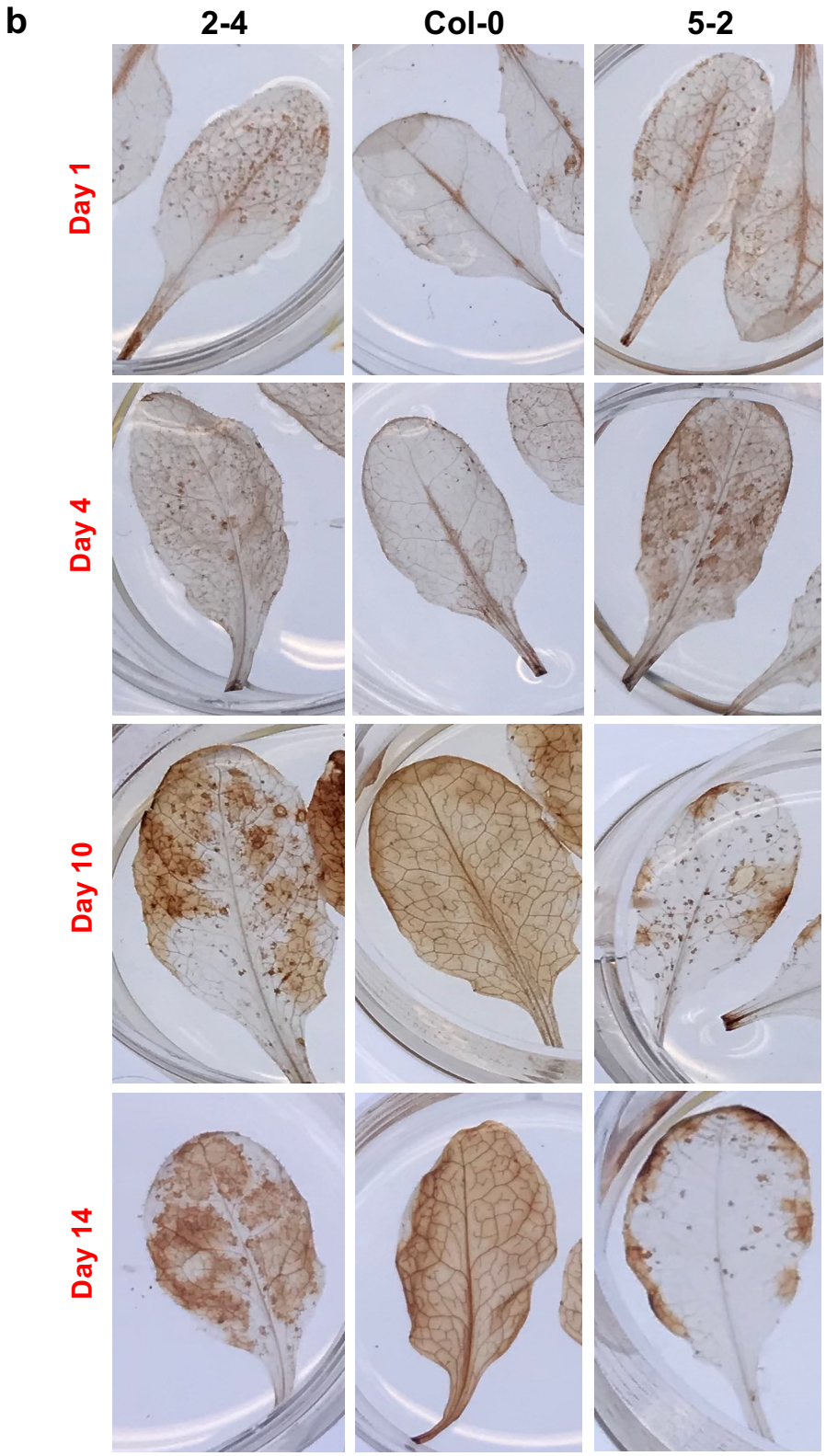
b
2-4
Col-0
5-2
Day 1
Day 4
Day 10
Day 14

Figure 3.5 – SDE1 induces reactive oxygen species (ROS) accumulation in sync with yellowing symptoms in *A. thaliana*. a) *A. thaliana* leaves from SDE1-expressing lines and wild-type control (Col-0) at 1, 4, 10, or 14 days post Dexamethasone (Dex) treatment (upper panels) and the same leaves after staining with 3,3'-diaminobenzidine (DAB) (lower panels). Brown dots (DAB precipitates) represent hydrogen peroxide (H_2O_2) accumulation in leaves, not overall brown color. Note yellowing symptoms in leaves correlate with increase in DAB precipitates (around day 10). Four leaves per sample timepoint are shown. **b)** Enlarged pictures of individual leaves from (a) to show DAB precipitates.

SDE1 transgenic citrus exhibit early yellowing after infection with CLas and have altered senescence-associated gene expression

Previously we generated *SDE1*-expressing transgenic citrus in the *Citrus paradisi* (L.) Macfadyen (Duncan grapefruit) background in collaboration with Dr. Nian Wang's group at the University of Florida (Chapter 2). These lines exhibit reduced total PLCP activity (**Chapter 2, Figure 2.9c**) and are more susceptible to *C*Las infection via grafting (**Chapter 2, Figure 2.12**). One line that allowed a particularly high *C*Las titer, SDE1-8, showed yellowing symptoms 1.5 months post *C*Las-infection, while infected control plants were still asymptomatic (**Figure 3.6**). Yellowing symptoms were not observed in *SDE1*-expressing transgenic citrus prior to *C*Las-infection; thus, the additional stress resulted from *C*Las-infection seems to be required for this accelerated disease symptom.

To understand the tentative role of senescence in the *SDE1*-expressing, *C*Las-infected lines, I utilized NanoString nCounter Elements technologies (hereafter NanoString) to measure direct digital counts of RNA transcripts of interest. Probes were custom designed to target a subset of senescence-associated genes (*SAGs*) and papain-like cysteine protease genes (*PLCPs*) predicted from citrus using the *Citrus sinensis* v1.1 and *C. clementina* v1.0 genomes (**Table 3.1**). These genes were selected based on homology to *A. thaliana* genes known to be associated with the senescence process or expressed during senescence. Lines SDE1-8, SDE1-9 were chosen for the analysis because they showed increased susceptibility to *C*Las and exhibited overall reduced PLCP activity, in addition to confirmed SDE1 protein expression (Chapter 2). Two control plants (Control-4 and Control-5) were used for comparison. Interestingly, out of the 11 *PLCP* genes tested, 7 were up-regulated in *C*Las-infected, *SDE1* transgenic lines relative to *C*Las-infected, Control lines (**Figure 3.7**, last column and **Figure 3.8**).

For the *SAG* genes, although at low levels, 6 out of the 9 genes tested were up-regulated, indicating a similar expression trend between *PLCP*s and *SAG*s in the *SDE1* transgenic citrus (**Figure 3.7, last column and Figure 3.8**).

Without *C*Las-infection *SAG* and *PLCP* expression in *SDE1*-expressing citrus lines had minimal differences compared to Controls, with the exception of the three *SAG12* subfamilies members, which showed increased expression in the SDE1 transgenic lines (**Figure 3.7, first column**). Post *C*Las-infection, up-regulation of *SAG12* subfamily members was still apparent in both Control and *SDE1*-expressing lines except for *orange1.1g018958m*, which was down-regulated, indicating a plausible differential role for this PLCP in the presence of SDE1 (**Figure 3.7**). The *PLCP* and *AALP* subfamily member, *orange1.1g036910m*, is also slightly more up-regulated in *SDE1*-expressing lines with *C*Las infection, when compared to *C*Las-infected Control lines directly (**Figure 3.7, last column and 3.8**). The *SAG*, *ORE1*, which is a NAC transcription factor associated with senescence (**Table 3.1**) is also up-regulated (**Figure 3.7, last column and 3.8**). However, *SEN1* is not strongly up-regulated in *SDE1*-expressing or *C*Las-infected citrus in general (**Figure 3.7, first 3 columns**), but when directly comparing *C*Las infected, *SDE1*-expressing and Control plants, there is an overall increase in expression of *SEN1* (**Figure 3.7, last column and 3.8**). This indicates that SDE1, in the presence of *C*Las-infection, can alter expression of some *SAG*s and *PLCP*s that are known to be related to senescence. As such, SDE1 may play a role in manipulation of citrus senescence during *C*Las infection by triggering differential gene expression either directly or via downstream signaling potentially through a PLCP inhibitory manner.

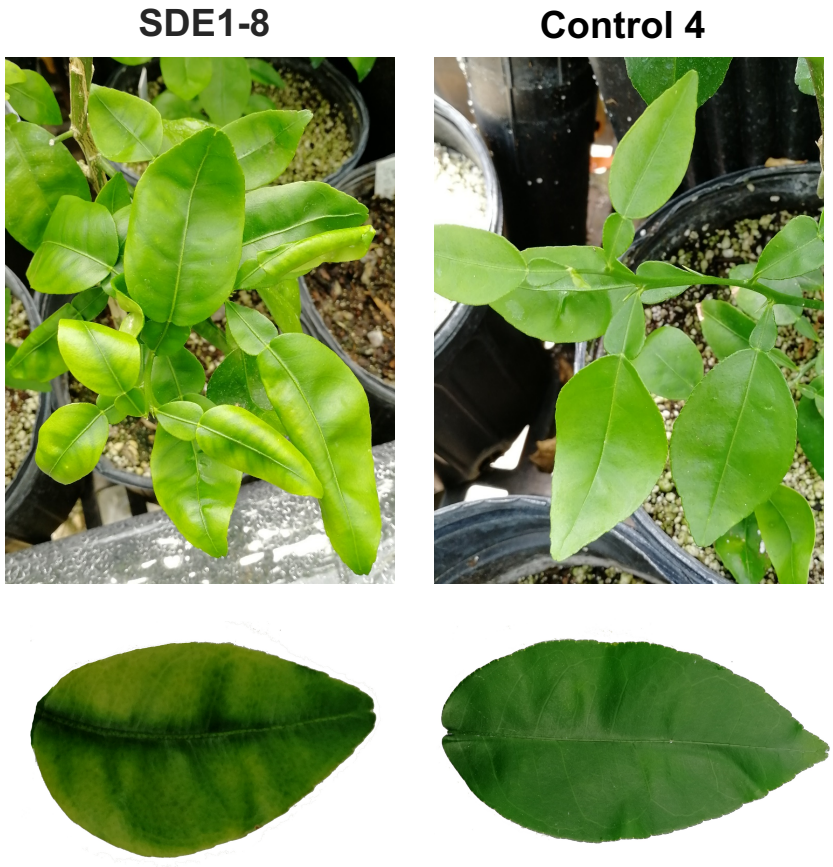

Figure 3.6 – SDE1 expression induces yellowing in citrus infected with *Candidatus* Liberibacter asiaticus (*C*Las). The SDE1-expressing transgenic line, SDE1-8, exhibits premature leaf yellowing 1.5 months post graft inoculation with *C*Las, while control plants remain asymptomatic. SDE1-expressing transgenic citrus was generated in the *Citrus paradisi* (L.) Macfadyen (Duncan grapefruit) background. Control plants are *C*Las-infected, Duncan grapefruit. Control 4 was chosen as a representative, but all control plants remained asymptomatic at this timepoint.

Table 3.1- Senescence-associated genes for NanoString analysis. Custom probes were designed based on homologs to sequences in *Citrus sinensis* v1.1 and *C. clementina* v1.0 genomes.

Gene name	Gene ID	Description	Arabidopsis homolog
SRG1A	orange1.1g035879m	senescence-related gene 1	AT1G17020
SRG1B	orange1.1g045260m	senescence-related gene 1	AT1G17020
SEN1	orange1.1t05190	senescence 1 homolog	AT4G35770
atg5	orange1.1g035508m	autophagy-related protein 5	AT5G17290
atg4	orange1.1g011418m	autophagy-related protein 4	AT2G44140
SAG102	orange1.1g045147m	senescence-associated family protein	AT2G44670
EIN2	orange1.1g000538m	ethylene-insensitive protein 2	AT5G03280
ORE1	orange1.1g018950m	NAC-domain transcription factor associated with senescence	AT5G39610
AED1	orange1.1g011600m	Aspartyl protease	AT5G10760

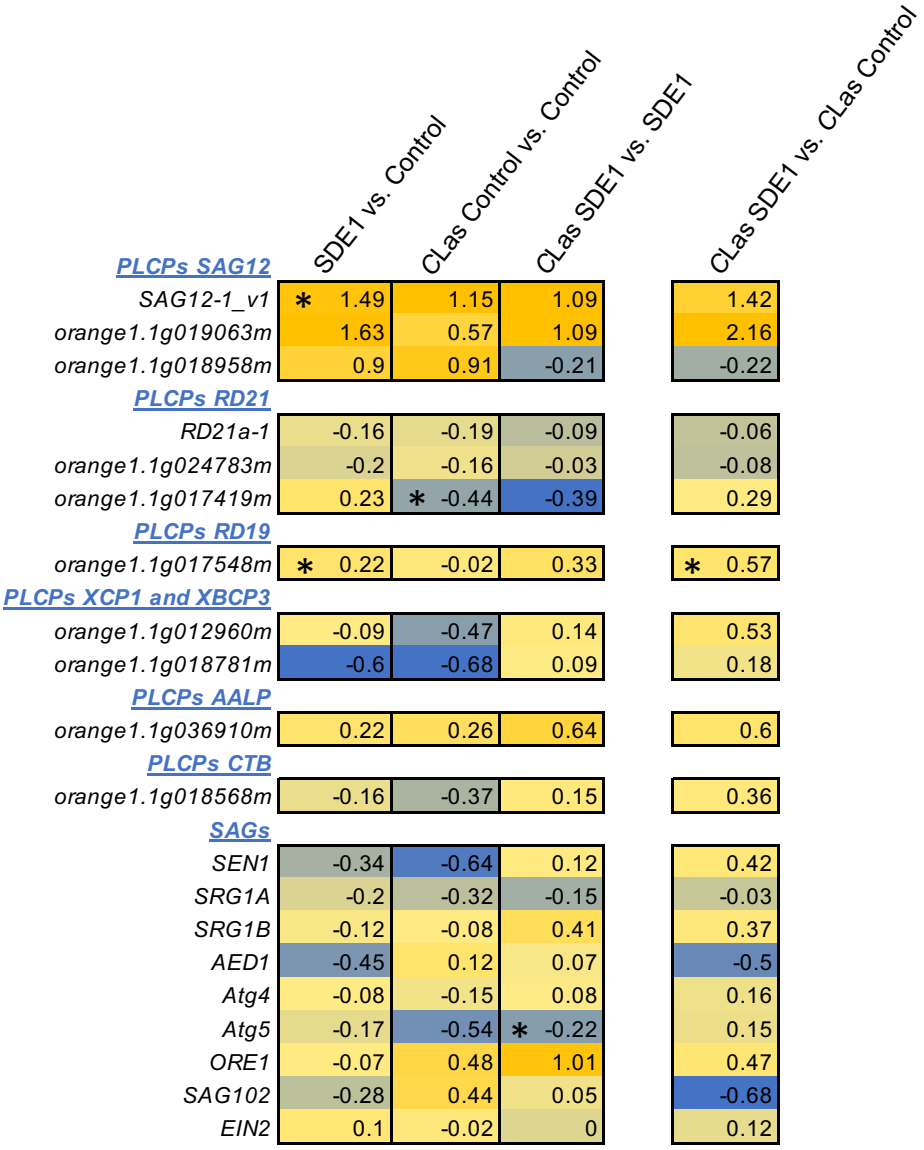

Figure 3.7 – Relative expression of senescence-associated genes (*SAG*s) and papain-like cysteine proteases (*PLPC*s) in SDE1-expressing citrus. Columns represent different comparisons of SDE1-expressing citrus and control citrus with and without *C*Las-infection. SDE1 = SDE1-expressing citrus lines SDE1-8 and -9, Control= control citrus plants -4 and -5. Transgenic and control citrus are in *Citrus paradisi* (L.) Macfadyen (Duncan grapefruit) background. *PLCP*s are grouped by subfamily. *SAG*s and *PLCP*s with up-regulated gene expression relative to control group are shown in gold and down-regulated shown in blue. Values are presented at Log_2 fold-change. Significant p-values indicated with (*) $p < 0.05$.

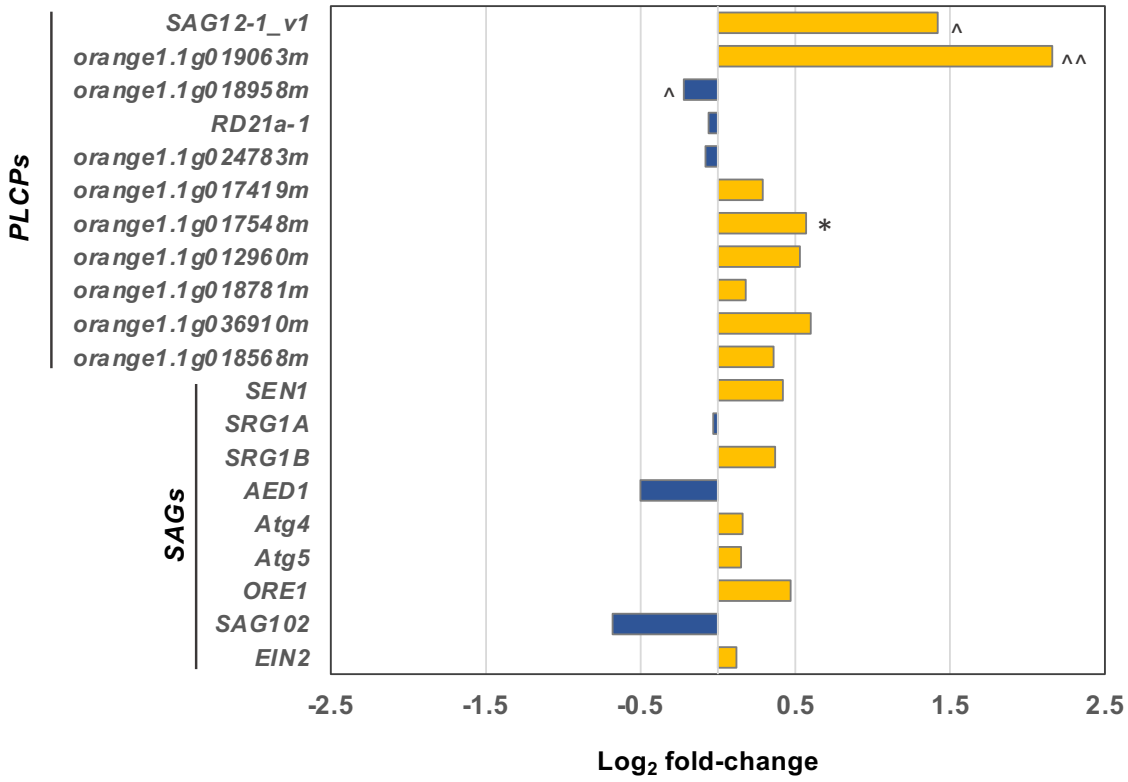

Figure 3.8 – Graphical representation of senescence-associated gene (*SAG)* and papain-like cysteine protease (*PLCP)* gene expression in *C*Las-infected, SDE1 transgenic citrus relative to infected controls. *SAG*s and *PLCP*s with up-regulated gene expression relative to control group are shown in gold and down-regulated shown in blue. Values are presented at Log_2 fold-change. (*) p-value < 0.05, other symbols represent nonsignificant p-values that are still low; (^^) p-value < 0.1 and (^) p-value < 0.17.

CONCLUSIONS AND DISCUSSION

Citrus Huanglongbing (HLB) remains a prominent threat to the citrus industry. Understanding the molecular mechanisms involved between the citrus host and the associated pathogen, *Candidatus* Liberibacter asiaticus (*C*Las) is in high demand. In particular, knowledge of the virulence strategies of *C*Las are key to uncovering information on phloem colonization and HLB disease progression. In this chapter, I further explored the function of the *C*Las effector, Sec-delivered effector 1 (SDE1). I demonstrated the role of SDE1 in the development of an HLB-like symptom, i.e. leaf yellowing, via *SDE1* expression in *A. thaliana* and citrus. *A. thaliana* lines expressing SDE1 protein exhibit severe leaf yellowing. This SDE1-induced yellowing is more prominent as leaves age, leading us to hypothesize this symptom occurs in a senescence-associated manner. Furthermore, senescence signatures including *At*SEN1 gene expression and reactive oxygen species (ROS) production are initiated. In citrus, early yellowing, reminiscent to HLB disease symptoms, was observed in one *SDE1* transgenic line, but only after *C*Las infection. Examination of senescence-associated genes (SAGs) and papain-like cysteine protease (PLCPs) genes also suggested alterations in citrus plants with SDE1 expression and after *C*Las infection. These results suggest a role for SDE1 in leaf yellowing, possibly through manipulation of the host senescence program. The implications and possible reasoning behind this response, plus inspiration for future research are discussed below.

SDE1-induced senescence signatures and their putative roles in HLB

The onset of leaf senescence is often associated with changes in leaf color and is known to require internal signals based on developmental stages [18,20]. Here, I found

expression of SDE1 in *A. thaliana* plants caused yellowing in mature leaves (**Figures 3.1 and 3.2**). This yellowing is reminiscent of both HLB symptoms and leaf senescence. Upregulation of senescence 1 (*AtSEN1*) gene expression was observed in leaves from *SDE1* transgenic *A. thaliana* lines, at up to 15-folds higher than in Col-0 (**Figure 3.3**). Age-dependency was also part of this response. Yellowing symptoms were only present in mature leaves and more severe in older leaves (**Figure 3.2**). In seedlings, *AtSEN1* expression was minimal (**Figure 3.4**) and SDE1-induced yellowing did not occur in *SDE1* transgenic lines.

Reactive oxygen species (ROS) production is an important part of the senescence program. Specific redox signaling can affect phytohormone levels and expression of transcription factors that regulate senescence [43]. Generation of ROS mainly occurs in the chloroplasts, [44] thus, chloroplast digestion would likely release a larger amount of ROS. To assess ROS production in *SDE1*-expressing leaves, I performed 3,3'-diaminobenzidine (DAB) staining and showed that, in tandem with SDE1-induced yellowing, DAB precipitates accumulate in mature leaves of transgenic plants, indicating H_2O_2 abundance (**Figure 3.5**). While this stain is only representative of H_2O_2 ROS forms, it is possible other ROS species are elicited during SDE1-induced yellowing and further experiments are needed to validate such hypotheses. It should also be noted that ROS accumulation in the *SDE1 A. thaliana* seedlings was not explored and would be of interest for further research into the age-dependency factor associated with senescence.

During senescence, major organelles are digested allowing nutrients to be recycled to younger, developing tissues [45]. In leaves, this occurs first in chloroplasts, which release large amounts of nitrogen for mobilization throughout the plant [45,46].

Digestion of chloroplasts and loss of chlorophylls is behind senescence-related color changes in leaves [18]. A previous report on SDE1-induced yellowing via transient expression of truncated SDE1 in *Nicotiana benthamiana* found a reduction in total chlorophylls and down-regulation of chlorophyll synthesis genes in these tissues [17]. These results further support a senescence role for SDE1. The same study also concluded starch accumulation is a major contributor to chloroplast thylakoid breakdown and subsequent yellowing. However, when I assayed starch levels in *SDE1* transgenic *A. thaliana* leaves via staining with Lugol's solution, I did not find a consistent correlation between starch accumulation and SDE1 expressing lines (**Figure 3.9**). Therefore, it is unclear if SDE1-yellowing in Arabidopsis is linked to starch accumulation and needs further exploration.

In citrus, it is interesting that premature yellowing symptoms only occurred in one *SDE1* transgenic line after infection with high *C*Las titers (**Figure 2.12 and Figure 3.6**), suggesting SDE1 only accelerates HLB symptom development but cannot induce yellowing without *C*Las infection. As senescence progresses in an organized manner and cell death does not proceed until nutrient mobilization has occurred [45], one possible explanation is that during *C*Las infection, SDE1 manipulates host senescence to recycle nutrients from highly infected tissues to other parts of the plant. This could allow for *C*Las colonization in distant tissues and longevity of the bacteria within the plant host. It is important to note that *C*Las has an uneven distribution in infected trees [47,48], thus such a strategy is consistent with previous observations. Espinoza et. al. (2007) proposed a similar scenario between viral pathogens and their hosts in which recycling of nutrients from infected leaves to distant tissues is thought to allow longer establishment of viral pathogens within the host [49]. For a phloem-limited, obligate pathogen such as *C*Las, this

approach is logical since the bacterium must extend its life in the plant host until acquisition and distribution by its insect vector. Thus, another possibility would be that early induction of yellowing symptoms is a ploy to attract insect vectors, further disseminating *C*Las propagules. Psyllids are not necessarily attracted to senescing leaves but, are known to be drawn to yellow color [50–52].

Relationship between senescence and papain-like cysteine proteases (PLCPs)

SDE1 was previously found to interact with and inhibit the activity of several papain-like cysteine proteases (PLCPs) in citrus [4]. As leaf senescence is accompanied by extensive protein degradation, PLCPs play a major role in the process and some up-regulated senescence-associated genes (*SAG*s) encode PLCPs [5,7,10,25]. PLCPs are also involved in other plant developmental processes and defense against pathogens [6,40,41]. Pruzinska et. al. (2017) found PLCPs from the AALP and RD21 subfamilies to be the largest contributors to dark-induced senescence in *A. thaliana* [10]. SDE1 can interact with citrus homologs from AALP and RD21 subfamilies and is known to inhibit the activity of an RD21 member (**Chapter 2, Figure 2.9**). Results from the NanoString analysis indicate the *AALP* subfamily member, *orange1.1g036910m*, has higher expression in *SDE1* transgenic citrus infected with *C*Las, more so than in the infected controls, and the *SAG12* subfamily members are highly expressed in transgenic citrus with or without *C*Las-infection (**Figure 3.7 and 3.8**). These results present an interplay between SDE1 and the senescence-associated PLCPs. It is possible SDE1 manipulates the function of a particular PLCP involved in senescence. For example, inhibition of a particular PLCP's activity could lead to an overcompensation effect, in which this or other PLCP(s) are induced at the transcription level leading to senescence symptoms. It should be noted

that the senescence-related genes studied here were selected for study based on their roles in *A. thaliana*; the same functions may not translate to citrus. Regardless, the connection between PLCPs and senescence, and previous research demonstrating a role of PLCPs in defense, provide a basis for further exploration of their roles in citrus and how it relates to HLB disease.

Potential role for SDE1-associated senescence in autophagy

Autophagy is another catabolic process that participates in cell maintenance by degrading and recycling impaired macromolecules or organelles and functions in senescence, stress response, and immunity in plants and animals [19,53,54]. As senescence and autophagy are connected cellular degradation processes, it is worth discussing the possible role of autophagy in SDE1-induced leaf yellowing. Interestingly, *A. thaliana* autophagy mutants exhibit premature senescence, but only under low nutrient or stressed conditions [55,56]. In plants, autophagy has been implicated in both restricting and promoting immune-related, programmed cell death [53]. Autophagy can confer resistance to pathogens including *Botrytis cinerea* [57] and *Pseudomonas syringae* [58,59]. Shindo et. al. (2012) found *At*RD21 contributes to defense against *Botrytis cinerea* [60] and silencing of *RD21* homologs in *N. benthamiana* phenocopies *atg3* autophagy mutants, illustrating a plausible role of PLCPs in autophagy as well [61]. In mammalian systems, specialized autophagy termed xenophagy can engulf intracellular bacteria and viruses [62,63]. Considering *C*Las is an intracellular pathogen an autophagic-like defense strategy against the associated pathogen is plausible; therefore, it is likely that *C*Las would adapt a counter mechanism to subvert host autophagy.

There are many examples of plant and animal pathogens which have evolved virulence strategies by targeting the autophagy process in the hosts. Dagdas et. al. (2018) found that the effector of *Phytophthora infestans*, PexRD54, can hijack autophagosome formation and outcompete the native cargo, Joka2, contributing to *Phytophthora* infection [64]. *Legionella pneumophila* secretes an effector that acts as a cysteine protease and incepts the role of autophagy-related protein, Atg4, in autophagosome formation [65]. Although our NanoString analysis did not show major changes in the two autophagy genes that I chose to examine (*atg4* and *atg5*, **Figure 3.7**), there are many more *atg*s that could be manipulated by SDE1 in the transgenic citrus. In addition, manipulation of the autophagy pathway could be post-translational. Atg4 plays an essential role in autophagosome formation via cleavage of Atg8 intermediates [66]. Atg4 is a cysteine protease (clan CA, family C54), although slightly different in fold from PLCPs (clan CA, family C1A). Thus, it is intriguing to speculate that SDE1 could potentially have inhibitory activity to the Atg4 homolog(s) in citrus, or to other proteases involved in the autophagy process. This could partially explain how SDE1 induces senescence, as Atg4 mutants in Arabidopsis display premature senescence due to failure of the autophagy program, but future experiments are required to explore this hypothesis.

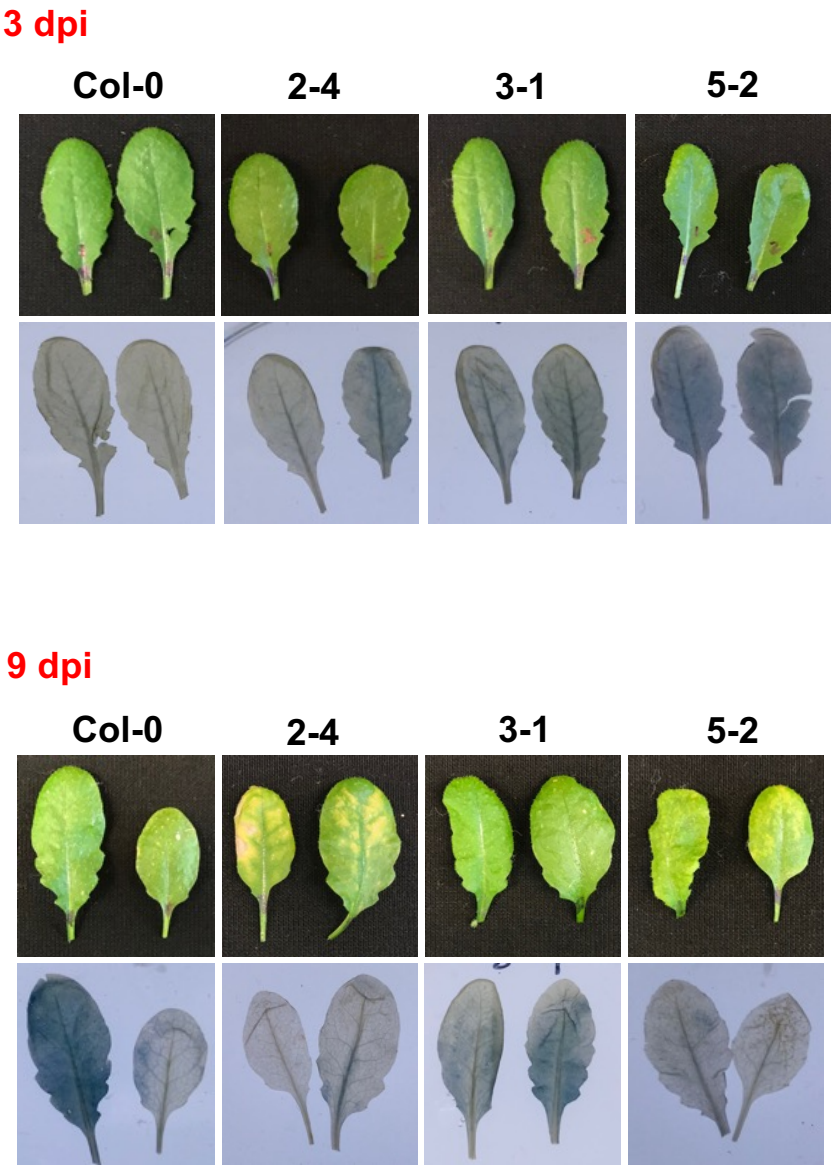

Figure 3.9 – Starch staining of *SDE1* *A. thaliana* leaves. SDE1 protein expression was induced in mature *A. thaliana* leaves via swabbing of individual leaves with 40μM Dex, leaves were bleached and stained with Lugol's solution to assess starch accumulation. Timepoints shown are 3- and 9-days post Dex induction (dpi). Top panels show leaves before staining for starch and bottom panels are the same leaves after starch staining. Dark blue color in stained leaves represents starch.

MATERIALS AND METHODS

Generation of SDE1-expressing transgenic Arabidopsis and growth conditions

Arabidopsis thaliana ecotype Columbia (Col-0) seeds were sown in soil and vernalized at 4°C for 2 days. The plants were then grown in a conditioned growth room at 22°C with a 12hr/12hr light/dark regime. Plants 4-6 weeks of age were used for all experiments and flowering plants (6-8 weeks) were used to generate SDE1 expressing lines. SDE1 full-length sequence (minus signal peptide) with an N-terminal 3xFLAG tag was cloned into the binary vector pTA7002 with Dexamethasone inducible promoter from Aoyama and Chua (1997) [42]. The recombinant plasmids were transformed into *Agrobacterium tumefacians* GV3101 and Col-0 plants were transformed using the floral dip method from Clough and Bent (1998) [67] and selected for on Murashige and Skoog (MS)-hygromycin plates using the rapid screening method in Harrison et. al. (2006) [68].

Dexamethasone induction of SDE1 expression

Prepare a final concentration of 40μM Dexamethasone (Dex) (Sigma, St. Louis, MO) solution in sterile water with 0.05% Silwet L-77 (LEHLE SEEDS, Round Rock, TX). Dex solution was applied to *A. thaliana* leaves from plants 3-4 weeks in age by spraying or swabbing with Q-tips. For spray application, Dex solution was suspended in a spray bottle and all leaves were evenly sprayed with Dex solution. For swabbing application, individual leaves were marked with a Sharpie and swabbed with Dex solution using Q-tips. Several leaves across several different plants were Dex-induced for use in the different experiments throughout this chapter.

Protein extraction and Western blotting

Leaf tissue was ground into a powder with liquid nitrogen and re-suspended in 2x Laemmli buffer [69]. Samples were then boiled for 5min and centrifuged to separate leaf solids and aqueous proteins. The soluble protein was then run on an 12% polyacrylamide gel via SDS-PAGE to verify protein loading. SDS-PAGE gels were then transferred to PVDF membrane paper (GE Healthcare, Chicago, IL) for Western blotting. For Western blotting, membranes were blocked in 5% non-fat skim milk solution, then incubated with anti-FLAG-HRP antibodies at a dilution of 1:2,000 (Sigma, St. Louis, MO). Before signal development unbound antibody was washed off membranes with TBS-T buffer (1xTBS pH 7.4, with 0.1% Tween-20). Signals were detected using SuperSignal West Pico PLUS Chemiluminescent Substrate (Thermo Scientific, Waltman, MA).

3,3'-diaminobenzidine (DAB) staining of Arabidopsis leaves

3,3'-diaminobenzidine (DAB) (Alfa Aesar, Haverhill, MA) solution was prepared fresh for each staining according to the protocol found in Daudi and O'Brien (2012) [70]. Briefly, *A. thaliana* leaves post Dex treatment were cut and submerged in DAB stain overnight, in the dark, with gentle shaking. The following day, leaves were de-stained by boiling in bleaching solution (ethanol: acetic acid: glycerol = 3:1:1) for 10min. DAB precipitates were imaged using UV white light transilluminator (Analytik Jena, Jena, Germany). Staining was repeated at multiple timepoints post Dex treatment, for multiple leaves.

Starch staining of Arabidopsis leaves

Post Dex-induction, mature *A. thaliana* leaves were cut from plants and bleached until white by boiling in 80% ethanol solution. Bleached leaves were then stained with 5-10 drops (until whole leaf was covered) of 2% Lugol's solution (2% Iodine, 4% Potassium Iodide, 94% distilled water) and allowed to stain for 5 minutes. To de-stain, leaves were rinsed in distilled water with gentle shaking. Stained leaves were imaged using UV white light transilluminator (Analytik Jena, Jena, Germany). Starch staining of SDE1-expressing *A. thaliana* leaves was repeated on three separates sets of plants at different timepoints with similar results.

RNA extraction from Arabidopsis and citrus tissues

Total RNA was extracted from *A. thaliana* tissues by grinding approximately 0.1g of leaf tissue in liquid nitrogen followed by re-suspension in 1mL TRIzol® (Ambion, Austin, TX). 200uL of chloroform was used to separate the solid and aqueous phases, followed by centrifugation at 12,000xg for 15min and 4°C. The aqueous phase (containing RNA) was precipitated for 20min at -20C in 1mL of isopropanol. Pellets were spun down and washed two times with 75% molecular grade ethanol, then air dried in the chemical hood before re-suspension in sterile water. RNA yield and quality were measured using the NanoDrop 2000 Spectrophotometer (Thermo Scientific, Waltham, MA). Total RNA was then subjected to DNAse treatment and used to make cDNA as described below.

Total citrus RNA was extracted using the TRIzol® (Ambion, Austin, TX) method described above. Citrus total RNA was assessed for quality using the NanoDrop and for

yield using the Qubit Fluorometer and Qubit RNA Broad Range assay kit (Thermo Scientific, Waltham, MA). RNA was used directly for NanoString analysis (below).

Quantitative PCR (qPCR) for senescence markers

RNA from four-week-old *A. thaliana* plants (RNA extraction described above) at different timepoints (24hr, 27hr, 30hrs, and 48hrs) post Dex-induction was used to make cDNA. RNA from dark-treated plants was used as a control for the *At*SEN1 gene marker. 1μg of total RNA was DNase-treated and reverse transcribed by RevertAid Reverse Transcriptase with RiboLock RNase Inhibitor at 42°C for one hour using oligo-dT as a primer (Kit from Thermo Scientific, Waltham, MA). 30X diluted cDNA was then subjected to quantitative PCR (qPCR) analysis using iQ SYBR Green Supermix (BioRad, Hercules, CA) and Bio-Rad CFX96 thermocycler. For the qPCR reaction *At*SEN1 and *At*Actin-2 primers (IDT Coralville, IA) were used at a final concentration of 5μM. Cycle conditions were an initial denaturation at 95°C for 2min followed by 42 cycles of 95°C for 15s, 56°C for 30s, and 72°C for 30s and a melt curve cycle at 65°C for 5s and 95°C for 5s. Relative expression levels were determined using *At*Actin-2 as the internal control and calculated by the $2^{-\Delta\Delta Ct}$ method. Bar graphs were generated in Excel, Microsoft Office v16.31.

NanoString Elements nCounter gene expression analysis

Total citrus RNA was diluted according to the NanoString nCounter Elements user manual (50ng total RNA per sample). Custom probes were designed by NanoString (Seattle, Washington) to target a subset of papain-like cysteine protease and senescence gene markers in citrus (**Table 3.1**). Gene sequences from the *Citrus*

sinensis v1.1 and *C. clementina* v1.0 (genomes accessed via Phytozome JGI database) were used for probe generation. Probe working stocks were added to nCounter Elements Tag-Set along with hybridization buffer. Hybridization of target specific probes to RNA was performed for 16hrs at 67°C in a thermocycler. After hybridization, sterile water was added to each sample to bring the total volume up to 30μL for loading in the NanoString SPRINT cartridge after which direct digital RNA counts were read by the nCounter SPRINT Profiler (NanoString, Seattle, WA). Samples were run using two biological replicates.

Data was analyzed using nSolver software version 4.0 (NanoString, Seattle, Washington). *Citrus sinensis* and *C. clementina, F-BOX*, *UPL7*, and *SAND* were used as housekeeping genes for data analysis. Along with internal positive and negative controls provided by NanoString to assess quality of the run. Comparisons of different samples to assess relative expression was performed in nSolver using the ratio data. All values are presented as Log_2 fold-change. Each comparison group contains at least two biological replicates.

ACKNOWLEDGEMENTS

For the results presented in this chapter I would like to acknowledge Dr. Zhiqian Pang and Dr. Nian Wang at the University of Florida, Lake Alfred for their contributions in generating the SDE1 transgenic citrus and performing *C*Las-infection via graft inoculation. I would also like to acknowledge the UC Riverside undergraduate students Shellen Lee, Thomas Forest, Caitlin Tong, and Abhi Gowder for helping to Dex-induce many Arabidopsis leaves and providing other assistance necessary for these experiments.

REFERENCES

1. Yan, Q. *et al.* Global gene expression changes in Candidatus Liberibacter asiaticus during the transmission in distinct hosts between plant and insect. *Mol. Plant Pathol.* **14**, 391–404 (2013).

2. Prasad, S., Xu, J., Zhang, Y. & Wang, N. SEC-Translocon Dependent Extracytoplasmic Proteins of Candidatus Liberibacter asiaticus. *Front. Microbiol.* **7**, (2016).

3. Pagliaccia, D. *et al.* A Pathogen Secreted Protein as a Detection Marker for Citrus Huanglongbing. *Front. Microbiol.* **8**, 2041 (2017).

4. Clark, K. *et al.* An effector from the Huanglongbing-associated pathogen targets citrus proteases. *Nat. Commun.* **9**, 1718 (2018).

5. Liu, H., Hu, M., Wang, Q., Cheng, L. & Zhang, Z. Role of Papain-Like Cysteine Proteases in Plant Development. *Front. Plant Sci.* **9**, (2018).

6. van der Hoorn, R. A. L. Plant Proteases: From Phenotypes to Molecular Mechanisms. *Annu. Rev. Plant Biol.* **59**, 191–223 (2008).

7. Roberts, I. N., Caputo, C., Criado, M. V. & Funk, C. Senescence-associated proteases in plants. *Physiol. Plant.* **145**, 130–139 (2012).

8. Lohman, K. N., Gan, S., John, M. C. & Amasino, R. M. Molecular analysis of natural leaf senescence in Arabidopsis thaliana. *Physiol. Plant.* **92**, 322–328 (1994).

9. James, M. *et al.* SAG12, a Major Cysteine Protease Involved in Nitrogen Allocation during Senescence for Seed Production in Arabidopsis thaliana. *Plant Cell Physiol.* **59**, 2052–2063 (2018).

10. Pružinská, A. *et al.* Major Cys protease activities are not essential for senescence in individually darkened Arabidopsis leaves. *BMC Plant Biol.* **17**, 4 (2017).

11. Spann, T. M. & Schumann, A. W. The Role of Plant Nutrients in Disease Development with Emphasis on Citrus and Huanglongbing. *Proc Fla State Hort Soc* 169–171 (2009).

12. Pustika, A. B. *et al.* Interactions between plant nutrition and symptom expression in mandarin trees infected with the disease huanglongbing. *Australas. Plant Dis. Notes* **3**, 112–115 (2008).

13. Zhao, H. *et al.* Small RNA Profiling Reveals Phosphorus Deficiency as a Contributing Factor in Symptom Expression for Citrus Huanglongbing Disease. *Mol. Plant* **6**, 301–310 (2013).

14. Stansly, P. A. *et al.* Vector control and foliar nutrition to maintain economic sustainability of bearing citrus in Florida groves affected by huanglongbing. *Pest Manag. Sci.* **70**, 415–426 (2014).

15. Killingbeck, K. T. Nutrients in Senesced Leaves: Keys to the Search for Potential Resorption and Resorption Proficiency. *Ecology* **77**, 1716–1727 (1996).

16. Cao, J., Cheng, C., Yang, J. & Wang, Q. Pathogen infection drives patterns of nutrient resorption in citrus plants. *Sci. Rep.* **5**, (2015).

17. Pitino, M., Allen, V. & Duan, Y. LasΔ5315 Effector Induces Extreme Starch Accumulation and Chlorosis as Ca. Liberibacter asiaticus Infection in Nicotiana benthamiana. *Front. Plant Sci.* **9**, 113 (2018).

18. Lim, P. O., Kim, H. J. & Gil Nam, H. Leaf Senescence. *Annu. Rev. Plant Biol.* **58**, 115–136 (2007).

19. Thomas, H. Senescence, ageing and death of the whole plant. *New Phytol.* **197**, 696–711 (2013).

20. Woo, H. R., Kim, H. J., Nam, H. G. & Lim, P. O. Plant leaf senescence and death - regulation by multiple layers of control and implications for aging in general. *J. Cell Sci.* **126**, 4823–4833 (2013).

21. Breeze, E. *et al.* High-Resolution Temporal Profiling of Transcripts during Arabidopsis Leaf Senescence Reveals a Distinct Chronology of Processes and Regulation. *Plant Cell* **23**, 873–894 (2011).

22. Bhattacharjee, S. Reactive oxygen species and oxidative burst: Roles in stress, senescence and signal transducation in plants. *Curr. Sci.* **89**, 1113–1121 (2005).

23. Buchanan-Wollaston, V. *et al.* The molecular analysis of leaf senescence – a genomics approach. *Plant Biotechnol. J.* **1**, 3–22 (2003).

24. Gan, S. Mitotic and Postmitotic Senescence in Plants. *Sci. Aging Knowl. Environ.* **38**, re7 (2003).

25. Gepstein, S. *et al.* Large-scale identification of leaf senescence-associated genes. *Plant J.* **36**, 629–642 (2003).

26. Häffner, E., Konietzki, S. & Diederichsen, E. Keeping Control: The Role of Senescence and Development in Plant Pathogenesis and Defense. *Plants* **4**, 449–488 (2015).

27. Obregón, P., Martín, R., Sanz, A. & Castresana, C. Activation of defence-related genes during senescence: a correlation between gene expression and cellular damage. *Plant Mol. Biol.* **46**, 67–77 (2001).

28. Quirino, B. F., Normanly, J. & Amasino, R. M. Diverse range of gene activity during Arabidopsis thaliana leaf senescence includes pathogen-independent induction of defense-related genes. *Plant Mol. Biol.* **40**, 267–278 (1999).

29. Schenk, P. M., Kazan, K., Rusu, A. G., Manners, J. M. & Maclean, D. J. The SEN1 gene of Arabidopsis is regulated by signals that link plant defence responses and senescence. *Plant Physiol. Biochem.* **43**, 997–1005 (2005).

30. Thaler, J. S., Humphrey, P. T. & Whiteman, N. K. Evolution of jasmonate and salicylate signal crosstalk. *Trends Plant Sci.* **17**, 260–270 (2012).

31. Buchanan-Wollaston, V. *et al.* Comparative transcriptome analysis reveals significant differences in gene expression and signalling pathways between developmental and dark/starvation-induced senescence in Arabidopsis. *Plant J.* **42**, 567–585 (2005).

32. Guo, P. *et al.* A Tripartite Amplification Loop Involving the Transcription Factor WRKY75, Salicylic Acid, and Reactive Oxygen Species Accelerates Leaf Senescence. *Plant Cell* **29**, 2854–2870 (2017).

33. Morris, K. *et al.* Salicylic acid has a role in regulating gene expression during leaf senescence. *Plant J.* **23**, 677–685 (2000).

34. He, Y., Fukushige, H., Hildebrand, D. F. & Gan, S. Evidence Supporting a Role of Jasmonic Acid in Arabidopsis Leaf Senescence. *Plant Physiol.* **128**, 876–884 (2002).

35. Liao, H.-L. & Burns, J. K. Gene expression in Citrus sinensis fruit tissues harvested from huanglongbing-infected trees: comparison with girdled fruit. *J. Exp. Bot.* **63**, 3307 (2012).

36. Fu, S., Shao, J., Zhou, C. & Hartung, J. S. Transcriptome analysis of sweet orange trees infected with 'Candidatus Liberibacter asiaticus' and two strains of Citrus Tristeza Virus. *BMC Genomics* **17**, 349 (2016).

37. Kim, J.-S., Sagaram, U. S., Burns, J. K., Li, J.-L. & Wang, N. Response of Sweet Orange (*Citrus sinensis*) to ' *Candidatus* Liberibacter asiaticus' Infection: Microscopy and Microarray Analyses. *Phytopathology* **99**, 50–57 (2009).

38. Martinelli, F. *et al.* Transcriptome profiling of citrus fruit response to huanglongbing disease. *PloS One* **7**, e38039 (2012).

39. Barth, C., Moeder, W., Klessig, D. F. & Conklin, P. L. The Timing of Senescence and Response to Pathogens Is Altered in the Ascorbate-Deficient Arabidopsis Mutant vitamin c-1. *Plant Physiol.* **134**, 1784–1792 (2004).

40. Ilyas, M. *et al.* Functional Divergence of Two Secreted Immune Proteases of Tomato. *Curr. Biol.* **25**, 2300–2306 (2015).

41. Misas-Villamil, J. C., van der Hoorn, R. A. L. & Doehlemann, G. Papain-like cysteine proteases as hubs in plant immunity. *New Phytol.* **212**, 902–907 (2016).

42. Aoyama, T. & Chua, N.-H. A glucocorticoid-mediated transcriptional induction system in transgenic plants. *Plant J.* **11**, 605–612 (1997).

43. Rogers, H. & Munné-Bosch, S. Production and Scavenging of Reactive Oxygen Species and Redox Signaling during Leaf and Flower Senescence: Similar But Different. *Plant Physiol.* **171**, 1560–1568 (2016).

44. Shapiguzov, A., Vainonen, J. P., Wrzaczek, M. & Kangasjärvi, J. ROS-talk – how the apoplast, the chloroplast, and the nucleus get the message through. *Front. Plant Sci.* **3**, (2012).

45. Bieker, S. & Zentgraf, U. Plant Senescence and Nitrogen Mobilization and Signaling. in *Senescence and Senescence-Related Disorders* (ed. Zhiwei, W.) (InTech, 2013). doi:10.5772/54392.

46. Ishida, H., Izumi, M., Wada, S. & Makino, A. Roles of autophagy in chloroplast recycling. *Biochim. Biophys. Acta BBA - Bioenerg.* **1837**, 512–521 (2014).

47. Tatineni, S. *et al.* In Planta Distribution of ' *Candidatus* Liberibacter asiaticus' as Revealed by Polymerase Chain Reaction (PCR) and Real-Time PCR. *Phytopathology* **98**, 592–599 (2008).

48. Li, W., Levy, L. & Hartung, J. S. Quantitative Distribution of ' *Candidatus* Liberibacter asiaticus' in Citrus Plants with Citrus Huanglongbing. *Phytopathology* **99**, 139–144 (2009).

49. Espinoza, C., Medina, C., Somerville, S. & Arce-Johnson, P. Senescence-associated genes induced during compatible viral interactions with grapevine and Arabidopsis. *J. Exp. Bot.* **58**, 3197–3212 (2007).

50. Hall, D. G., Sétamou, M. & Mizell, R. F. A comparison of sticky traps for monitoring Asian citrus psyllid (Diaphorina citri Kuwayama). (2010).

51. Paris, T. M., Allan, S. A., Udell, B. J. & Stansly, P. A. Evidence of behavior-based utilization by the Asian citrus psyllid of a combination of UV and green or yellow wavelengths. *PloS One* **12**, e0189228 (2017).

52. Sathe, T. V., Gophane, A. & Shendage, N. Colour attractivity and occurrence of some cell sap sucking pests on crop plants. *Biolife* **3**, 540–546 (2015).

53. Hayward, A. P. & Dinesh-Kumar, S. P. What Can Plant Autophagy Do for an Innate Immune Response? *Annu. Rev. Phytopathol.* **49**, 557–576 (2011).

54. Wang, P., Mugume, Y. & Bassham, D. C. New advances in autophagy in plants: Regulation, selectivity and function. *Semin. Cell Dev. Biol.* **80**, 113–122 (2018).

55. Thompson, A. R., Doelling, J. H., Suttangkakul, A. & Vierstra, R. D. Autophagic Nutrient Recycling in Arabidopsis Directed by the ATG8 and ATG12 Conjugation Pathways. *Plant Physiol.* **138**, 2097–2110 (2005).

56. Yoshimoto, K. *et al.* Autophagy Negatively Regulates Cell Death by Controlling NPR1-Dependent Salicylic Acid Signaling during Senescence and the Innate Immune Response in Arabidopsis. *Plant Cell* **21**, 2914–2927 (2009).

57. Li, Y., Kabbage, M., Liu, W. & Dickman, M. B. Aspartyl Protease-Mediated Cleavage of BAG6 Is Necessary for Autophagy and Fungal Resistance in Plants. *Plant Cell* **28**, 233–247 (2016).

58. Henry, E., Fung, N., Liu, J., Drakakaki, G. & Coaker, G. Beyond Glycolysis: GAPDHs Are Multi-functional Enzymes Involved in Regulation of ROS, Autophagy, and Plant Immune Responses. *PLOS Genet.* **11**, e1005199 (2015).

59. Patel, S. & Dinesh-Kumar, S. P. Arabidopsis ATG6 is required to limit the pathogen-associated cell death response. *Autophagy* **4**, 20–27 (2008).

60. Shindo, T., Misas-Villamil, J. C., Hörger, A. C., Song, J. & van der Hoorn, R. A. L. A Role in Immunity for Arabidopsis Cysteine Protease RD21, the Ortholog of the Tomato Immune Protease C14. *PLoS ONE* **7**, (2012).

61. Shindo, T. Investigating the role of papain-like cysteine protease RD21 in plant-pathogen interactions. (Max-Planck-Institut, 2009).

62. Kimmey, J. M. & Stallings, C. L. Bacterial Pathogens versus Autophagy: Implications for Therapeutic Interventions. *Trends Mol. Med.* **22**, 1060–1076 (2016).

63. Wu, Y.-W. & Li, F. Bacterial interaction with host autophagy. *Virulence* **10**, 352–362 (2019).

64. Dagdas, Y. F. *et al.* Host autophagy machinery is diverted to the pathogen interface to mediate focal defense responses against the Irish potato famine pathogen. *eLife* **7**, e37476 (2018).

65. Choy, A. *et al.* The Legionella Effector RavZ Inhibits Host Autophagy Through Irreversible Atg8 Deconjugation. *Science* **338**, 1072–1076 (2012).

66. Yoshimoto, K. *et al.* Processing of ATG8s, Ubiquitin-Like Proteins, and Their Deconjugation by ATG4s Are Essential for Plant Autophagy. *Plant Cell* **16**, 2967–2983 (2004).

67. Clough, S. J. & Bent, A. F. Floral dip: a simplified method for Agrobacterium-mediated transformation of Arabidopsis thaliana. *Plant J. Cell Mol. Biol.* **16**, 735–743 (1998).

68. Harrison, S. J. *et al.* A rapid and robust method of identifying transformed Arabidopsis thaliana seedlings following floral dip transformation. *Plant Methods* **2**, 19 (2006).

69. Laemmli, U. K. Cleavage of Structural Proteins during the Assembly of the Head of Bacteriophage T4. *Nature* **227**, 680–685 (1970).

70. Daudi, A. & O'Brien, J. Detection of Hydrogen Peroxide by DAB Staining in Arabidopsis Leaves. *BIO-Protoc.* **2**, (2012).

GENERAL CONCLUSIONS AND DISCUSSION

Huanglongbing (HLB) remains a threat to the citrus industry and understanding the molecular mechanisms behind disease progression is pivotal to provide strategies for management. In particular, knowledge on the virulence mechanisms of the associated-pathogen, *Candidatus* Liberibacter asiaticus (*C*Las) is key to uncovering potential resistance and/or susceptibility genes in citrus. In this thesis, I employed Sec-delivered-effectors (SDEs) of *C*Las to gain mechanistic insight and elucidate possible avenues for HLB disease management.

To summarize, I used the *C*Las secreted effectors, SDE1 and SDE2 to improve antibodies applied to serological detection platforms for *C*Las. These results demonstrated that secreted proteins of *C*Las can serve as useful detection biomarkers. Future *C*Las detection could employ other SDEs as biomarkers using the same pipeline, antibodies generated against additional biomarkers could be mixed as a cocktail to enhance detection robustness. In addition, knowledge from this work could be used in the development of serological-based detection for other vascular-limited pathogens via use of secreted pathogen components as markers.

Further, I utilized SDE1 to identity effector host targets in citrus and characterize effector function, broadening our knowledge on *C*Las virulence mechanisms and HLB pathogenesis. My results concluded that SDE1 can interact with and inhibit the activity of papain-like cysteine proteases (PLCPs) in citrus and promote *C*Las growth, likely in a PLCP-inhibitory manner. In the future, characterization of the interaction interface between SDE1 and PLCPs would provide useful information for genetic modification of citrus. For example, specific residues found to confer SDE1-PLCP interaction could be modified to prevent SDE1's inhibitory function (i.e. resistance to SDE1) and thus

generate HLB tolerant or resistant citrus cultivars. In addition, assessment of PLCP expression and activity levels in different citrus species could help citrus breeders determine potential defense associated PLCPs to use for hybrid generation.

Finally, I found SDE1 to contribute to an HLB-like symptom (i.e. leaf yellowing) in Arabidopsis and citrus. My results indicate this yellowing could be linked to the induction of leaf senescence as PLCPs and other senescence-associated genes have altered gene expression in *SDE1* transgenic citrus. The role of SDE1 and citrus PLCPs in leaf senescence still needs further exploration, in addition to the potential contributions of *C*Las SDEs to HLB symptom development.

APPENDIX

Table A.1 – Vectors and strains used in Chapter 1

No.	Vector name	Strain	Purpose
1	pRSF-Sumo::SDE1 (partial)	DH5alpha	Plasmid for further protein expression
2	pRSF-Sumo::SDE1 (full)	DH5alpha	Plasmid for further protein expression
3	pRSF-Sumo::SDE1-1 (partial)	BL21 (RIL)	Protein expression
4	pRSF-Sumo::SDE1 (full)	BL21 (RIL)	Protein expression
5	pRSF-Sumo::EV	DH5alpha	Empty vector control
6	pRSF-Sumo::EV	BL21 (RIL)	Empty vector control
7	pET28a::gIII-SDE1-His	DH5alpha	Plasmid for periplasmic protein expression
8	pET28a::gIII-His-SDE1	DH5alpha	Plasmid for periplasmic protein expression
9	pET28a::NativeSP-SDE1-His	DH5alpha	Plasmid for periplasmic protein expression
10	PET28a::NativeSP-His-SDE1	DH5alpha	Plasmid for periplasmic protein expression
11	pET28a::gIII-CsSAG12-1-His	DH5alpha	Plasmid for periplasmic protein expression
12	pET28a::gIII-CsSAG12-63-His	DH5alpha	Plasmid for periplasmic protein expression
13	pET28a::gIII-RCR3-dsm3-His	DH5alpha	Plasmid for periplasmic protein expression
14	pET28a::gIII-RCR3-lyc-His	DH5alpha	Plasmid for periplasmic protein expression
15	pET28a::gIII-RCR3-pim-His	DH5alpha	Plasmid for periplasmic protein expression
16	pET28a::gIII-RD21a-1-His	DH5alpha	Plasmid for periplasmic protein expression

17	pET28a::gIII-RD19a-1-His	DH5alpha	Plasmid for periplasmic protein expression
18	pET28a::gIII-SDE1-His	BL21 (DE3)	Periplasmic protein expression
19	pET28a::gIII-His-SDE1	BL21 (DE3)	Periplasmic protein expression
20	pET28a::NativeSP-SDE1-His	BL21 (DE3)	Periplasmic protein expression
21	PET28a::NativeSP-His-SDE1	BL21 (DE3)	Periplasmic protein expression
22	pET28a::gIII-CsSAG12-1-His	BL21 (DE3)	Periplasmic protein expression
23	pET28a::gIII-CsSAG12-63-His	BL21 (DE3)	Periplasmic protein expression
24	pET28a::gIII-RCR3-dsm3-His	BL21 (DE3)	Periplasmic protein expression
25	pET28a::gIII-RCR3-lyc-His	BL21 (DE3)	Periplasmic protein expression
26	pET28a::gIII-RCR3-pim-His	BL21 (DE3)	Periplasmic protein expression
27	pET28a::gIII-RD21a-1-His	BL21 (DE3)	Periplasmic protein expression
28	pET28a::gIII-RD19a-1-His	BL21 (DE3)	Periplasmic protein expression
29	pET28a::EV	BL21 (DE3)	Empty vector control
30	pET28a::SDE1	DH5alpha	Plasmid for further protein expression (from Dr. Jinxia Shi)
31	pET14b::SDE2	DH5alpha	Plasmid for further protein expression (from Dr. Jinxia Shi)
32	pET28a::SDE1	BL21 (DE3)	Protein expression (from Dr. Jinxia Shi)
33	pET14b::SDE2	BL21 (DE3)	Protein expression (from Dr. Jinxia Shi)
34	pEG103::SDE1+GFP	C58C1	Protein expression in Nicotiana benthamiana (from Dr. Jinxia Shi)

35	pEG103::SDE1+GFP	C58C1	Protein expression in Nicotiana benthamiana (from Dr. Jinxia Shi)
36	pEG103::SDE2+GFP	C58C1	Protein expression in Nicotiana benthamiana (from Dr. Jinxia Shi)
37	pEG103::SDE2+GFP	C58C1	Protein expression in Nicotiana benthamiana (from Dr. Jinxia Shi)
38	pEG103::SDE1	GV3101	Protein expression in Nicotiana benthamiana (from Dr. Jinxia Shi)
39	pEG103::SDE2	GV3101	Protein expression in Nicotiana benthamiana (from Dr. Jinxia Shi)

A.2 – Vectors and strains used in Chapter 2

No.	Vector name	Strain	Purpose
1	pGBKT7::EV	DH5alpha	Y2H bait plasmid (from Dr. Jinxia Shi)
2	pGBKT7::SDE1	DH5alpha	Y2H bait plasmid (from Dr. Jinxia Shi)
3	pGBKT7::EV	AH109	Y2H bait yeast (from Dr. Jinixa Shi)
4	pGBKT7::SDE1	AH109	Y2H bait yeast (from Dr. Jinixa Shi)
5	pGADT7::XM_006475194	DH5alpha	Y2H prey plasmid
6	pGADT7::XM_006489385	DH5alpha	Y2H prey plasmid
7	pGADT7::XM_006488247	DH5alpha	Y2H prey plasmid
8	pGADT7::XM_006467144	DH5alpha	Y2H prey plasmid
9	pGADT7::XM_006467400	DH5alpha	Y2H prey plasmid
10	pGADT7::XM_006493578	DH5alpha	Y2H prey plasmid
11	pGADT7::*Cs*SAG12-1 full-length	DH5alpha	Y2H prey plasmid
12	pGADT7::CsSAG12-1 truncate 1	DH5alpha	Y2H prey plasmid
13	pGADT7::CsSAG12-1 truncate 2	DH5alpha	Y2H prey plasmid
14	pGADT7::CsSAG12-2 truncate 1	DH5alpha	Y2H prey plasmid
15	pGADT7::CsSAG12-2 truncate 2	DH5alpha	Y2H prey plasmid
16	pGADT7::*Cs*AALP truncate 1	DH5alpha	Y2H prey plasmid
17	pGADT7::CsAALP truncate 2	DH5alpha	Y2H prey plasmid
18	pGADT7::CsRD21a truncate 1	DH5alpha	Y2H prey plasmid

19	pGADT7::CsRD21a truncate 2	DH5alpha	Y2H prey plasmid
20	pGADT7::CsXBCP3 truncate 2	DH5alpha	Y2H prey plasmid
21	pGADT7::CsRD19 truncate 2	DH5alpha	Y2H prey plasmid
22	pGADT7::CsCTB truncate 2	DH5alpha	Y2H prey plasmid
23	pGADT7::CsSAG12-63 truncate 2	DH5alpha	Y2H prey plasmid
24	pGADT7::CsSAG12-34 truncate 2	DH5alpha	Y2H prey plasmid
25	pGADT7::CsSAG12-58 truncate 2	DH5alpha	Y2H prey plasmid
26	pGADT7::EV	DH5alpha	Empty vector control
27	pRSF-Sumo::SDE1 (full)	BL21 (RIL)	Protein expression for inhibition assays
28	pET14b::SDE2	BL21 (DE3)	Protein expression for inhibition assay
29	pGEX-4T2-GST::EV	DH5alpha	Plasmid for in vitro pull-down
30	pGEX-4T2-GST::EV	BL21 (DE3)	Plasmid for in vitro pull-down
31	RCR3-dms3 (unknown vector)	Unknown Agrobacterium	Protein expression in Nicotiana benthamiana (from Dr. Suomeng Dong)
32	RCR3-dms3 (unknown vector)	Unknown Agrobacterium	Protein expression in Nicotiana benthamiana (from Dr. Suomeng Dong)
33	pGEX-4t2-GST::CsSAG12-1 truncate 1	DH5alpha	Plasmid for in vitro pull-down
34	pGEX-4t2-GST::CsSAG12-1 truncate 2	DH5alpha	Plasmid for in vitro pull-down
35	pGEX-4t2-GST::CsSAG12-1 truncate 1	BL21 or SHuffle	In vitro pull-down

36	pGEX-4t2-GST::CsSAG12-1 truncate 2	BL21 or SHuffle	In vitro pull-down
37	pGEX-4t2-GST::CsRD21a truncate 1	BL21 or SHuffle	In vitro pull-down
38	pGEX-4t2-GST::CsRD21a truncate 2	BL21 or SHuffle	In vitro pull-down
39	pGEX-4t2-GST::CsAALP truncate 2	DH5alpha	Plasmid for in vitro pull-down
40	pGEX-4t2-GST::CsAALP truncate 2	BL21 or SHuffle	In vitro pull-down
41	pGEX-4t2-GST::RCR3 (dms3)	DH5alpha	Plasmid for in vitro pull-down
42	pGEX-4t2-GST::RCR3 (dms3)	BL21 or SHuffle	In vitro pull-down
43	pGEX-4t2-GST::EV	BL21	Empty vector control
44	pGEX-4t2-GST::*At*DRB4	BL21	In vitro pull-down (from Dr. Yi Zhai)